UCLouvain

AGRO LOUVAIN

Faculté des bioingénieurs

Vulnerability assessment of Qatar desalination plants to oil spills

Auteur : Thomas Anselain

Promoteur : Prof. Emmanuel Hanert (UCLouvain)

Lecteurs : Prof. Essam Heggy (QEERI, Qatar Foundation)

Prof. Patrick Bogaert (UCLouvain)

Année académique : 2020 - 2021

Bioingénieur : Sciences agronomiques

Abstract

Water scarcity is an issue at least once a year for 70% of the global population. As water scarcity increases, desalination plants are on the rise. Today, desalinated water represents about half of the entire water supply of Qatar. However, the desalination plants and, by extension, Qatar are very sensitive to oil spill pollution. The Arabian Gulf being one of the most oil-polluted environment in the World, Qatar is continuously threatened by oil spills, which could lead to the closure of desalination plants. To efficiently manage its water supply, Qatar needs to monitor its coastal waters in order to detect as early as possible oil spills that could potentially threaten its desalination plants.

In this study, we perform a vulnerability assessment of Qatar desalination plants to oil pollution originating from both shipping activities and offshore oil platforms. In order to simulate oil drift dispersal, we used the open-source model OpenOil, which takes into account the different physical processes driving oil dispersal as well as most of the oil weathering processes. To assess the exposure to oil pollution originating from shipping activities, we first identify the oil risk area around a desalination plant and then combine this risk information with the density of ships in the Gulf. In a second step, a connectivity study was performed to highlight which oil fields are the most dangerous for Qatar.

Overall, the results show a strong seasonal variability of the oil exposure patterns, which reflects changes in the atmospheric and oceanic in the Gulf. When Shamal winds are blowing in summer and winter, risk is usually located mostly Northwest of Qatar. However, when winds weaken in spring and autumn, the risk area tends to shift East and be more isotropic. It is during summer, that the circulation is the most intense and hence that oil spills could travel the largest distances before reaching a desalination plant. Higher temperatures and more intense wave activity however increase the oil weathering rate and hence reduce the associated risk. Among Qatar's three main desalination plants, Ras Laffan, located on the northeastern coast of Qatar, is the one most at risk of being impacted by oil spills.

Despite the model is not validated by previous oil spill observations, our results could inform Qatar authorities on ways to optimize their oil spill management strategy. This study could also inspire new research about desalination plants vulnerability throughout the Arabian Gulf and promote the development of oil spills forecasting and monitoring capacities in order to reduce the impact of oil pollution on water production.

Acknowledgments

My first thanks go to Emmanuel Hanert, who has been an invaluable support throughout the completion of this thesis. He was always available to check my progresses and redirect me if necessary. Working under his supervision and his optimistic personality has been a pleasant and rewarding experience.

I would also like to thank Thomas Dobbelaere for guiding me through the OpenOil codes. He never hesitated to help me whenever I needed it. I am grateful to Antoine Saint-Amand, Valentin Vallaeys and David Vincent whose ideas are allowed to improve this study.

I would then like to thank my readers for their valuable comments on this thesis. Prof. Bogaert learns me to making numbers meaningful, a useful skill in the scientific field. Special thanks to Essam Heggy for his interest in the water production sustainability in Qatar.

I would like to thank my friends and my thesis colleagues for the mutual support.

Finally, I would like to express my gratitude to my girlfriend. Thank you a lot for your precious support. Thanks also to my family not only for this master thesis but also for giving me important key in the life path.

The end of my study through this master thesis constitute a major step in my life. The achievement of this task would not have been possible without the support of many people not mentioned before. Many thanks to them.

Glossary

CMEMS: Copernicus Marine Environment Monitoring Service.

ECMWF: European Centre for Medium-Range Weather Forecasts.

EEZ: Exclusive Economic Zone.

ERA5: ERA refers to "ECMWF ReAnalysis", with ERA5 being the fifth global reanalysis produced by ECMWF.

NOAA: National Oceanic and Atmospheric Administration.

NEMO: Nucleus for European Modelling of the Ocean.

MSF: Mutli Stage Flash distillation.

MED: Multiple Effect Distillation.

RO: Reverse Osmosis.

Key words

Arabian Gulf • Water scarcity • Offshore platforms • Qatar • Oil spill • OpenOil • Shipping lane • Desalination • Hydrodynamic model

Contents

1 Introduction 8

2 Material and Methods 14

2.1 Area of interest 14
a. Qatar and the Arabian Gulf 14
b. Desalination plants in Qatar 15
c. Shipping routes and oil platforms in the Arabian Gulf 17
2.2 Ocean circulation in the Gulf 18
a. General circulation patterns and their seasonal variability 18
b. Hydrodynamic model (NEMO) 19
2.3 Oil spill modelling 20
a. Chemical and physical processes driving oil spills dispersal 20
b. Oil dispersal model (OpenOil) 22
c. Input data 25
2.4 Vulnerability indicators 27
a. Vulnerability to oil spills from shipping 27
b. Vulnerability to oil spills from drilling platforms 31

3 Results 33

3.1 Circulation patterns around Qatar 33
3.2 Desalination plants risk maps 34
3.3 Arrival time maps 37
3.4 Shipping exposure maps 40
3.5 Oil platforms exposure maps 43
3.6 Total monthly exposure timeseries 45

4 Discussion 47

4.1 Influence of ocean and wind circulation on oil pathways 47
4.2 Identification of dangerous areas, sensitive stations and risky periods 48

5 Conclusion 51

6 References 53

7 Appendices 57

A. Circulation pattern in the Arabian Gulf 58
B. Minimum arrival time maps 60
C. Oil risk density maps 72
D. Oil exposure maps from ships 84
E. Qatari coasts exposure to oil from oil fields 96

List of Figures

Figure 1.1 : Number of months per year in which blue water scarcity exceeds 1 8
Figure 1.2 : Map of country most at risk of water scarcity 9
Figure 1.3 : Evolution of global desalinated water production and number of desalination plants 10
Figure 1.4 : Evolution of total water withdrawal in Qatar 11
Figure 1.5 : Sources of oil pollution..... 12
Figure 1.6 : Map of all oil spills detected (pink areas) in the Arabian Gulf in 2017 13

Figure 2.1 : Political map of the Arabian Gulf..... 14
Figure 2.2 : Qatar's power and desalination plants 16
Figure 2.3 : Shipping density ranges map in the Arabian Gulf in 2013..... 17
Figure 2.4 : Location of the oil and gas fields considered in this study..... 18
Figure 2.5 : Diagram of the water circulation in the Arabian Gulf during warm months..... 19
Figure 2.6 : Diagram of the behaviour and weathering processes of oil in water..... 20
Figure 2.7 : Diagram of the physical steps of an Opendrift simulation 23
Figure 2.8 : (**a**) Evolution of oil weathering as simulated by OpenOil for QATAR MARINE oil and (**b**) evolution of oil viscosity and density 24
Figure 2.9 : Risk zones and receptor points associated to each stations in Qatar 26
Figure 2.10 : Example of a 5 days backward simulation starting from a receptor points at Ras Laffan desalination plant..... 28
Figure 2.11 : Example of a minimum arrival time map for Ras Laffan in March 2019 28
Figure 2.12 : Example of a risk distribution function with the associated Total risk for Ras Laffan in March 2019..... 29
Figure 2.13 : Shipping density distribution in a sub zone of Arabian Gulf in 2013 30
Figure 2.14 : Example of an exposure map with the associated Total exposure for Ras Laffan in March 2019 31
Figure 2.15 : Partition of Qatar's coastline in ten coastal segments 31
Figure 2.16 : Connection table between offshore platforms and Qatari coasts for Ras Laffan in March 2019 including oil weathering processes 32

Figure 3.1 : Seasonal variability of the monthly-averaged ocean circulation around Qatar as simulated by the ocean model NEMO in 2019 34
Figure 3.2 : Seasonal varability of oil risk probability density for Ras Laffan in 2019..... 35
Figure 3.3 : Seasonal variability of oil risk probability density for Umm al Houl in 2019 36
Figure 3.4 : Seasonal variability of oil spill minimum arrival time for Ras Laffan in 2019.... 38

Figure 3.5 : Seasonal variability of oil spill minimum arrival time for Umm al Houl in 2019 39
Figure 3.6 : Seasonal variability of exposure to ships oil spill for Ras Laffan in 2019 41
Figure 3.7 : Seasonal variability of exposure to ships oil spill for Umm al Houl in 2019..... 42
Figure 3.8 : Seasonal variability of oil mass fraction stranded on Qatari coasts originating from oil rigs in 2019..... 44
Figure 3.9 : Evolution of Qatari desalination plants exposure to (**a**) ships oil spill and (**b**) oil from oil rigs, in 2019 and 2020 46

Figure 4.1 : Evolution of Qatari desalination plants exposure to oil from oil rigs in 2019 49
Figure 4.2 : Evolution of oil weathering for (**a**) 'QATAR MARINE' (850.3 kg/m^3) and (**b**) 'Yombo, Amoco' (950.6 kg/m^3) 50

Figure 7.1 : Seasonal variability of the monthly-averaged ocean circulation around Qatar as simulated by the ocean model NEMO in 2019 59
Figure 7.2 : Minimum arrival time of oil spill for Ras Laffan in 2019 61
Figure 7.3 : Minimum arrival time of oil spill for Umm al Houl in 2019..... 63
Figure 7.4 : Minimum arrival time of oil spill for Abu Fontas in 2019 65
Figure 7.5 : Minimum arrival time of oil spill for Ras Laffan in 2020 67
Figure 7.6 : Minimum arrival time of oil spill for Umm al Houl in 2020..... 69
Figure 7.7 : Minimum arrival time of oil spill for Abu Fontas in 2020 71
Figure 7.8 : Maps of oil risk probability density for Ras Laffan in 2019 73
Figure 7.9 : Maps of oil risk probability density for Umm al Houl in 2019 75
Figure 7.10 : Maps of oil risk probability density for Abu Fontas in 2019 77
Figure 7.11 : Maps of oil risk probability density for Ras Laffan in 2020 79
Figure 7.12 : Maps of oil risk probability density for Umm al Houl in 2020 81
Figure 7.13 : Maps of oil risk probability density for Abu Fontas in 2020 83
Figure 7.14 : Exposure to ships oil spill for Ras Laffan in 2019 85
Figure 7.15 : Exposure to ships oil spills for Umm al Houl in 2019 87
Figure 7.16 : Exposure to ships oil spills for Abu Fontas in 2019..... 89
Figure 7.17 : Exposure to ships oil spills for Ras Laffan in 2020..... 91
Figure 7.18 : Exposure to ships oil spills for Umm al Houl in 2020 93
Figure 7.19 : Exposure to ships oil spill for Abu Fontas in 2020 95
Figure 7.20 : Oil mass fraction stranded on Qatari coasts originating from oil rigs in 2019... 97
Figure 7.21 : Oil mass fraction stranded on Qatari coasts originating from oil rigs in 2020... 99

1 Introduction

Water scarcity is a global threat that affects every continent (WWF 2014 and Worldvision 2018). While water shortages were first documented during the 19th century, it became a major issue during the 20th century when about 11 billion people died due to a lack of freshwater. Only since 1993, the United Nations have designated the 22th March as World Water Day to focus on the importance of freshwater. Despite this action, more than 70% of the global population still finds water scarce at least one month of the year (*fig. 1.1*) (Mekonnen and Hoekstra 2016).

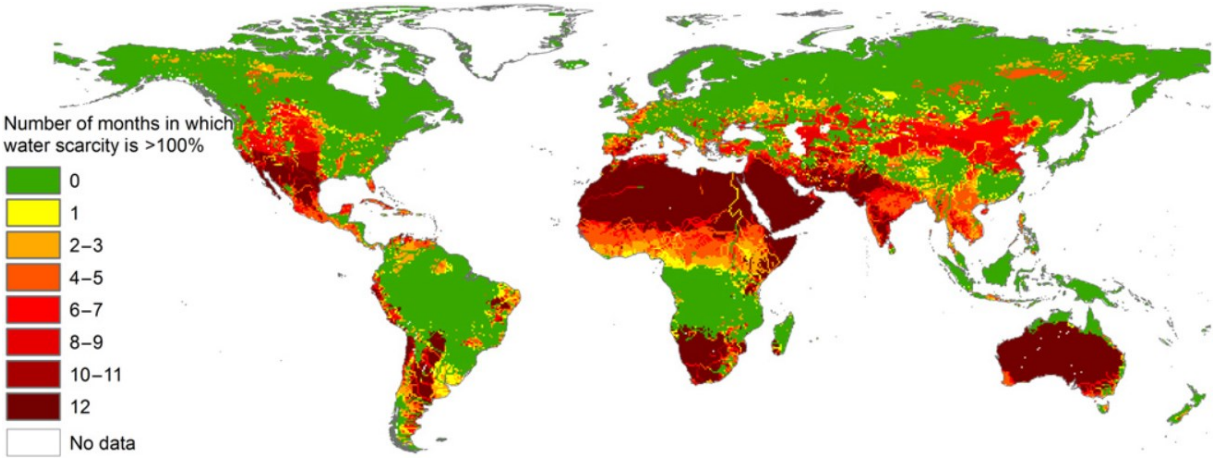


Figure 1.1 : Number of months per year in which blue water scarcity exceeds 1. The blue water scarcity level is measured by ratio between blue water consumption and net water withdrawal. (Mekonnen and Hoekstra 2016)

Water scarcity is due to several causes at both the global and local levels. The first is climate change. Global climate is changing fast, with more extreme heat events and more variable rainfall patterns. On the one hand, some areas in World are now facing droughts almost on a yearly basis while others are exposed to floods of increasing intensity. 74% of natural disasters between 2001 and 2018 were related to water and this number is expected to increase as climate change intensifies (UNICEF 2021). On the other hand, global population will keep on increasing. This increase is highly correlated with the water demand. In 2050, the World population is expected to be 30% larger than today and water demand will at least increase by the same amount (UNICEF 2021 and Schleifer 2017). Population growth also leads to an increase in water demand by the agricultural sector. Agriculture represents 70% the freshwater use and 60% of this water is wasted (WWF 2014). In addition, the use of fertilizers and pesticides pollutes both surface and groundwater. The latter is further depleted by irrigation, which becomes more and more frequent as rainfall declines. Finally, the management of wastewater is usually rather limited as 80% of wastewaters are released in the nature without treatments or reuse (Schleifer 2017).

Water scarcity has an impact on human population in many different ways. Only 117 countries have sufficient data to assess availability of drinking water and sanitation services (Sustainable Development Goal 6 on water and sanitation 2021). Despite this bias, 30% of the World population did not have access to safely managed drinking water services in 2017. Lack of drinking water is also related to poor sanitation services. In 2017, only 40% of world population in the 117 countries assessed used safely managed sanitation services (Sustainable Development Goal 6 on water and sanitation 2021). Patients suffering from diseases related to lack of clean water represent half of the world's hospital beds occupied at any given time (Tzanakakis and al. 2020). Globally, 2.3 billion people are living in country with severe water scarcity and this number is expected to keep on increasing (Tzanakakis and al. 2020; Sustainable Development Goal 6 on water and sanitation 2021; Mekonnen and Hoekstra 2016). The World Resources Institute (WRI 2019) identified 17 countries that are most at risk of water scarcity (*fig. 1.2*). Most of these countries are located in the Middle-East and in North Africa but there are also hotspots in South Asia, Europe and South Africa.

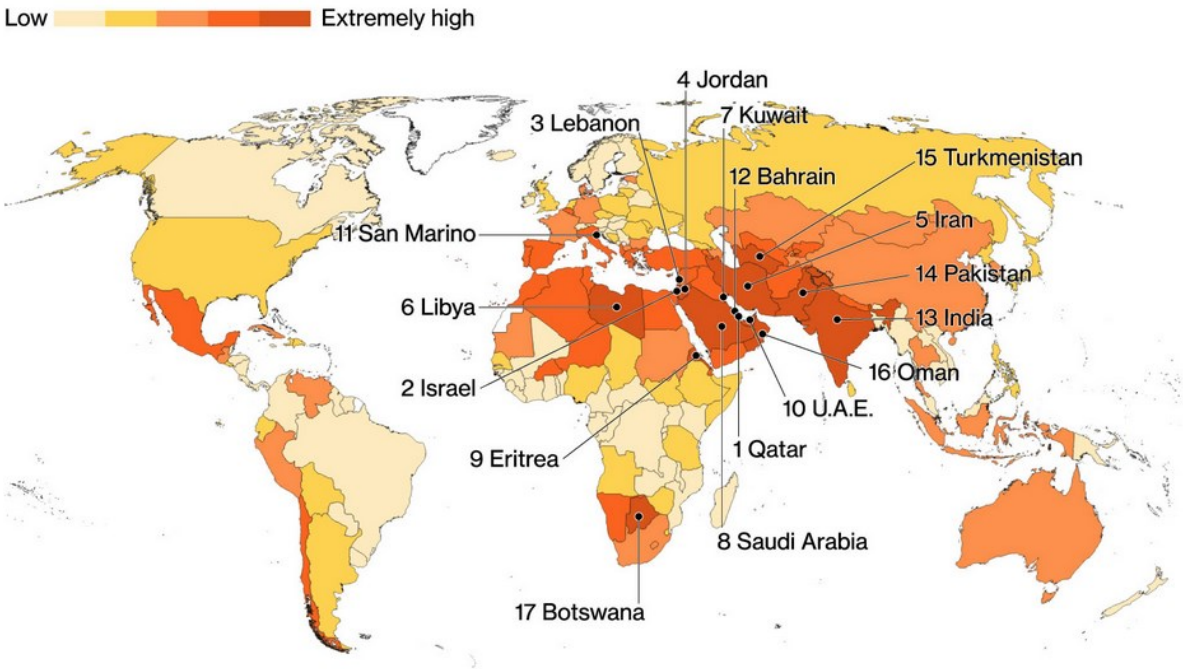


Figure 1.2 : Map of country most at risk of water scarcity. The highlighted 17 countries face the risk of extremely high water stress. (*Bloomberg.com* 2019 based on WRI's Aqueduct data)

As water scarcity increases, desalination plants are on the rise (FAO AQUASTAT). Seawater desalination is a process whereby salty seawater is transformed into freshwater. Plants are used to separate the salt and the water either by distillation or by reverse osmosis. Desalination plants therefore need to be built by the sea in order to be close to the seawater intake and brine outfall systems. Seawater desalination is nowadays a key water source in many arid countries to fill in the gap between water demand and water supply. Since 1980, desalinated water production keeps on increasing (*fig. 1.3*). Today, almost 16 000 desalination plants produce on average 100 million m^3 of desalinated water per day.

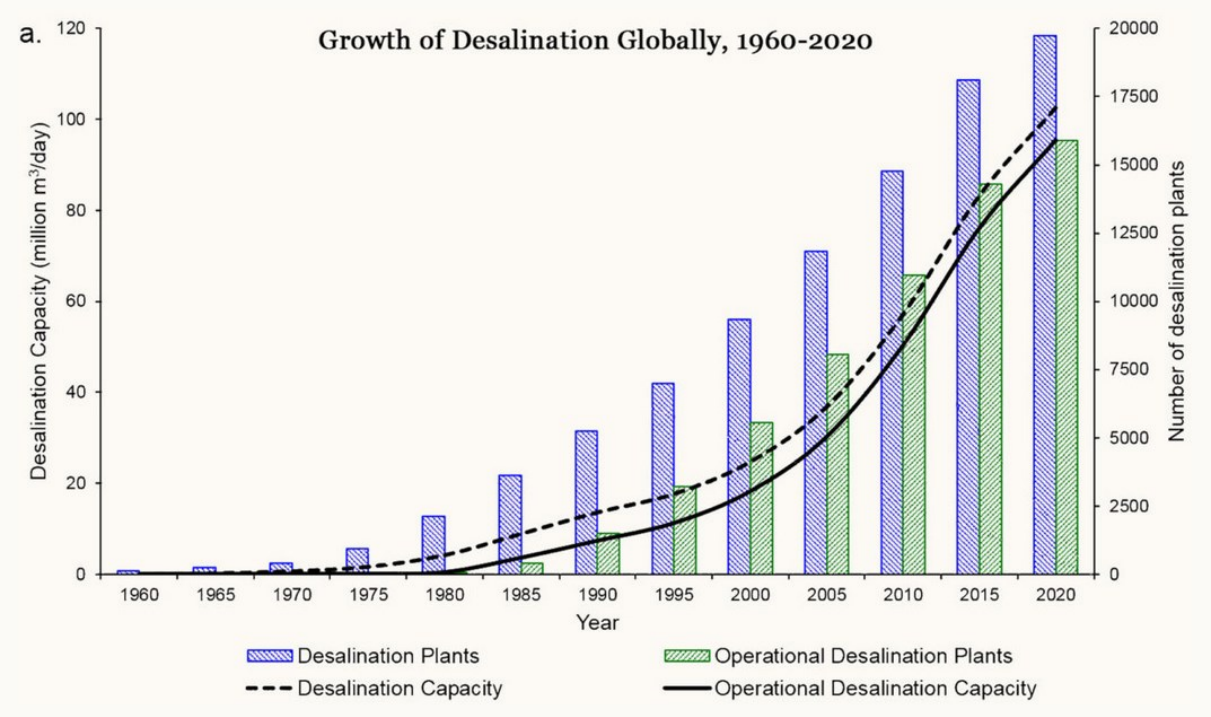


Figure 1.3 : Evolution of global desalinated water production and number of desalination plants (Jones et al. 2019)

The desalination capacity in the Middle East and North Africa represents almost half of the global desalination capacity (Jones et al. 2019). Most of the desalination capacity is located in the six Gulf Cooperation Council (GCC) states. This council is formed by six countries around the Arabian Gulf which are Bahrain, Kuwait, Oman, Qatar, Saudi Arabia and United Arab Emirates. In the GCC states, desalinated water produces 80% of the total drinking water (Mogielnicki 2020). In Bahrain, Kuwait, Qatar, and UAE, 50% of all the water used comes from desalination plants production (Dawouda and al. 2020).

However, seawater desalination does not come without risks as it relies on a steady intake of seawater. If that intake is disturbed, water production can be completely shut off. A number of countries therefore rely heavily on a small number of very exposed coastal desalination plants. They are facing several risks, including terrorist attacks, algal blooms and marine pollution. The latter is particularly acute in the Arabian Gulf because of the presence of many oil platforms and a very intense oil tanker traffic. The Arabian Gulf is thus very polluted and oil spills of different sizes and origins are always present. If such spills were to reach a desalination plants, the consequences could be major. As an example, the city of Sharjah (UAE, 20 km North of Dubai) was left without drinking water for one day after its desalination plant had to be shut off after being exposed to an oil spill from a grounded ship (Mogielnicki 2020).

According to WRI's national water stress rankings, Qatar is the country most at risk of water scarcity (*fig. 1.2*). Since 1987, it has therefore been relying extensively on seawater desalination. Its groundwater reserves are now threatened by over-extraction and seawater infiltration. The aquifer will be depleted in about 30 years if groundwater extraction continues at the current rate. Desalination is thus essential to fulfil the needs of the agricultural, industrial and municipal sectors (*fig. 1.4*). Today, desalinated water represents half of the general Qatari water supply. The remaining half Qatari water consumption is covered at 36% by groundwater and 14% by treated wastewater. In urban areas (such as in municipality of Doha), almost 100% of the water supplies comes from desalination (Hussein and Lambert 2020).

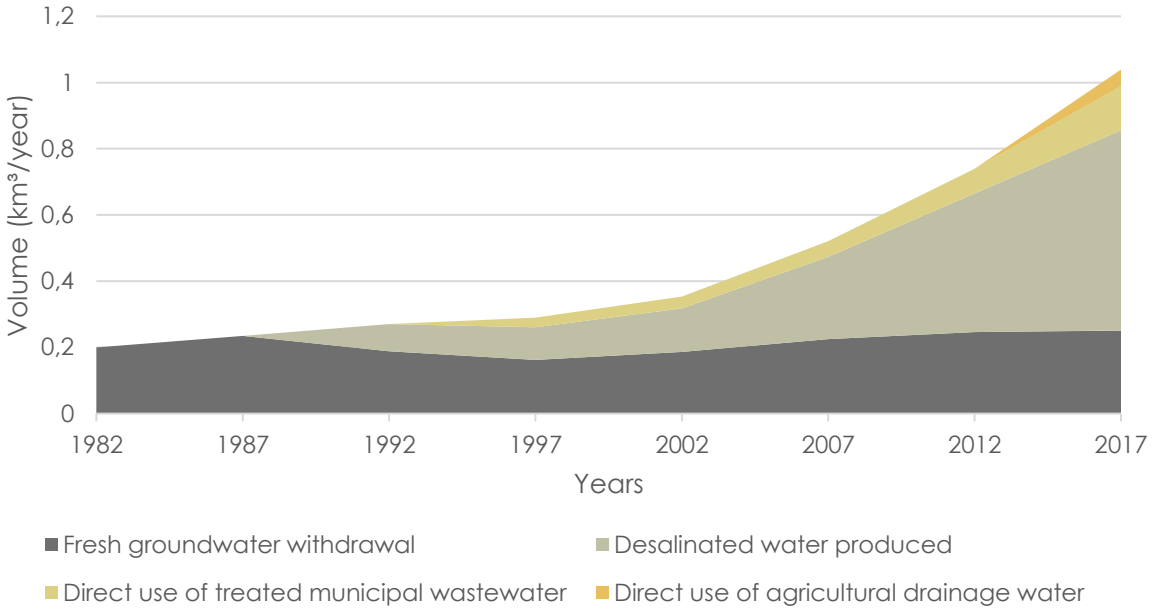


Figure 1.4 : Evolution of total water withdrawal in Qatar (based on data from FAO AQUASTAT 2020)

Such a reliance on desalinated water carries substantial risk. As a peninsula located in the center of the Arabian Gulf, Qatar is exposed to several geopolitical and environmental threats. Oil spill pollution is one of those and it could have dire consequences on Qatar society. If massive oil spills, such as those observed during the two Gulf wars, were to reach Qatar eastern coast, it would shut off the production of its three main desalination plants, which are just 100 km apart. With its current water reserves, that would leave the Qatari capital, Doha, with only 3 days of drinking water supply (Name 2015).

While massive oil spills are very rare, the Arabian Gulf continuously experiences oil pollution. There are three main type of oil pollutions: natural pollution, land-based pollution and sea-based pollution. Sea-based pollution is clearly the most dangerous for desalination plants. It is almost always related to accidental or intentional oil releases from offshore platforms, pipelines and ships (Zhang and al. 2019). Accidental releases can be due to vessel accidents, blowouts at offshore platforms, ship abandonment, pipeline leaks, terrorist attacks, and so on. Intentional releases are practiced by offshore platforms and all types of vessels to ensure their proper functioning. In the case of vessels, it usually involves the cleaning of tanks at sea to avoid the cost of performing that operation in a port. The statistics about oil sources are generally very wide from one source to another. Nevertheless, the figures are still very alarming regarding pollution from ships (*fig. 1.5*).

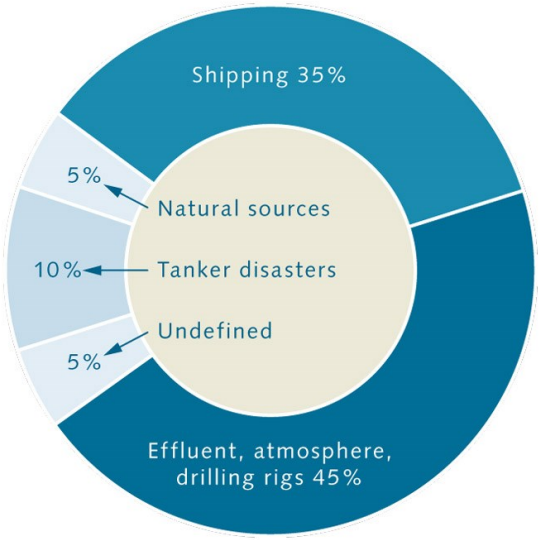


Figure 1.5 : Sources of oil pollution (World Ocean Review 2010)

The Arabian Gulf is one of the most oil-polluted environment in the World. It is a major passage for ships and especially oil tankers, with about 20-30 thousand tanker movements per year (ScanEx 2018). 25% of the world's oil supply passes through the Gulf each day (Ismail 2015). As mentioned before, ships are an important source of oil spills through their operational discharges namely tank washings, ballast water discharges and discharges of ship waste containing oil products but also through unintentional discharges following terrorist attacks or accidents. In addition, the Arabian Gulf counts not less than 34 oilfields exploited by 800 wells. On average 100 to 160 thousands tons of oil and oil products are released in Arabian Gulf every year (*fig. 1.6*). This level of oil pollution is 47 times larger than the World's average pollution level (ScanEx 2018).

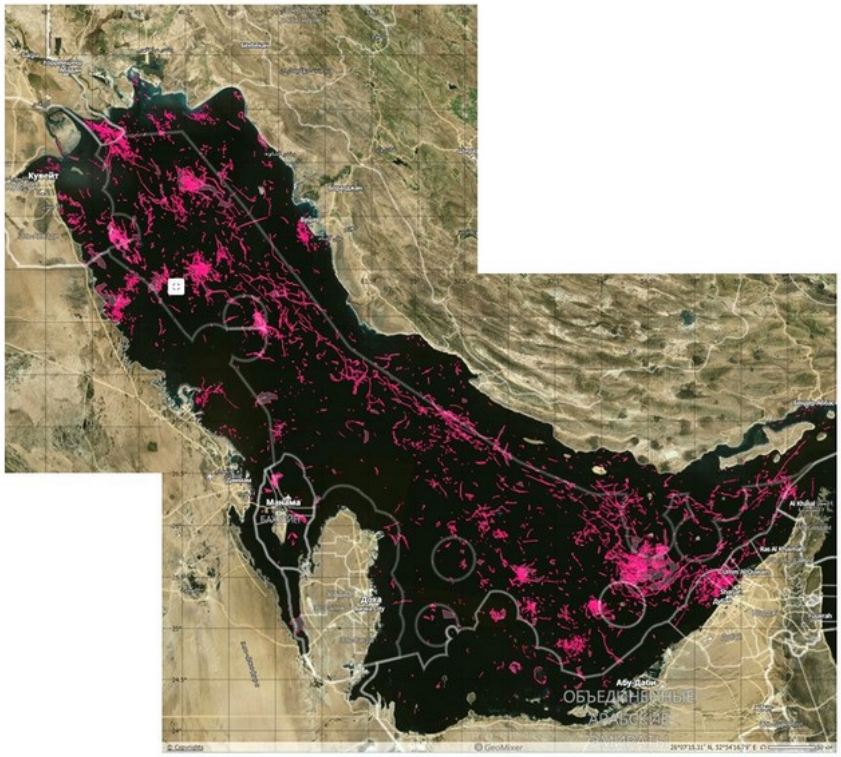


Figure 1.6 : Map of all oil spills detected (pink areas) in the Arabian Gulf in 2017. Information are provided by Sentinel-1A and Sentinel-1B SAR images. Gray line show boundaries of terrestrial waters. (ScanEx 2018)

Despite its wealth, Qatar carries a double burden. It is at the same time severely exposed to water scarcity and also to oil pollution. To efficiently manage its water supply, it therefore has to continuously monitor its coastal waters in order to detect as early as possible oil spills that could potential threaten its desalination plants. This requires both advanced early-detection monitoring capacities and also forecasting capacities to predict the evolution of an observed spill. The objective of this thesis is to contribute to the development of oil spills monitoring and forecasting capacities by assessing the vulnerability of Qatar desalination plants to oil spills originating both from shipping and from offshore oil and gas platforms. We will identify which offshore areas present the greatest risk to Qatar desalination plants if oil was released there. Our assessment will consider both diffuse oil sources related to shipping and localised sources related to oil platforms. We will consider the interannual variability of the ocean circulation through the Gulf over two consecutive years (2019 and 2020) in order to provide robust overview of the space-time evolution of oil spill risk and the resulting vulnerability.

2 Material and Methods

2.1 Area of interest

a. Qatar and the Arabian Gulf

Qatar is a small peninsular country on the eastern coast of the Arabian Gulf. The capital Doha is situated in middle of the eastern coast. The peninsula is about 160 km long and 80 km wide. The land area amounts to about 11 610 km^2, which is just a bit more than a third of Belgium's area. Over land, Qatar has just one border, with Saudi Arabia in the North (CIA 2021). Qatar's population in 2021 reached 2.9 million (Worldometer 2021; WorldPopulationReview 2021). Almost 90% of the population are non-Qatari. These consist mostly of expatriates from India, Iran and Pakistan, which have been attracted by the economic growth of the country (Britannica 2021). Qatar is well-known for its prosperity that relies on its oil and gas reserves. As the other countries of Arabian Gulf, Qatar possesses a large amount of oil reserves. Most importantly, Qatar is a major producer of natural gas. Its North field is one of the largest offshore gas field in the World (Britannica 2021). Qatar's climate is arid with extremely high temperatures and low precipitations of only 75 mm per year (Rahman and Zaidi 2018). Hence, Qatar is considered like a desert and 96% of its population lives in urban areas.



Figure 2.1 : Political map of the Arabian Gulf (nationsonline 2018)

On a larger scale, Qatar is located in the Persian Gulf, also known as the Arabian Gulf, and often simply called "the Gulf" (*fig. 2.1*). It covers an area of 250,000 km^2. The Gulf extends between 24°N and 30°N latitude and 48°E and 57°E longitude. It is about 1000 km long and between 200 and 300 km wide (Vaughan and al. 2019). It is surrounded by deserts, which makes drinking water particularly scarce for the populations living on its shores. The Gulf itself has a low water supply. Indeed, the sea water comes mainly from the Arabian Sea through the Strait of Hormuz. The main influx of freshwater comes from Iraq, Iran and Kuwait through the Tigris, Euphrates, Karun and Mand rivers. The evaporation rates are very high and not compensated by the fluvial contributions and the precipitations, which are negligible. This leads to a net loss of water within the Gulf and hence a high salinity. The actual evaporation rate estimated is 2m/year (Reynolds 1993; Kaempf and Sadrinasab 2006). While precipitation accounts for 0.07 m/year and riverine inputs are of the order of 0.45 m/year (Reynolds 1993; Johns et al. 2003). As result, the water in the Gulf has a salinity of about 40 grams of salt per kg of seawater (40 PSU), a value much higher than open ocean conditions. The seawater temperatures strongly fluctuate through the seasons. Temperatures can go down around 20°C in winter but can rise to 35°C in the summer (Vaughan and al. 2019). The overall water depths in the Gulf are shallow, with a maximum depth of 90 m and average depth of around 35 m. The bottom is constituted by harder areas of rock or salt and allows the hosting of rare ecosystems such as coral reefs, seaweed beds, seagrass meadows, mangrove forests, mud and sand flats (Vaughan and al. 2019).

b. Desalination plants in Qatar

As mentioned before, Qatar is facing major water stresses. It is ranked first among countries most exposed to water stress (WRI 2019). There is no permanent river and groundwater is already partly depleted and only useful for a minority of farmers. To overcome this issue, the country has been very proactive in building desalination plants (*table 2.1*). Desalination now covers 50% of all the water consumed in Qatar for both domestic and industrial use. There are 3 main types of desalination plants in Qatar. The oldest one is based on Multiple Effect Distillation (MED). MED uses the principle of distillation and applies it in series to reduce energy consumption. The Multi Stage Flash Distillation (MSF) is also based on distillation but this time energy is reintroduced in the next stage by countercurrent heat exchangers. The last process is Reverse Osmosis (RO). This process is more and more recommended due to its low energy consumption. RO is based on physical process that let water with a high salt concentration move towards a zone with lower salt concentration. This movement takes places over a semi permeable membrane to allow the flow of water and gradually reduce the salt concentration (SSWM 2009).

Plant	Capacity (MIGD)	Technology	Commissioning year
Ras Abu Fantas	55	MSF	(1997-1983) (1994)
Ras Abu Fantas b	33	MSF	1977-1998
Ras Laffana	40	MSF	2003-2004
Ras Laffan-b Qatar power	60	MSF	2006-2008
Abu Samra	0.2	RO	1982
Qaeedat al Shamal	0.2	MSF	1993
Ras Abu Fantas A1	45	MSF	2010
Ras Abu Fantas B2	30	MSF	2008
Ras Qertas	63	MED	2010-2011
Dukan	2	MED	1997
Ras Abu Fantas A3	36	RO	2016
Umm al houl	60 76	RO MSF	2016-2017
Total	500		

Table 2.1 : Desalination plants of Qatar. 1 MIGD = 4.546 million litres per day (Rahman and Zaidi 2018; Qatar Electricity & Water 2021)

We have selected three largest plants in Qatar to perform our risk assessment and all three are located on the east side. The three stations are respectively located in Ras Laffan, Ras Abu Fontas and Umm al Houl (*fig. 2.2*).

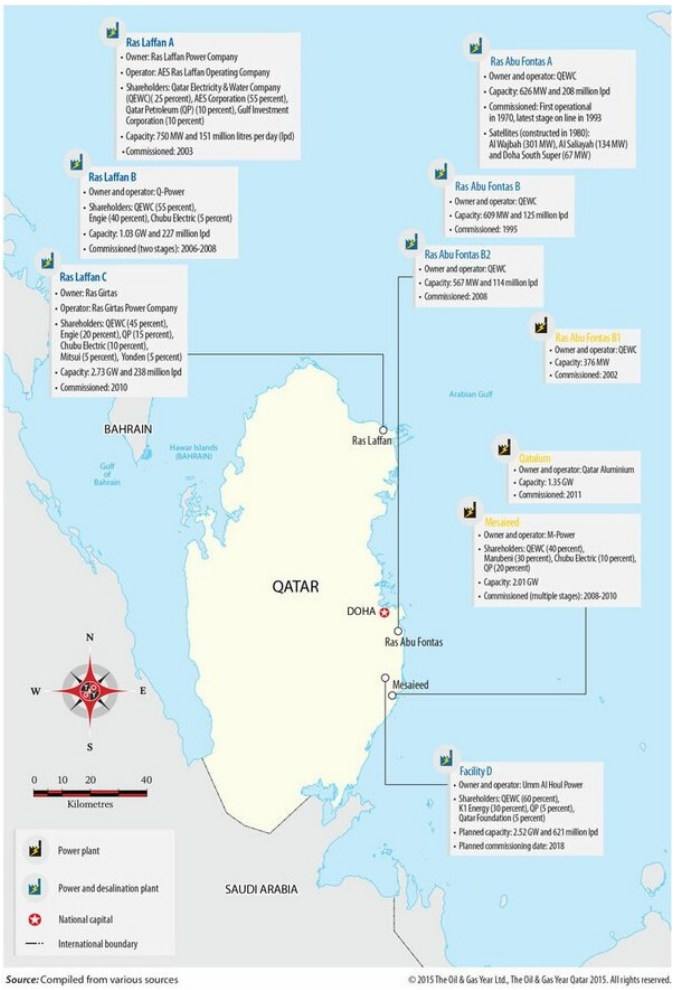


Figure 2.2 : Qatar's power and desalination plants (The Oil & Gas Year Qatar 2015)

c. Shipping routes and oil platforms in the Arabian Gulf

To assess the oil risk involved by the desalination plants, a good knowledge of dangerous areas of the Gulf is important. These areas can be risky because of a high shipping rate or the presence of offshore platforms. As mentioned before, the Arabian Gulf is a major shipping lane especially for tankers and 25% of the world's oil supply passes through the Gulf each day (Ismail 2015). The shipping density data is based on tracking information retrieved from the automatic identification system (AIS) that has to be fitted on all ships with more than 300 gross tonnage and all passenger ships (Halpern et al. 2015) (*fig. 2.3*). The data has been collected throughout 2013. The shipping could of course have changed from 2013 to 2019. Here we make the assumption that the overall shipping patterns remain the same. Changes in amplitude won't have any impact on our results as the shipping density will subsequently be normalized.

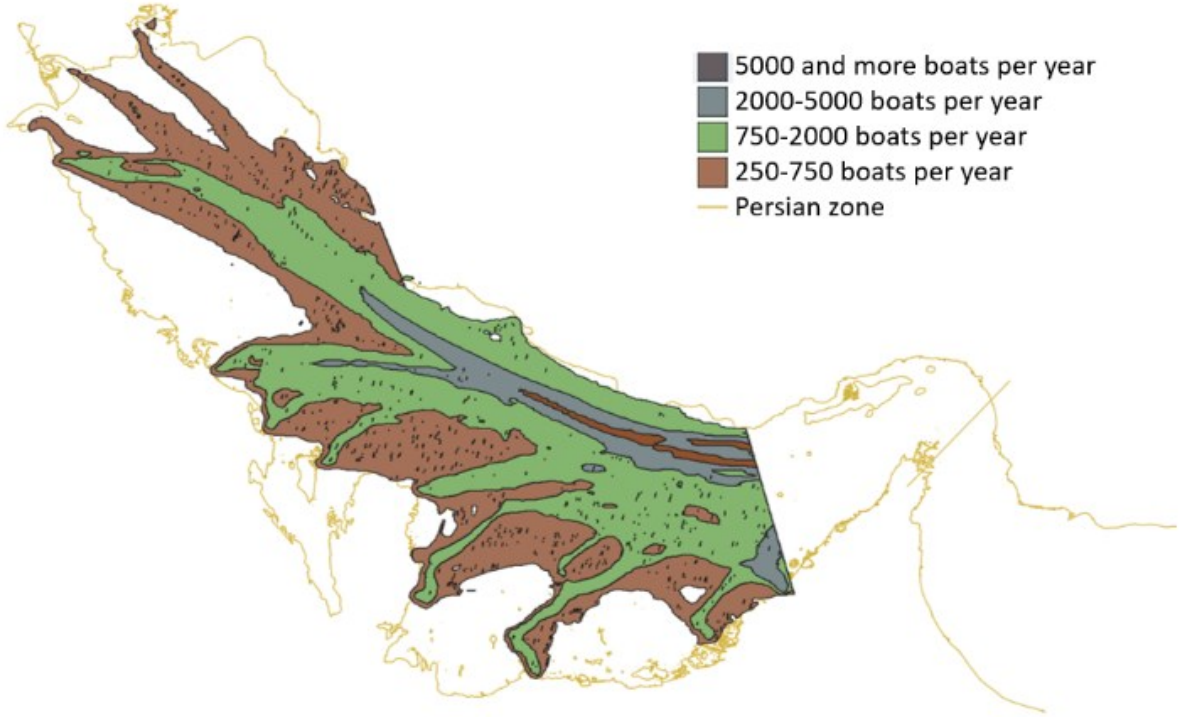


Figure 2.3 : Shipping density ranges map in the Arabian Gulf in 2013 (Halpern et al. 2015)

Offshore platforms are another potential source of pollution. The Arabian Gulf is home to about 800 offshore oil and gas platforms including some of the largest in the world (Albano et al. 2016). Here we selected only the largest oil and gas fields, which can include several platforms, and only those that were sufficiently close to Qatar to threaten its coastline (Le Grand Atlas De Boeck 2014; CIA 2007). We tried to take points within the oil fields representing the drilling wells. These wells were chosen for their large oil reserves and for their high geographical variability between them in order to assess the risk from different locations in the Arabian Gulf (*fig. 2.4*).

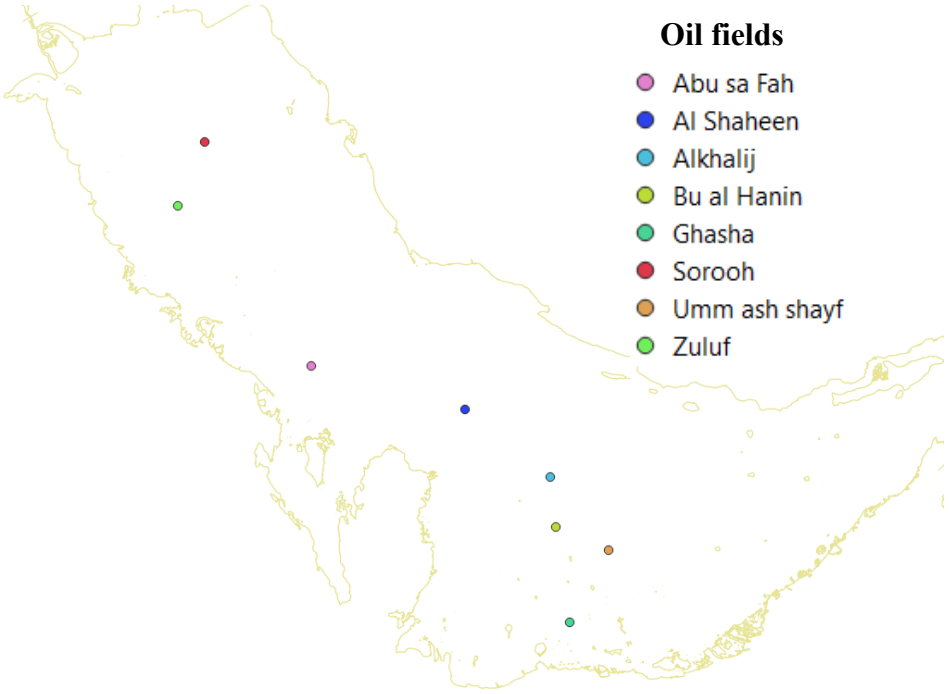


Figure 2.4 : Location of the oil and gas fields considered in this study

2.2 Ocean circulation in the Gulf

a. General circulation patterns and their seasonal variability

The circulation in the entire of the Arabian Gulf change through the seasons (Vaughan and al. 2019). Beside the tides, there are 2 major processes regulating the circulation in the Gulf. The first one are the forces related to the density gradients generated by a high evaporation rate (Reynolds 1993; Kaempf and Sadrinasab 2006). The second is the wind, which plays a major role, especially the dominant northwest shamal winds. During the warm months, the increase of temperature and the decrease of wind intensity lead to a cyclonic currents extended all over the Gulf. The surface waters enter in the Gulf through the Strait of Hormuz and then flow along the coast of Iran. It then turns around near Saudi Arabia and moves along the western side of the Gulf before exiting the Gulf through the Strait (*fig. 2.5*). In autumn, the water temperature decrease and the shamal winds increase inducing an instable circulation. This produces persistent meso-scale eddies in the center of the Gulf. In spring, the circulation becomes again directional and cyclonic due to the increase of temperature.

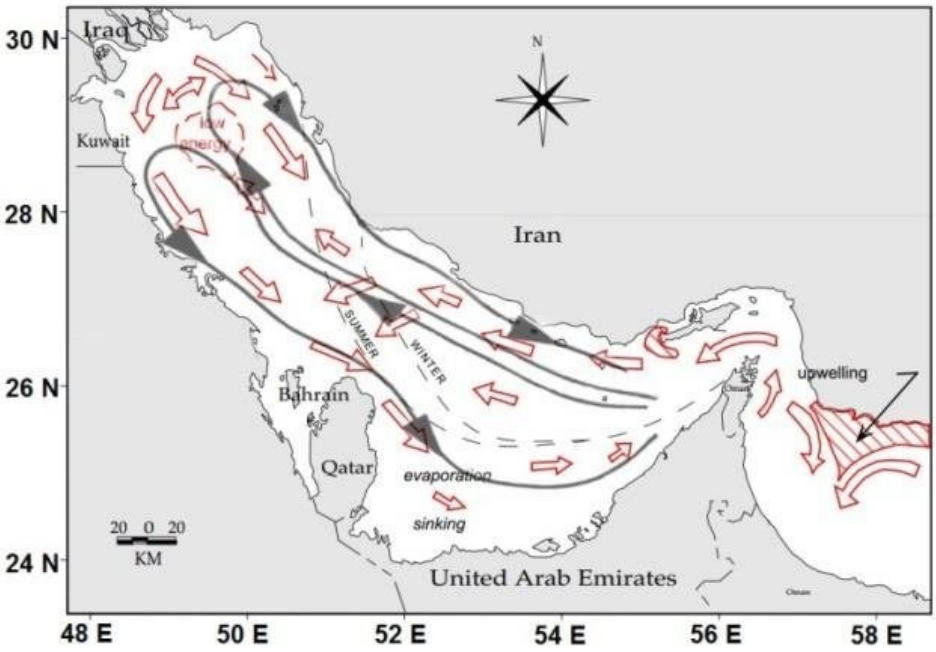


Figure 2.5 : Diagram of the water circulation in the Arabian Gulf during warm months (Pakhirehzan and al. 2018)

b. Hydrodynamic model (NEMO)

We model the regional circulation the Gulf by using the global ocean circulation model NEMO[1]. The physical ocean component of NEMO solves the 3D ocean circulation primitive equations for the velocity field, sea surface elevation, temperature and salinity. It uses a global curvilinear orthogonal grid in the horizontal direction and a mixture of *z* and *s* coordinates in the vertical. NEMO is well suited to regional and global ocean circulation problems down to kilometric scale.

NEMO model outputs are distributed by Mercator Ocean, the French center for analysis and forecasting of the global ocean. Mercator Ocean operates global forecasting systems and produces global and regional reanalysis, all based on NEMO ocean model, coupled to a data assimilation system. For this project, we used the outputs of the global forecasting system, which are available on the Copernicus web interface. They include hourly mean surface fields for sea level height, temperature and currents. The global ocean output files are displayed with a 1/12º horizontal resolution and 50 vertical levels ranging from 0 to 5500 meters.

[1] NEMO: Nucleus for European Modelling of the Ocean (http://www.nemo-ocean.eu)

2.3 Oil spill modelling

a. Chemical and physical processes driving oil spills dispersal

After being released in the water, an oil slick will continuously evolve. There are many different types of oil according to their density and viscosity. These properties will influence the behaviour of the oil in sea. Oil density is usually expressed in API degree (CESBC 2016). The high API degree is associated to a low oil density which results in a higher evaporation rate. Viscosity influences the thickness of the slick and hence its movements and its weathering. The oil environment will also impact its fate. For instance, the sea surface temperature will influence the oil evaporation rate. The waves, currents and winds will also drive the slick dispersal and weathering.

Oil undergoes many weathering processes all along its drift (Daniel 2012; Lee et al. 2016). First, when an oil spill occurs, it tends to spread in every directions. The area of spreading depends on the oil viscosity. The more an oil slick spreads, the more it has an negative impact on the environment. The oil slick will move according to the currents and, if it is at the sea surface, it will also be influenced by wind and waves. Oil is also able to move vertically within the water column (Röhrs et al. 2018). This vertical movement depends on the oil density, which changes through time due to weathering processes, and also on breaking waves, which are generally often correlated to the wind. This process is called submergence and can be reversed by oil droplets resurfacing.

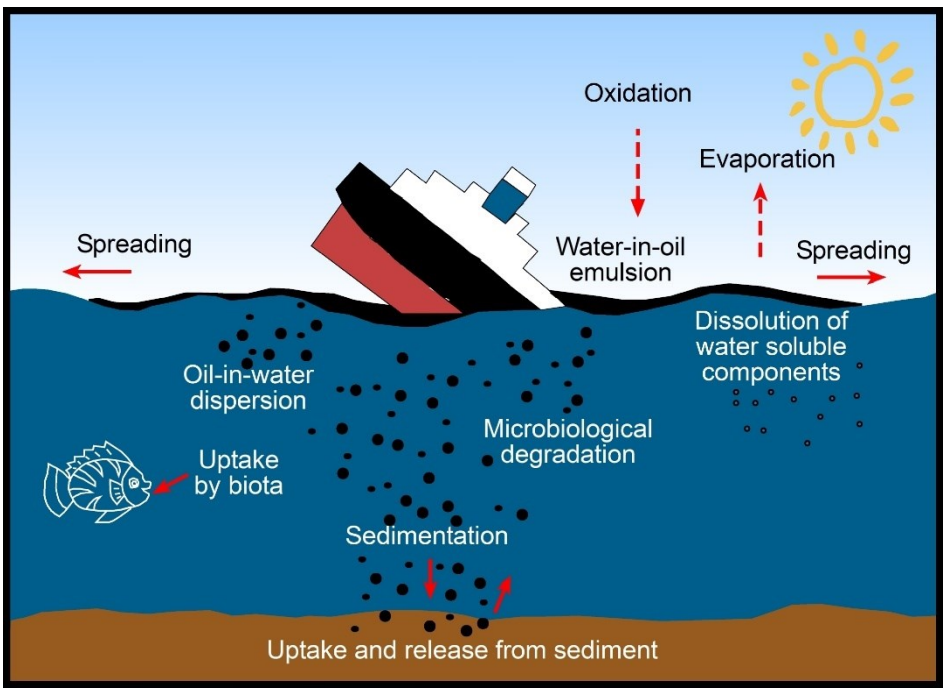


Figure 2.6 : Diagram of the behaviour and weathering processes of oil in water (Seos Project 2014)

From a degradation point of view, the oil slick first undergoes evaporation. This change of state occurs during the first few hours and strongly modifies the oil slick properties. Evaporation is generally more important if the oil density is low and if the water temperature is high. The fraction of oil that can be evaporated usually vanishes within a day (Reed et al. 1999). The dissolution involves the same oil fraction that can evaporate (Mishra and Kumar 2015). Since evaporation occurs quickly, dissolution is a minor process. However, oil dissolved in water increases the water toxicity. Breaking waves can carry seawater into the oil slick (Tarr et al. 2016; Zhang et al. 2019). Water droplets are then incorporated into the oil slick and increase the density and viscosity of the slick. This process is called emulsification. It is considered to be a protection of the oil by the water, which cannot undergo further weathering processes. Breaking waves can also break oil droplets into smaller particles (Zhang et al. 2019). This dispersion process facilitates the removal of oil by increasing the total surface area of particles in a slick. The application of dispersants aims to promote this phenomenon. The photodegradation affects the composition of the oil. The solar radiation oxidize the oil and change its chemistry (Tarr et al. 2016; Zhang et al. 2019). The oxygenated products are more soluble in water and more persistent than the original oil. This alteration is not yet well understood but it could increase the oil toxicity. Next, biodegradation is the only biological process and it is an important way to decrease the oil mass (Zhang et al. 2019). Microorganisms will break down the molecules that make up the oil. Biodegradation can take place on the surface or within the water column. This process is accelerated at higher temperatures or if the oil contains more biodegradable compounds. As mentioned before, the oil density will change because of evaporation and emulsification. These processes can lead to oil sinking if its density exceed than that of water. Oil and its residues have the ability to interact with sediments in the water column (Tarr et al. 2016; Zhang et al. 2019). A sinking oil particle can sometimes bind with detritus, minerals and so on. And in turn, these aggregates can sink and settle on the seabed. This process is called sedimentation and can be a major player in the removal of an oil slick. Unfortunately, it remains poorly documented and difficult to predict.

Oil weathering include all the processes modifying the physical or chemical properties of the oil spill. However, from the desalination plants point of view, we need to make distinction between alteration processes and removal processes. Alteration processes change the composition or physical status of the oil but without completely removing the hazard due to the oil. On the other hand, removal processes reduce the oil concentration and hence also reduce the associated hazard. This segmentation only valid for desalination plants are based on the current understanding of the processes (*table 2.2*).

Removal	Alteration
Evaporation	Dispersion
Biodegradation	Dissolution
Sedimentation	Emulsification
	Photooxidation
	(Submergence)

Table 2.2 : Summary of the main oil weathering processing and distinction between those that reduce the oil concentration (removal) and those that simply change the oil composition (alteration).

b. Oil dispersal model (OpenOil)

In order to simulate oil drift dispersal, we will use an open-source oil transport model called OpenDrift (Dagestad et al. 2018). The source code is in Python and was developed mainly by the Norwegian Meteorological Institute. It is a Lagrangian trajectory model that represents the drift of particles within a fluid. Opendrift can handle different types of particles such as microplastics, planktons, oil, pelagic eggs and so on. Each type of particle has a specific OpenDrift subclass. Here, we will use the OpenOil subclass to simulate the evolution of an oil spill. OpenOil has been thoroughly parameterized and validated, and is operationally used by the Norwegian Meteorological Institute. The oil particles are considered as Lagrangian elements representing a certain volume of oil (Röhrs et al. 2018; Dagestad et al. 2018).

From a physical point of view, each oil element is driven horizontally by three main processes. First, each element drifts with the ocean currents, whether it is at the surface or submerged. Secondly, the elements are also driven by surface wave propagation, through the so-called Stokes drift, which decreases with depth (Breivik and al. 2016). Thirdly, the elements at the surface are also moved by the direct action of the wind with a velocity equal to 2% of the wind velocity. Since the surface Stokes drift velocity is usually parametrized as 1.5% of the wind velocity, we end up at the surface with an additional component equal to 3.5% of the wind velocity that is added to current velocity (Ardhuin et al. 2009; C. E. Jones et al. 2016). Since the Stokes drift and the current velocity change with depth, it is therefore important to know how the vertical position of the oil elements will change. Firstly, oil elements on the surface are likely to be entrained by breaking waves into the ocean. The emergence of this phenomenon is calculated as a probability in function of time (C. E. Jones et al. 2016). In addition to breaking waves, the buoyancy of oil elements will determine its vertical dynamics. It depends on oil viscosity, oil density, seawater temperature, salinity and on the oil droplet size distribution (Tkalich and Chan 2002). Finally, within the water column, the oil elements are subject to vertical turbulence. All these physical processes concerning the particles are expressed and

parametrized based on the literature (Dagestad et al. 2018; Röhrs et al. 2018; C. E. Jones et al. 2016). A diagram summarizing the different steps performed by OpenOil is shown in *fig. 2.7*.

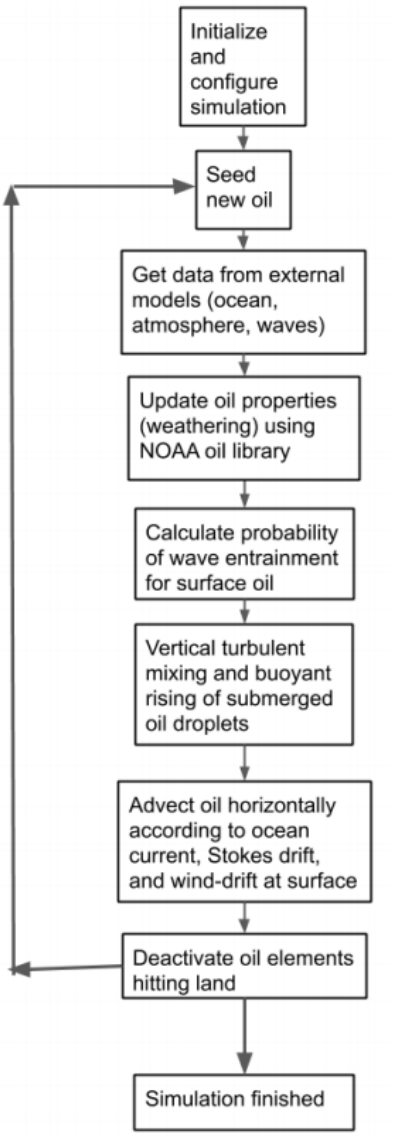


Figure 2.7 : Diagram of the physical steps of an Opendrift simulation

OpenOil also takes the oil weathering into account in order to correctly represent the degradation of the oil spill. Since that degradation is very sensitive to the type of oil, OpenOil uses a very detailed oil library developed by the National Ocean and Atmospheric Administration (NOAA) (Androulidakis et al. 2020; Dagestad et al. 2018). The different oil types are listed and can be use in OpenOil model. This NOAA library allows OpenOil to know the properties of a large number of oil types. In this study, we will consider 'QATAR MARINE' oil with an initial density and viscosity of 850.296 kg/m^3 and 9.277 x 10^{-6} mPa.s, respectively. Droplet size and entrainment rate were set to default values (Dagestad et al. 2018). In addition, the seawater temperature and salinity are respectively set by default to 30 degrees and 40 PSU.

The evolution of several oil properties as well as the different fraction of oil that have been weathered can be followed throughout the simulation (*fig. 2.8*). The sharp decrease of the oil fraction at the surface during the first few hours is due to evaporation. Lighter oil quickly evaporates in contact with warm water, hence increasing the remaining oil density (Zhang et al. 2019; Tarr et al. 2016). In our case, we are working with medium density oil that loses more or less 50% of its mass during the first hours of the oil spill.

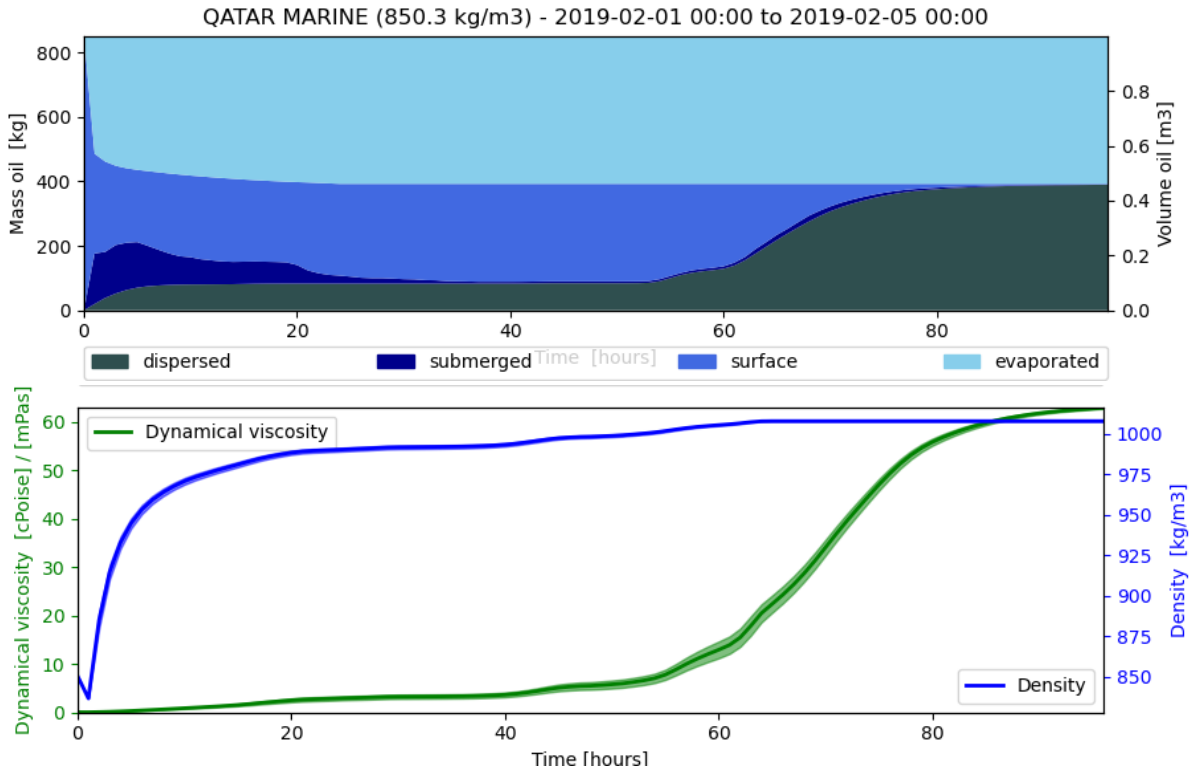


Figure 2.8 : (**a**) Evolution of oil weathering as simulated by OpenOil for QATAR MARINE oil and (**b**) evolution of oil viscosity and density. The simulation was carried out in the middle of the Gulf with an initial oil mass of 850.3 kg and lasted 4 days.

There are 2 ways to simulate the evolution of an oil spill with OpenOil: forward and backward in time. With the forward method, we start with an initial oil elements distribution and simulate its future evolution. We can hence find out where it will go. At the end of the simulation, we can evaluate what fraction of the initial oil reached the desalination plant. This method allows us to explicitly take into account oil weathering processes. However, the probability that a particle released from a specific location in the Gulf will reach a desalination plant on the coast is very low. A very large number of particles would thus be required to evaluate such low probability, which would not be very efficient. This is the reason why we will also perform backward simulations. In this case, we release oil elements at the desalination plan and simulate their transport backward in time. We can hence find out where the particle came from and what trajectory it followed on its way to the desalination plant. That allow us to identify the area from which oil particles would be transported to the station and also estimate the time it would take to reach the station. The backward approach is thus more efficient than

the forward approach to identify the offshore area that presents the largest risk to the desalination plant. However, when going backward in time, weathering processes cannot be taken into account and the mass of each oil particle thus remains constant.

Both methods are used in this study but the duration of both types of simulations will be different. Since weathering is not taken into account when doing a backward simulation, we have to be careful not to run a simulation that unrealistically long and which would hence overestimate the extent of the risk area. We have therefore chosen to run backward simulations during only 5 days. After that duration, most of the oil in the spill will have been weathered. This can be seen in *fig. 2.8a* where almost no oil is left at surface after 75 hours of drift and only the dispersed or submerged oil fractions remain. These are less of a threat to the station. With the forward simulations, weathering is explicitly taken into account and the mass of the oil elements hence decays over time. We will therefore run longer simulations of 10 days in order to capture the tail of the risk distribution corresponding to rare long-distance events. Finally, since oil degradation rate depends on water temperature, we will take into account the average monthly sea surface temperature (SAS 2020).

c. Input data

First, we need to define the release locations of the oil elements. These areas depend on the method used. With the backward method, the elements will start from the stations, which will be represented by a circular risk area with a radius of 2 km (*fig. 2.9* and *table 2.3*) (Ciappa and Costabile 2014). Oil particle will be released from the border of this risk area. Oil particles are released every day at midnight throughout the year and their final positions are aggregated for each month of the year. The forward method is employed to evaluate the risk related by an offshore platforms. In this case, we therefore released oil elements from each oil field (*fig. 2.4*).

Location	**Capacity (m^3/day)**	**Coordinates (decimal degrees – WGS84)**		**Risk zone radius (decimal degrees)**	**Number of receptor points (width = 0.0001 decimal degrees)**
		Lon	**Lat**		
Ras Laffan	454 690	51.5500	25.9464	0.01	21
Ras Abu Fontas	904 830	51.6269	25.2061	0.01	18
Umm al Houl	618 380	51.6295	25.0643	0.01	20

Table 2.3 : Description of desalination plants along the Qatari coast selected for oil spill assessment

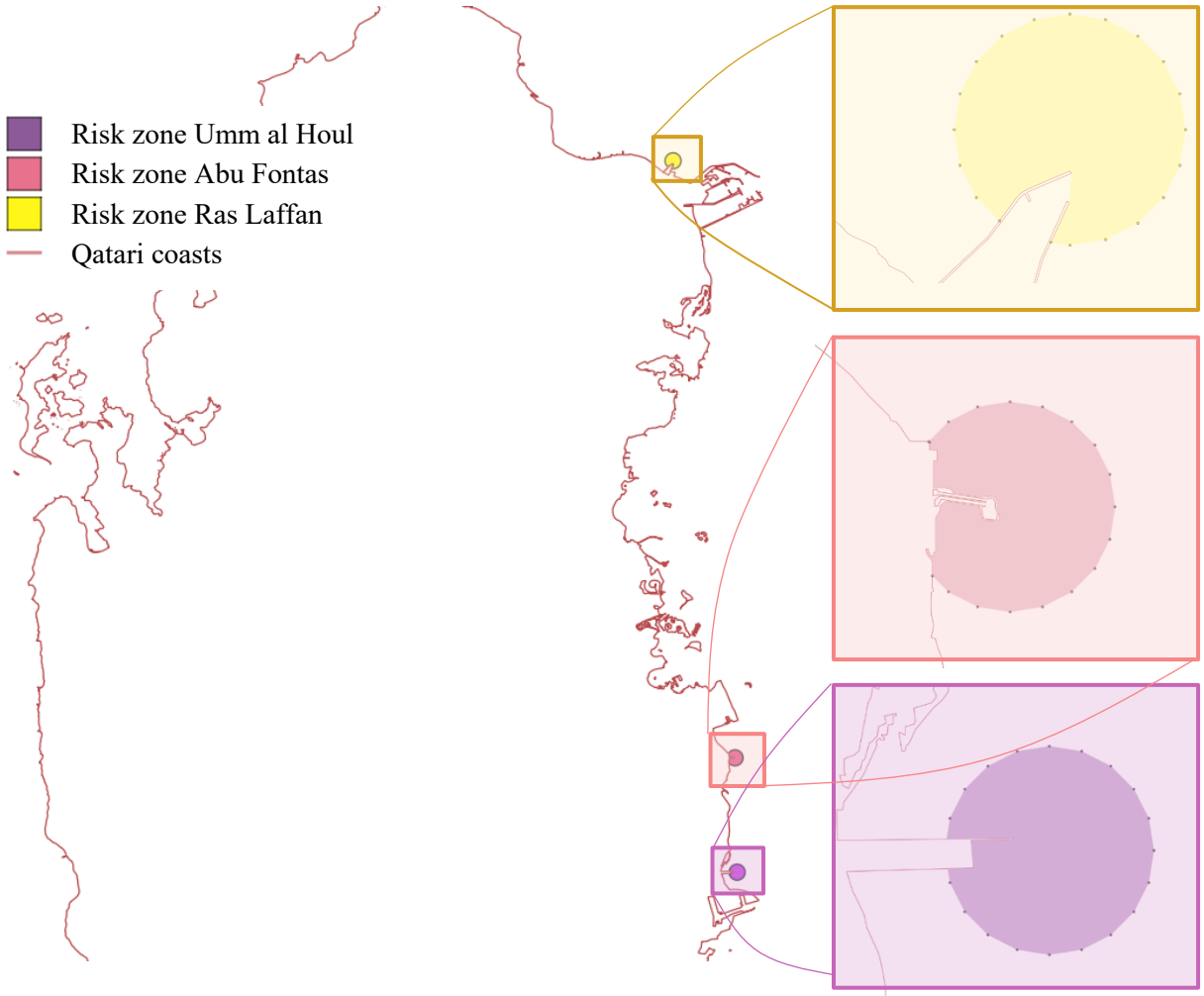


Figure 2.9 : Risk zones and receptor points associated to each stations in Qatar

Finally, OpenOil needs forcing data to drift the oil slick all along simulations. These data are the wind, currents, and waves which have a significant impact on the movement of oil elements. This data must be in NetCDF format in order to be readable by OpenOil. All information regarding forcing data can be found in *table 2.4*.

Source	**Parameters**	**Year used**	**Resolution :**		
			Temporal	**Horizontal**	**Vertical**
ERA5 model of ECMWF (ERA5)	Wind	2019, 2020	Hourly	0.25°	Surface
CMEMS (CMEMS)	Wave	2019, 2020	3h	1/10°	50 layers
CMEMS (CMEMS)	Current	2019, 2020	Daily	1/12°	50 layers

Table 2.4 : Summary of data used for the simulations and the maps creation

2.4 Vulnerability indicators

In OpenOil, when we simulate an oil spill, each oil particle is tracked. We give in input the total drifting time, the timestep, the location of release, the forcing data, etc. During a timestep, an oil particle moves according to the forcing data (wind and oceanic current). At the end of a timestep, the location of the particle as well as the fraction of oil as well as the fraction of oil lost through each of the weathering processes is stored. Then, the model recalculates the forcing data for the new location of the oil particle and this particle drifts again during the next timestep. This simulation pattern is repeated until it reaches the total drifting time (provided in input). The data collected at the end of each timestep of the simulation are the building blocks to create all the risk and vulnerability indicators presented in this section.

a. Vulnerability to oil spills from shipping

As mentioned before, the connection between an area in the Gulf and a very specific location on a coast is a low-probability event. In our case, the number of oil particles released is too small to be able to assess the risk of an oil spill using a simple forward method. We therefore adopted the opposite approach by using the target-to-source path. For this purpose, we have used backward simulations. The principle is to start with oil elements at the target location (i.e. the desalination plant), and then go back in time to understand where the oil elements threatening the plant came from. Starting from the station, we will be able to identify the trajectories of the elements as they move backward in time and hence identify the offshore that presents a risk to the station (*fig. 2.10*). It is important to note that an oil particle is evaluated all along its drift. The final location of the oil is not the only dangerous area. Oil released along the backward trajectories is also a threat for the desalination plant. In order to take this information into account, we keep track of all the successive positions of each oil element as it moves backward in time.

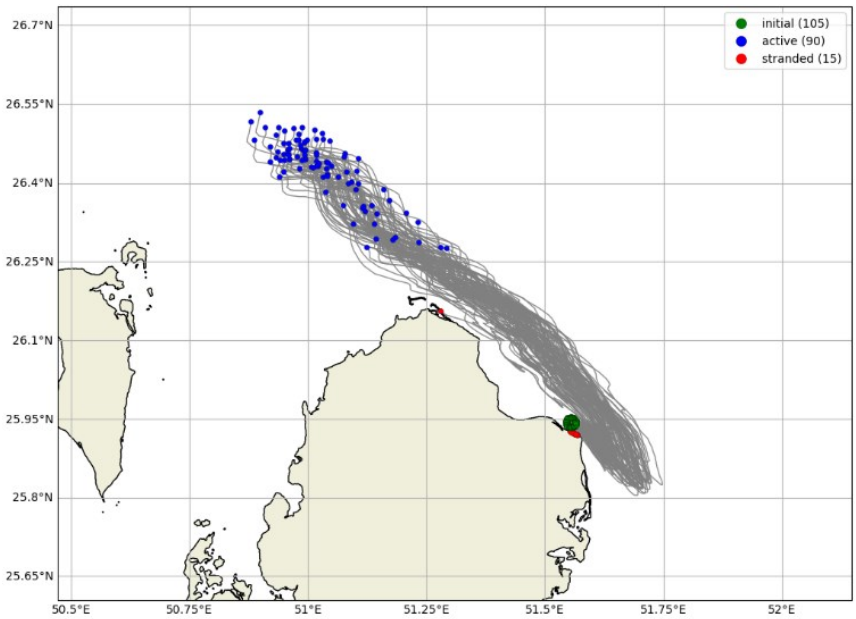


Figure 2.10 : Example of a 5 days backward simulation starting from a receptor points at Ras Laffan desalination plant. The green points are the initial positions of the particles at the beginning of the backward simulation, the blue points are the places where the oil particles were 5 days before reaching the station and the red points are elements that come from the shore (and hence not considered here). In addition, the gray trajectories highlight where the oil elements were as they moved backward in time from the station. Any oil elements released along these trajectories also represent a risk to the station.

From these backward simulations, we will create three different types of maps. By combining all the simulation results obtained at each day of a given month, we obtain maps that include all the variability present in the different forcing throughout the month.

First, we create arrival time maps, which indicate the time it would take for an oil spill to reach a desalination plant. We assess all oil particles of each timestep (*fig. 2.10*) and we distinguish them according to the time they have already been drifting : < 1 day, between 1 and 2 days, between 2 and 3 days, between 3 and 4 days and between 4 and 5 days. We are in backward hence, if we reverse to a forward simulation, these drifting times will indicate the time it will take for the element to reach the plant. These drifting ranges are stored and the same process is performed every days of the month. By combining all the ranges of the same arrival time during the month, we obtain a single plume of arrival time. The last step is to display them in order of risk. The map represents a minimum arrival time for a month-station combination (*fig. 2.11*).

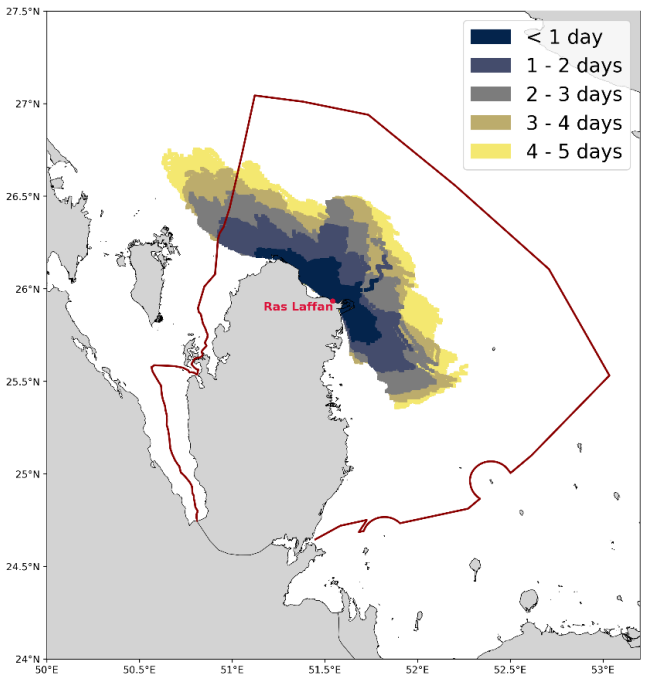


Figure 2.11 : Example of a minimum arrival time map for Ras Laffan in March 2019. The dark red line shows the limits of Qatar exclusive economic zone (EEZ).

The second indicators estimates the spatial distribution of the oil spill risk for a given desalination plant. To construct that indicator, we first build a grid that covers the entire Gulf with pixels of 0.02×0.02 decimal degree. As with the previous indicator, we look at the position of all the oil elements at every timestep of the backward simulation (*fig. 2.10*) and count the number of elements in each pixel of the grid. This count over the entire grid allows us to identify which pixels are the most hazardous according to the number of elements reported in that pixel for a backward simulation. We perform the same process on the same grid for every backward simulation of a month. At the end, we obtain a distribution that highlights where oil elements were the most likely to be during their 5-days backward motion. The distribution is subsequently normalized to make it independent of the drift time, the number of timestep, the number of oil element released and pixel area (*Eq. 2.1*). It is important to note that the integral of this probability density is smaller than 1 as we discard all particles that end up being stranded during their backward motion. Those particles would correspond to oil spills released from the land, which are not considered her. Nevertheless, the integral of this oil spill risk distribution function is a global measure of offshore oil spill risk (*Eq. 2.2*). These risk distribution functions are computed for every month and every desalination plant (*fig 2.10*).

Equation 3.1 : Probability density

$$\frac{\dfrac{\text{Number of particles per pixel}}{\text{Total number of particles released}} * \dfrac{\text{Timestep}}{\text{Total drift time}}}{\text{Pixel area}}$$

Equation 3.2 : Total risk

$$\sum(Probability\ density * Pixel\ area)$$

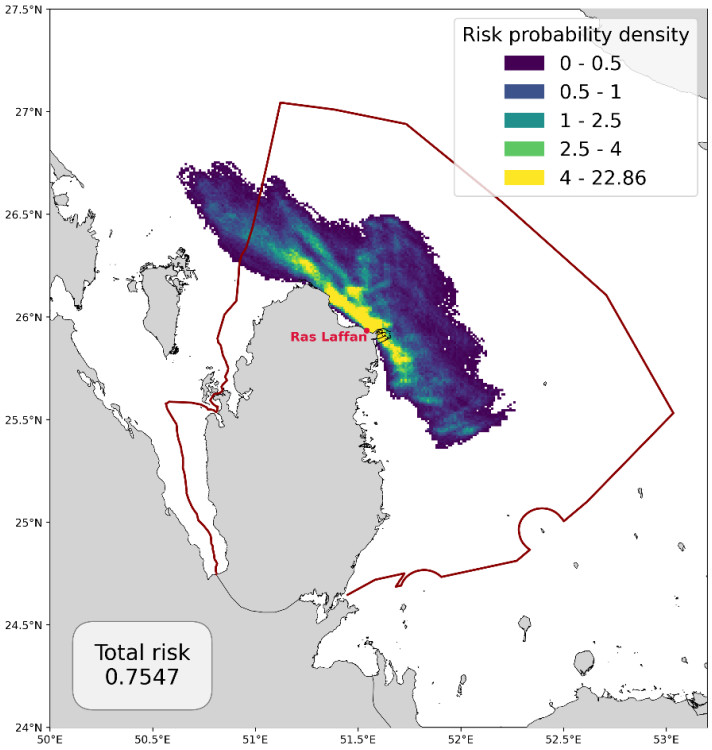


Figure 2.12 : Example of a risk distribution function with the associated Total risk for Ras Laffan in March 2019

Using the risk distribution function that we have just computed, we can derive an exposure function to oil spills resulting from shipping activities by using a shipping density function. The goal here is to determine which the areas are most hazardous to a given desalination plant because of marine traffic. We do that by multiplying the risk distribution function (*fig. 2.12*) with a ship density function (*fig. 2.13*). This amounts to assume that the probability of an oil spill being produced at a certain location will be proportional to shipping density at that location. We hence only consider marine traffic as a potential source of oil. We therefore normalize the ship density function to obtain a ship probability distribution function (with a surface integral equal to 1 (*fig. 2.13*) and multiply it with the risk distribution function (*Eq. 3.3*). The resulting shipping exposure maps are again computed for every month and every desalination plant. As we the risk distribution function, we can compute the surface integral of the shipping exposure distribution function to obtain the total monthly exposure of a given desalination plant to shipping activity (*fig. 2.14*). That indicator is particularly useful to compare the vulnerability of the three plants and identify which months are the most hazardous.

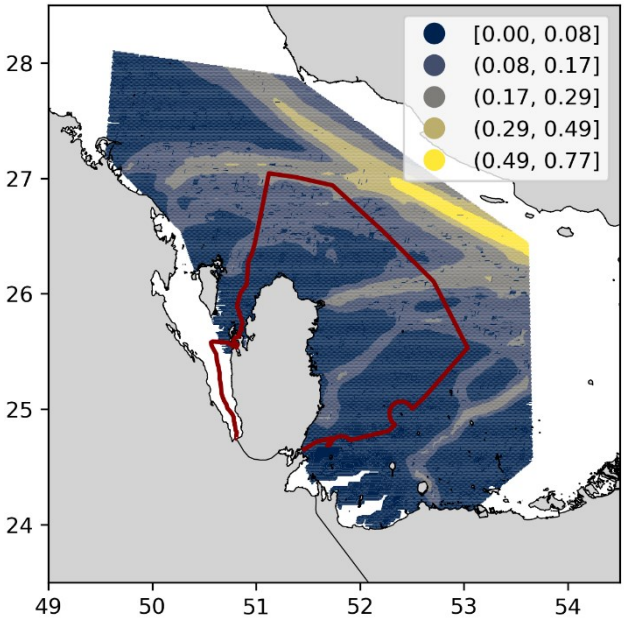


Figure 2.13 : Shipping density distribution in a sub zone of Arabian Gulf in 2013. The sub-area boundaries are determined by the fact that neither oil elements coming from outside of this zone could threat a station in 5 days.

Formula 3.3 : Product of densities

$$\frac{\text{Probability density risk}}{\text{Pixel area}} * \frac{\text{Probability density ships}}{\text{Pixel area}}$$

Formula 3.4 : Total exposure

$$\sum Product\ of\ densities * Pixel\ area$$

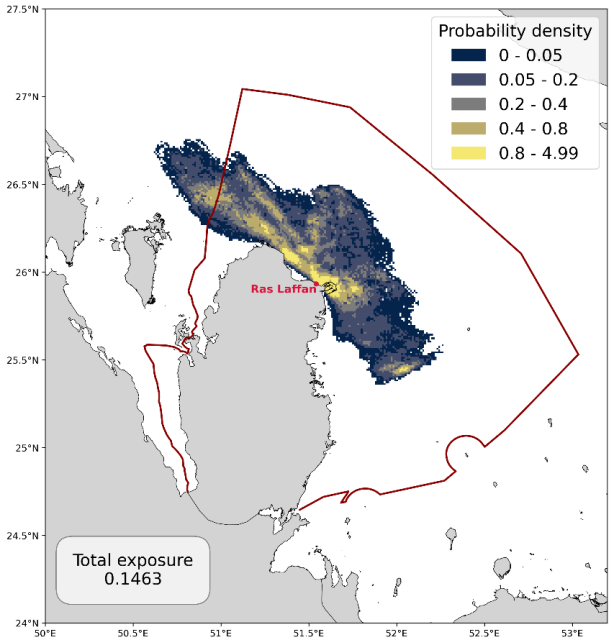


Figure 2.14 : Example of an exposure map with the associated Total exposure for Ras Laffan in March 2019

b. Vulnerability to oil spills from drilling platforms

So far, we have only considered a generic oil spill risk distribution function and an oil spill exposure function that only takes marine traffic into account. However, oil spill can also be produced by other sources. One obvious source of oil pollution in the Gulf are offshore oil and gas platforms (*fig. 2.4*). These platforms are generally clustered together over oil fields. We will therefore consider another exposure indicators for oil spills originating from these oil fields. Unlike marine traffic, oil fields are rather localised, and we therefore follow a different approach. We will now consider forward oil spill simulations from a source (i.e., the oil fields) to a destination (i.e., a portion of Qatar's coastline). Qatar's coastline has been divided in 10 different segments (*fig. 2.15)* corresponding to particular coastal cities or assets. When running

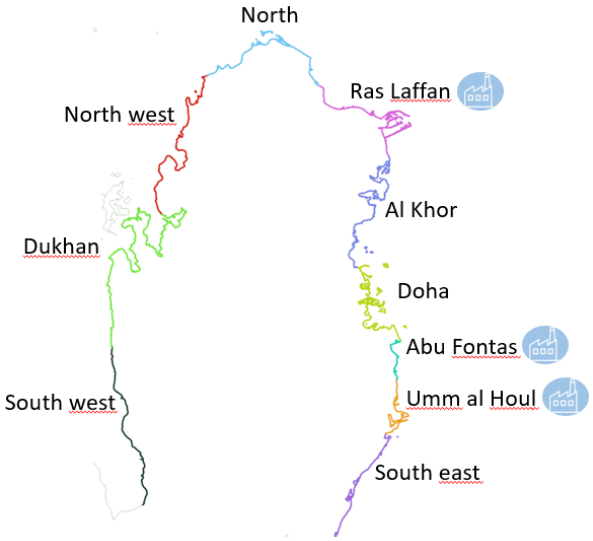


Figure 2.15 : Partition of Qatar's coastline in ten coastal segments. Three of these segments correspond to desalination plants (highlighted by an icon).

forward oil dispersal simulations, we can now explicitly take oil weathering into account. This means that oil particles will naturally degrade (and hence lose mass) as they move forward in time. We can therefore run longer simulations to take into account the low probability of long-distance dispersal events. The simulation duration is thus increased to 10 days. As with the previous backward simulations, we run simulations that start every day and do that for the entire years 2019 and 2020.

For each of these simulations, we compute a connectivity matrix that indicates what amount of oil released at a given oil field reaches a given segment of Qatar's coast. All the daily connectivity matrices for a given month are then summed together to have one unique monthly connectivity matrix (*fig. 2.16*). Each row in that matrix is then normalised by the total amount of oil released at the corresponding oil field to obtain a normalised connectivity matrix. In that matrix, each desalination plant corresponds to a particular column. By summing all the entries in each of those columns, we can estimate the exposure of each desalination plant to oil spill pollution originating from offshore platforms. The connectivity matrix can be visualised as a graph where each non-zero entry in the matrix corresponds to an edge in the graph, between an oil platform and a coastal segment.

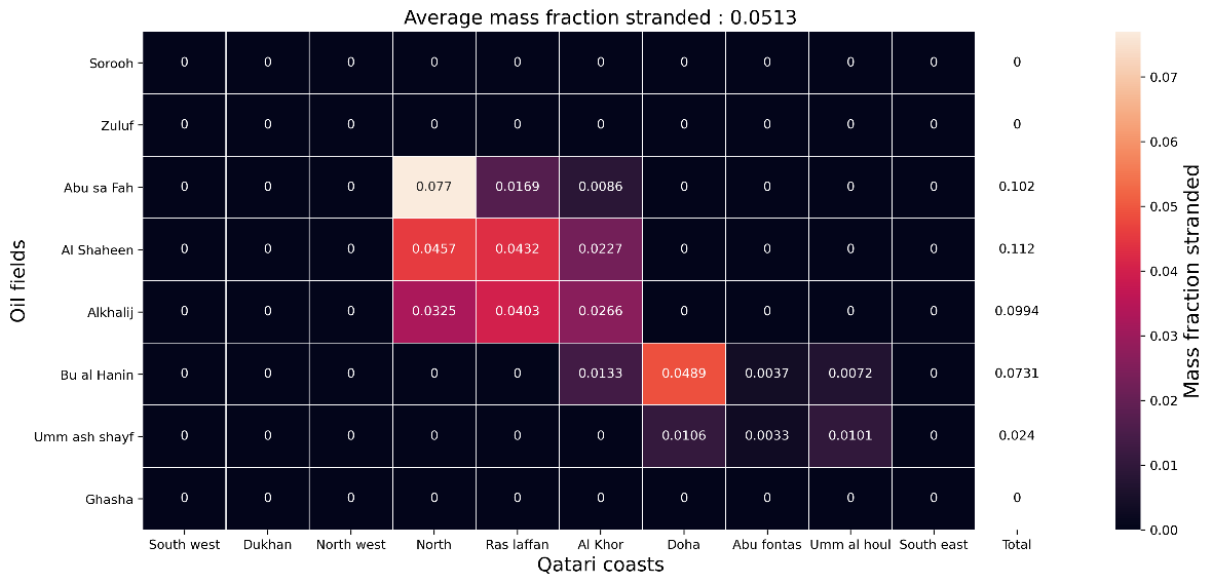


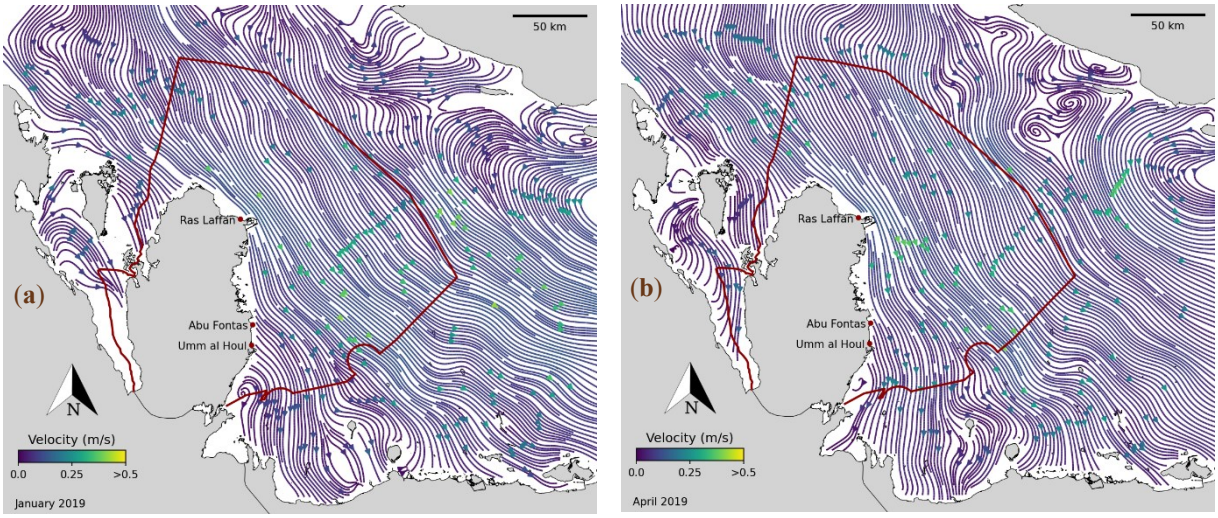
Figure 2.16 : Connection table between offshore platforms and Qatari coasts for Ras Laffan in March 2019 including oil weathering processes

3 Results

In this section, we will produce several maps that show how the oil spill risk that Qatar desalination plants are facing varies spatially and temporally. We will consider different risk indicators that are related to oil spills originating from both shipping activities and offshore oil platforms. All these indicators are computed for each month of the year in 2019 and 2020. For the sake of brevity, we will only show results for 2019 and for the months of January, April, July and October. That will allow us to better highlight the importance of the seasonal variability of oil spill risk. We will also only show results for the stations of Ras Laffan and Umm al Houl as the latter is very close to the station of Abu Fontas. The risk maps for Umm al Houl and Abu Fontas are therefore very close. The interested reader is referred to Appendices section to see the entirety of our results for the three stations, all months and both years.

3.1 Circulation patterns around Qatar

The regional ocean circulation around Qatar is characteristic of the circulation in the entire Arabian Gulf, which is mostly driven by changes in the stratification and wind regime. The wind-induced currents in the Gulf are predominantly towards south/southeast due to the northerly winds including shamal winds. During the summer, surface waters warm up and lead to very stratified conditions that result in a stable cyclonic circulation that extends to almost the entire Gulf. In autumn, surface waters cool down and wind intensifies leading to a decreasing stratification and hence a destabilisation of the circulation, which produces smaller meso-scale eddies. The stronger mesoscale activity during the winter leads to a weaker mean circulation. In spring, the increase of temperature leads to a slow restratification, which reduces the mesoscale eddy activity and leads to a more directional circulation.



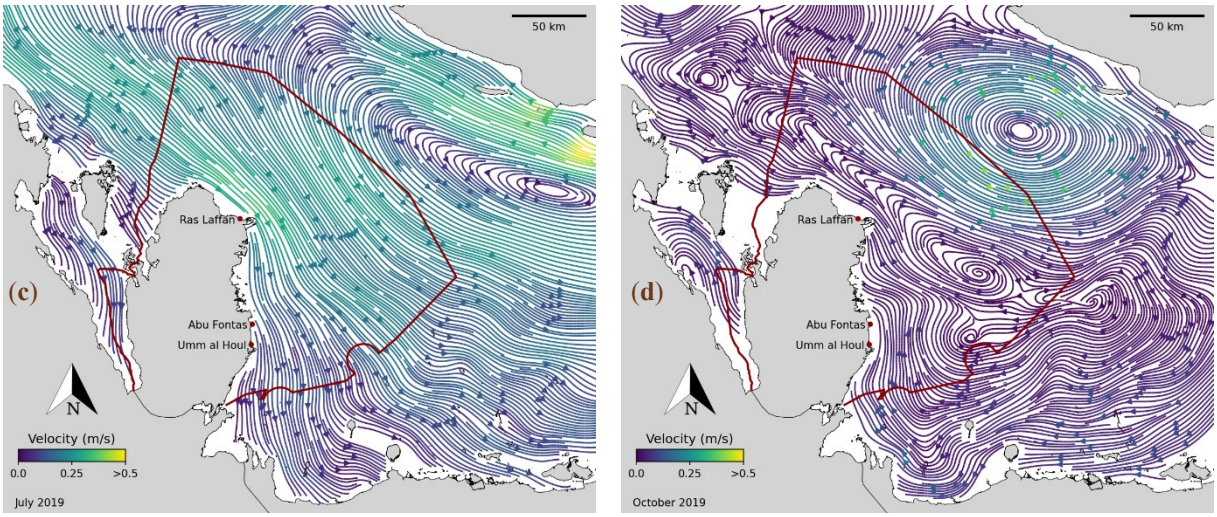


Figure 3.1 : Seasonal variability of the monthly-averaged ocean circulation around Qatar as simulated by the ocean model NEMO in (**a**) January 2019, (**b**) April 2019, (**c**) July 2019 and (**d**) October 2019

3.2 Desalination plants risk maps

In January and April, the large-scale circulation offshore of Ras Laffan is rather weak. Oil dispersal is therefore mostly tidally-driven and the resulting risk plumes are quite isotropic in southeast-northwest direction, which corresponds to the direction of the tidal currents (*fig. 3.2*). In the summer, there is a strong gyre in the center of the Arabian Gulf that generates stronger currents North of Qatar that flow in the southeast direction. Ras Laffan is therefore exposed to oil spills coming from the northwest and potentially from well outside Qatar EEZ. In autumn, the circulation is more variable, with smaller eddies, and often directed to the northwest. Ras Laffan is thus exposed to a risk coming mostly from the southeast.

Around Umm al Houl, the large-scale circulation is generally weaker. Oil dispersal will therefore be mostly driven by the tidal currents (leading to a rather isotropic dispersal) and by wind. The wind in that area are generally coming from the north west and weaker than the Shamal wind at the middle of the Gulf (Khonkar and al. 2009). The oil risk is rather isotropic and remains rather close to coast even if it extends out of Qatar EEZ (*fig. 3.3*). In summer, the risk plume is the smallest and mostly located north of Umm al Houl.

Throughout the year, Ras Laffan appears to be more at risk of being disturbed by an oil spill than the stations of Umm al Houl and Abu Fontas. This total is computed by integrating over the sea the risk distribution function. Except during autumn, Ras Laffan faces a risk 50-80% larger than the other two stations.

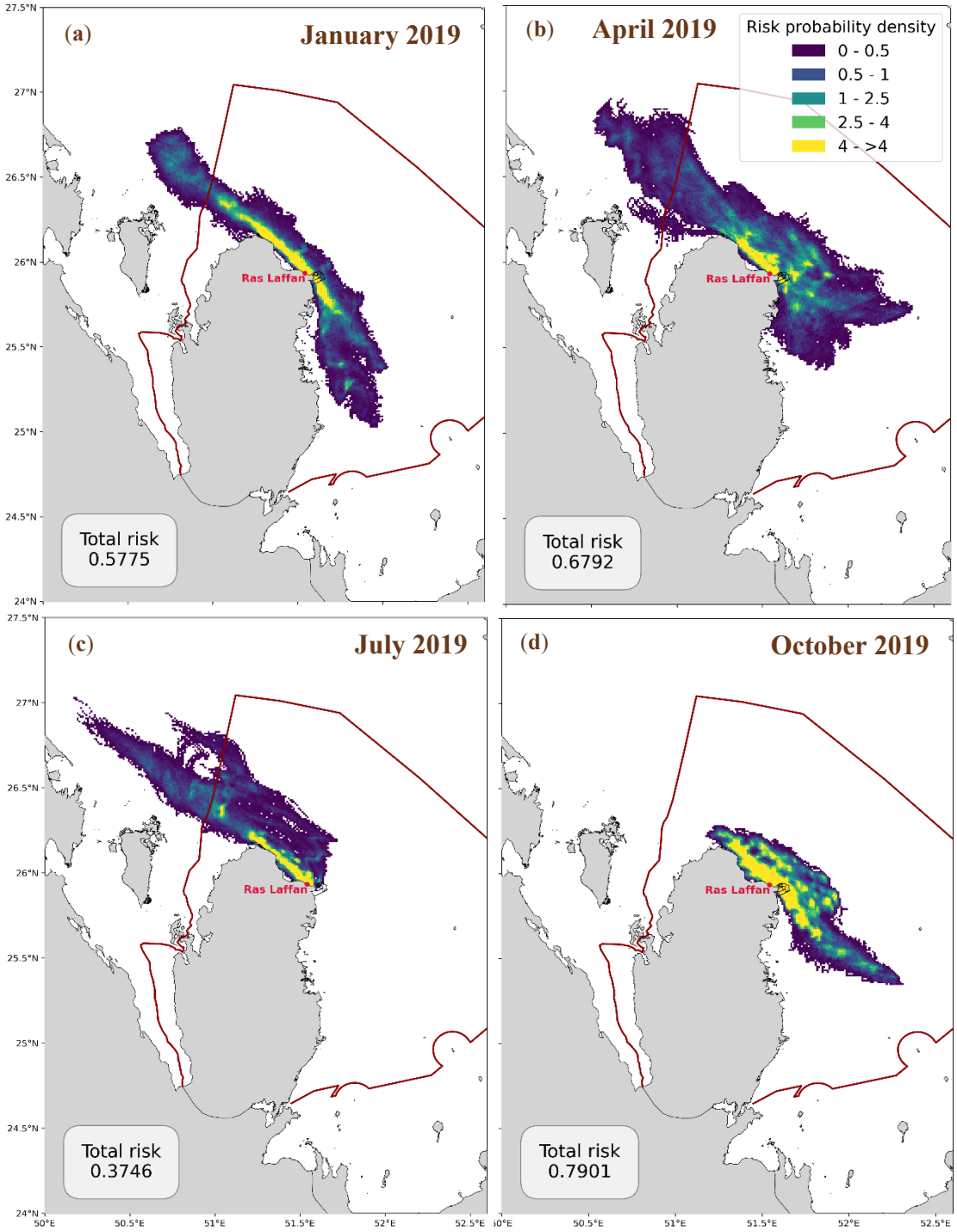


Figure 3.2 : Seasonal varability of oil risk probability density for Ras Laffan in (**a**) January 2019, (**b**) April 2019, (**c**) July 2019 and (**d**) October 2019

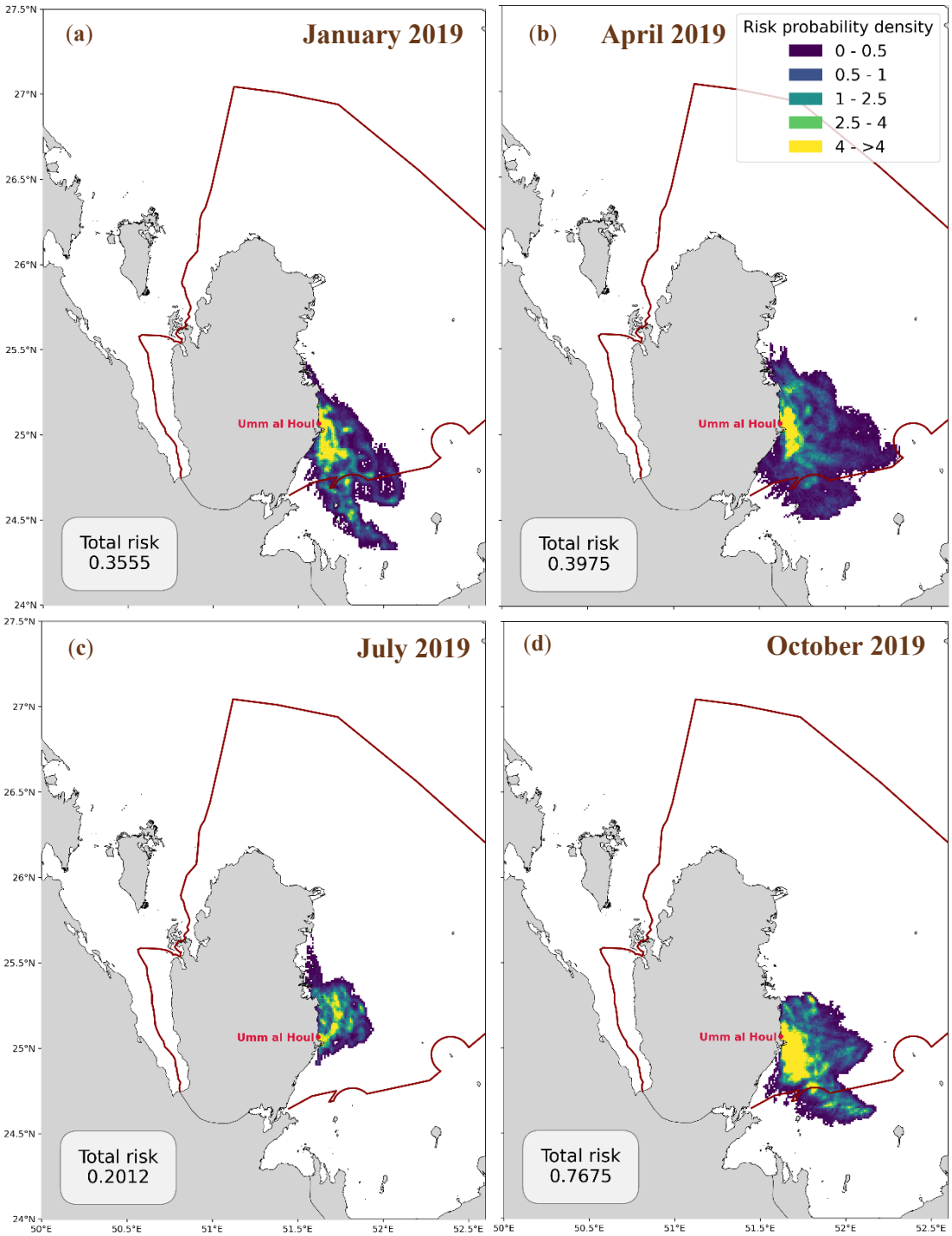


Figure 3.3 : Seasonal variability of oil risk probability density for Umm al Houl in (**a**) January 2019, (**b**) April 2019, (**c**) July 2019 and (**d**) October 2019

3.3 Arrival time maps

The minimum arrival time maps shows the time it would take for an oil spill to reach a desalination plan. In Ras Laffan, the circulation is sometimes strong which increase the distance that an oil spill can travel in a couple of days. In January, April and July, an oil spill originating from Bahrain EEZ could reach Ras Laffan in less than 2 days (*fig. 3.4*). Umm al Houl (and Abu Fontas) desalination plants are also exposed to spills originating from outside of Qatar EEZ. These two stations could indeed be impacted by oil spills originating from the UAE EEZ in less than 2 days as well (*fig. 3.5*).

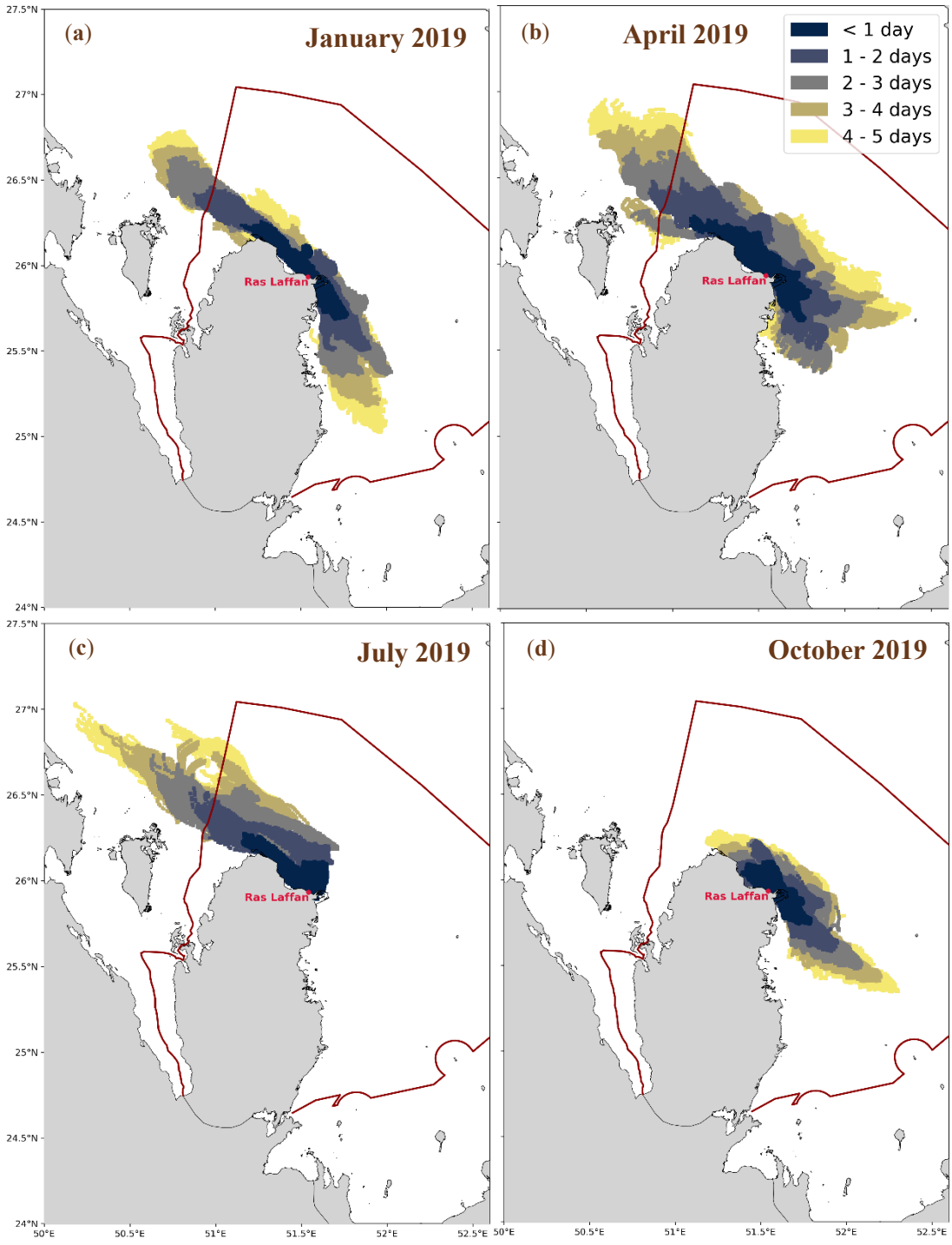


Figure 3.4 : Seasonal variability of oil spill minimum arrival time for Ras Laffan in (**a**) January 2019, (**b**) April 2019, (**c**) July 2019 and (**d**) October 2019

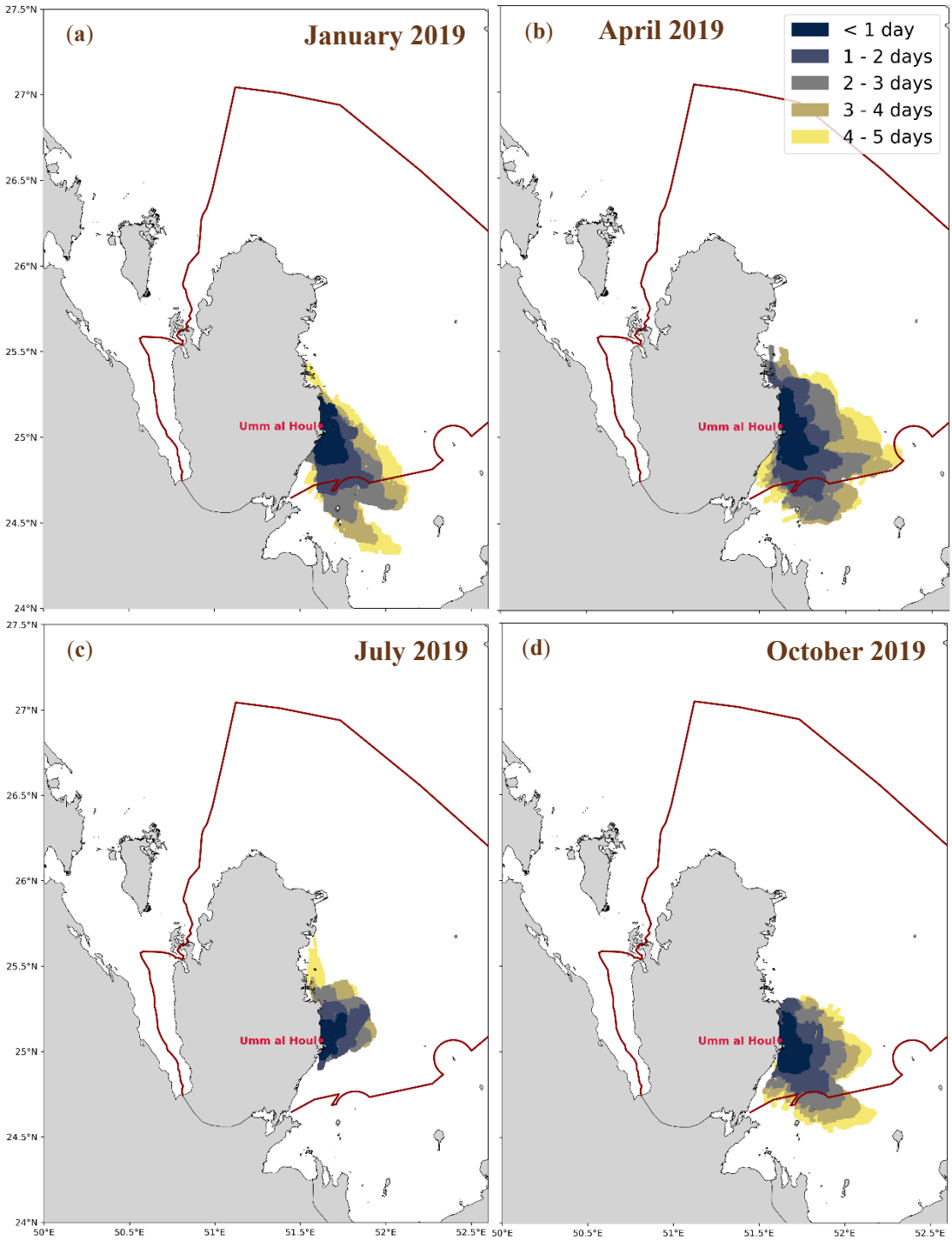


Figure 3.5 : Seasonal variability of oil spill minimum arrival time for Umm al Houl in (**a**) January 2019, (**b**) April 2019, (**c**) July 2019 and (**d**) October 2019

3.4 Shipping exposure maps

Exposure maps combine the risk of being impacted by a spill and the probability for the spill to originate from a certain location. Here we assume that this probability is directly proportional to the density of the shipping traffic (*fig. 3.6a*). The latter is particularly important in the center of the Arabian Gulf, along the main shipping route that goes from the Strait of Hormuz to the oil terminals in Iraq and Kuwait, and also along all the secondary routes that connect the main route to all the ports and terminals along the coast. Ras Laffan desalination plant being closer to the center of the Gulf and next to the gas terminal of Ras Laffan it is much more exposed to oil spills originating from shipping accidents than the stations of Umm al Houl and Abu Fontas. The exposure is the largest during summer and takes non-negligible values even outside of Qatar EEZ.

Ras Laffan appears to be vulnerable to oil spills released along 3 shipping routes (*fig. 3.6a*): the route going to Bahrain in the North (R1), the route going straight to the gas terminal of Ras Laffan(R2) and the route going to Doha and Abu Fontas in the South (R3). In January, the desalination plant is exposed to all three routes but the overall exposure is rather limited. In April, the exposure is larger on mostly concentrated along R2 with also some exposure to R1 (*fig. 3.6b*). In July, the stronger northwest currents lead to an increase of the exposure to R1 while the overall exposure remains limited (*fig. 3.6c*). Finally, in October, the exposure shifts South and is mostly located along R2 and, to a lesser extent, along R3 (*fig. 3.6d*).

The exposure of Umm al Houl (and Abu Fontas) is much weaker, by about a factor of 5. Among the three routes described before, only R3 presents a risk for these two stations but it is rather limited as the risk distribution is generally skewed towards the South and hence does not overlap much with that shipping route (*fig. 3.7*). The vulnerability pattern therefore appears to be more isotropic and probably influenced by smaller vessels that operate more locally do not necessarily follow the more important shipping routes.

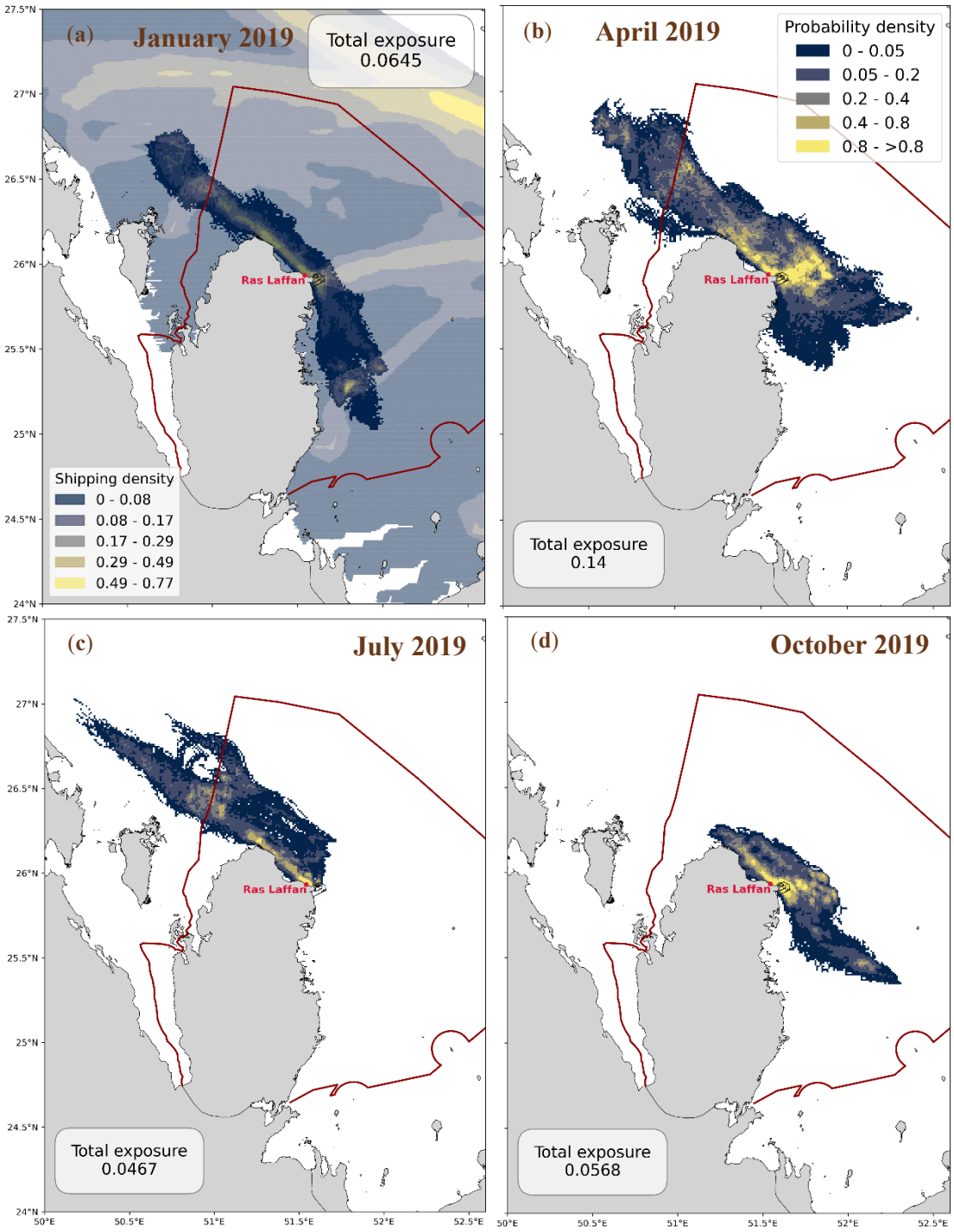


Figure 3.6 : Seasonal variability of exposure to ships oil spill for Ras Laffan in (**a**) January 2019, (**b**) April 2019, (**c**) July 2019 and (**d**) October 2019

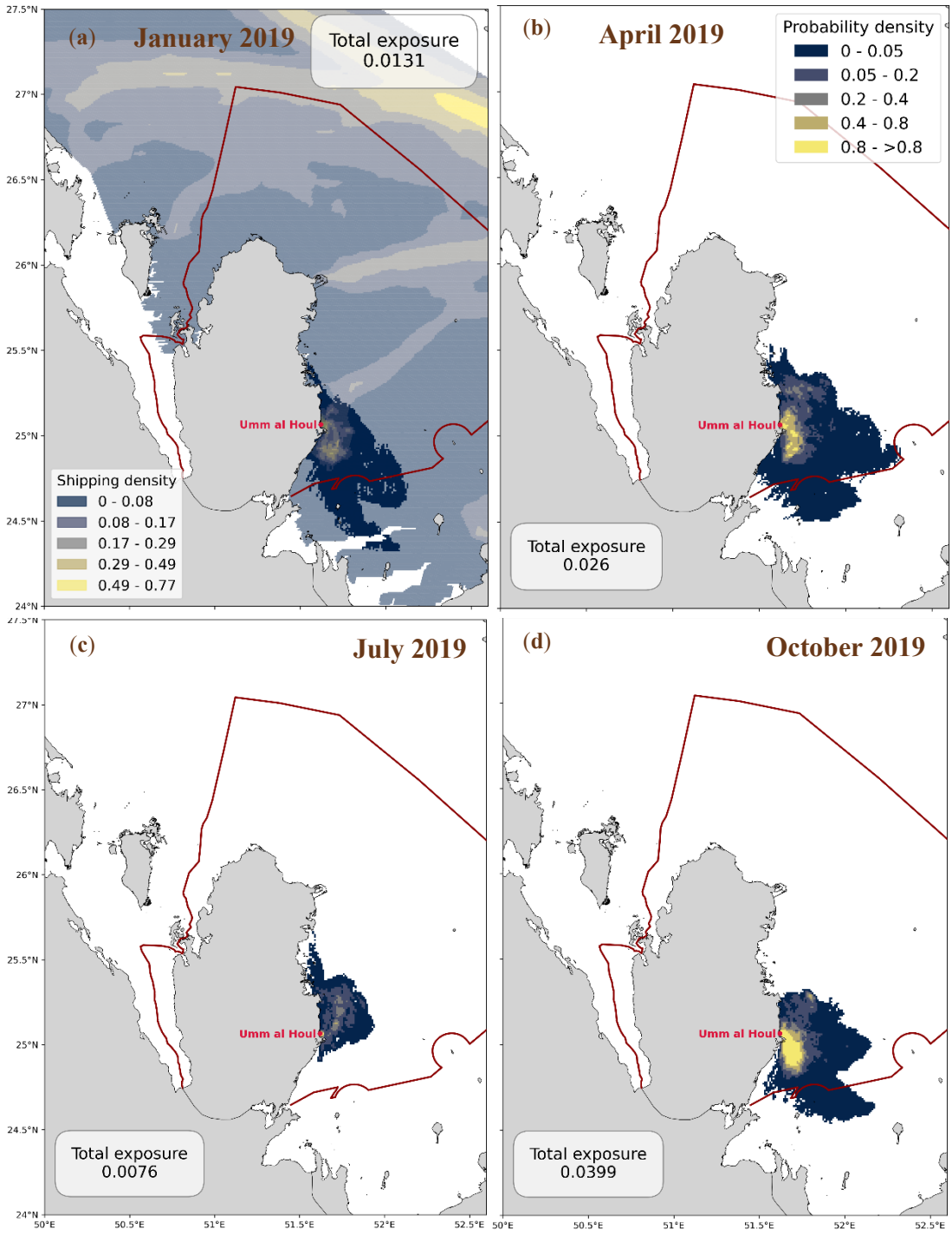


Figure 3.7 : Seasonal variability of exposure to ships oil spill for Umm al Houl in (**a**) January 2019, (**b**) April 2019, (**c**) July 2019 and (**d**) October 2019

3.5 Oil platforms exposure maps

There are three oil and gas (O&G) fields in Qatar EEZ but they are rather far from the coast. Currents therefore need to be quite strong and directional during a long period in order to carry an oil spill from one of these platforms to the coast of Qatar. In winter, spring and autumn, the currents are mostly directed to the south/south east and rather weak. Most of the risk therefore comes from O&G field of Abu sa Fah, which can potentially impact the station of Ras Laffan but not the two others (*fig. 3.8a,b,d*). In the summer, the currents are both stronger and more consistently directed to the Southeast. They can therefore transport oil spills over larger distances. As a result, the distant Zuluf oil field (KSA) can represent a risk to the Ras Laffan station and also to Abu Fontas (*fig. 3.8c*).

The average fractions of oil stranded are the similar in January, April and July. Stranding is weakened in October as the circulation is more unstable and weaker so that oil spills have a lower probability of reaching the coast.

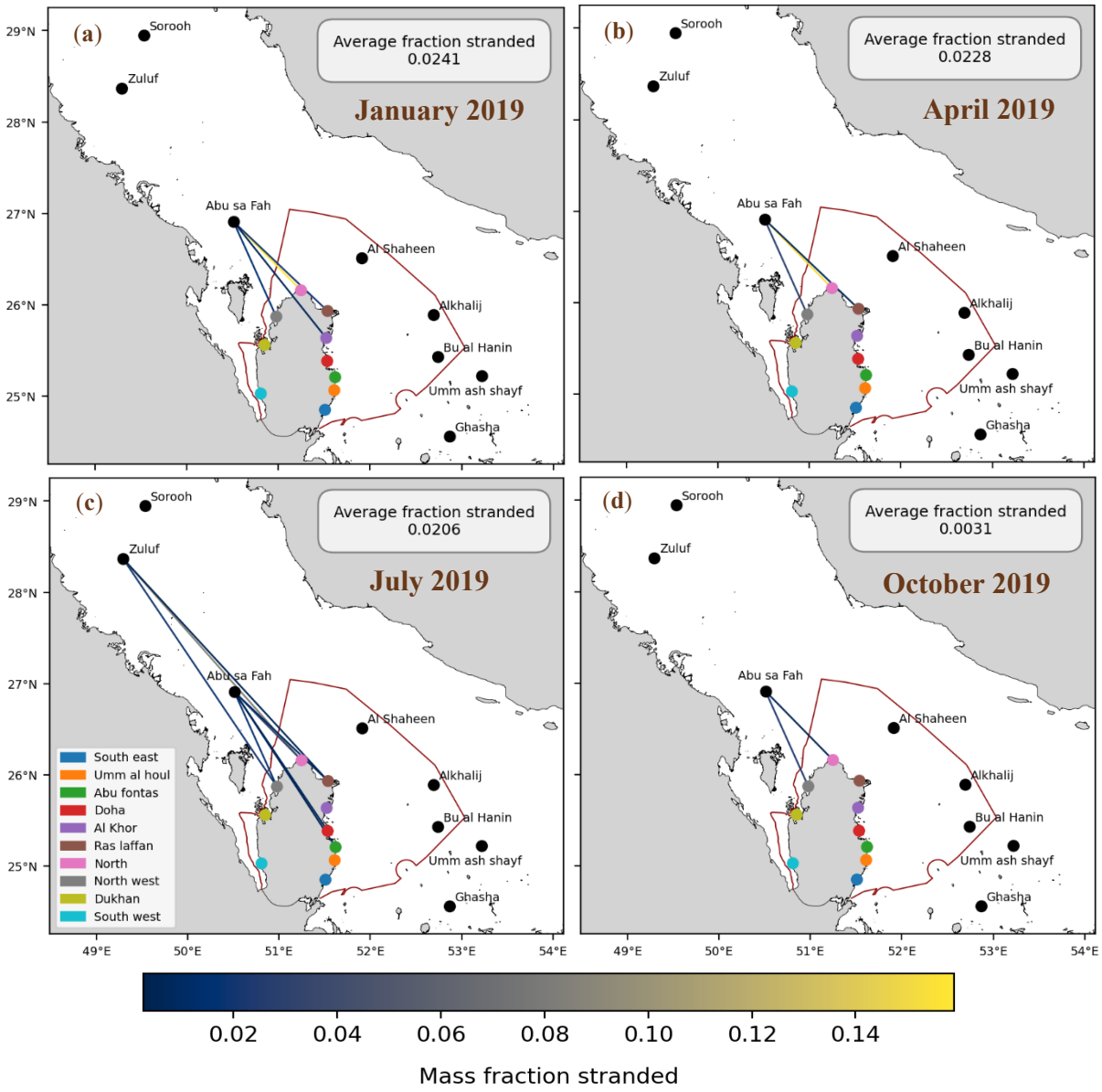


Figure 3.8 : Seasonal variability of oil mass fraction stranded on Qatari coasts originating from oil rigs in (**a**) January 2019, (**b**) April 2019, (**c**) July 2019 and (**d**) October 2019

3.6 Total monthly exposure timeseries

The total exposures and the average oil fractions stranded can be compilated for the years 2019 and 2020 (*fig. 3.9*). The evolution of total exposure and average fraction stranded show the variation of exposure of oil from ships and the variation of exposure of oil from offshore platforms.

Among the three main desalination plants of Qatar, Ras Laffan is the most exposed to oil spills throughout the year and from both shipping and O&G platforms. Abu Fontas and Umm al Houl have a similar exposure that is markedly smaller than the one of Ras Laffan.

The timeseries for 2019 and 2020 suggest that oil spill vulnerability is the largest in spring. During that period oil exposure is large for both shipping and offshore platforms. Autumn also appears to be a period of high vulnerability but mostly to shipping. However, since the circulation is less stable at that time of the year, we expect more variability from one year to the next. In contrast, summer and especially July generally represent a weaker exposure. However, because of the stronger circulation, that exposure is less localised and hence potentially more difficult to detect.

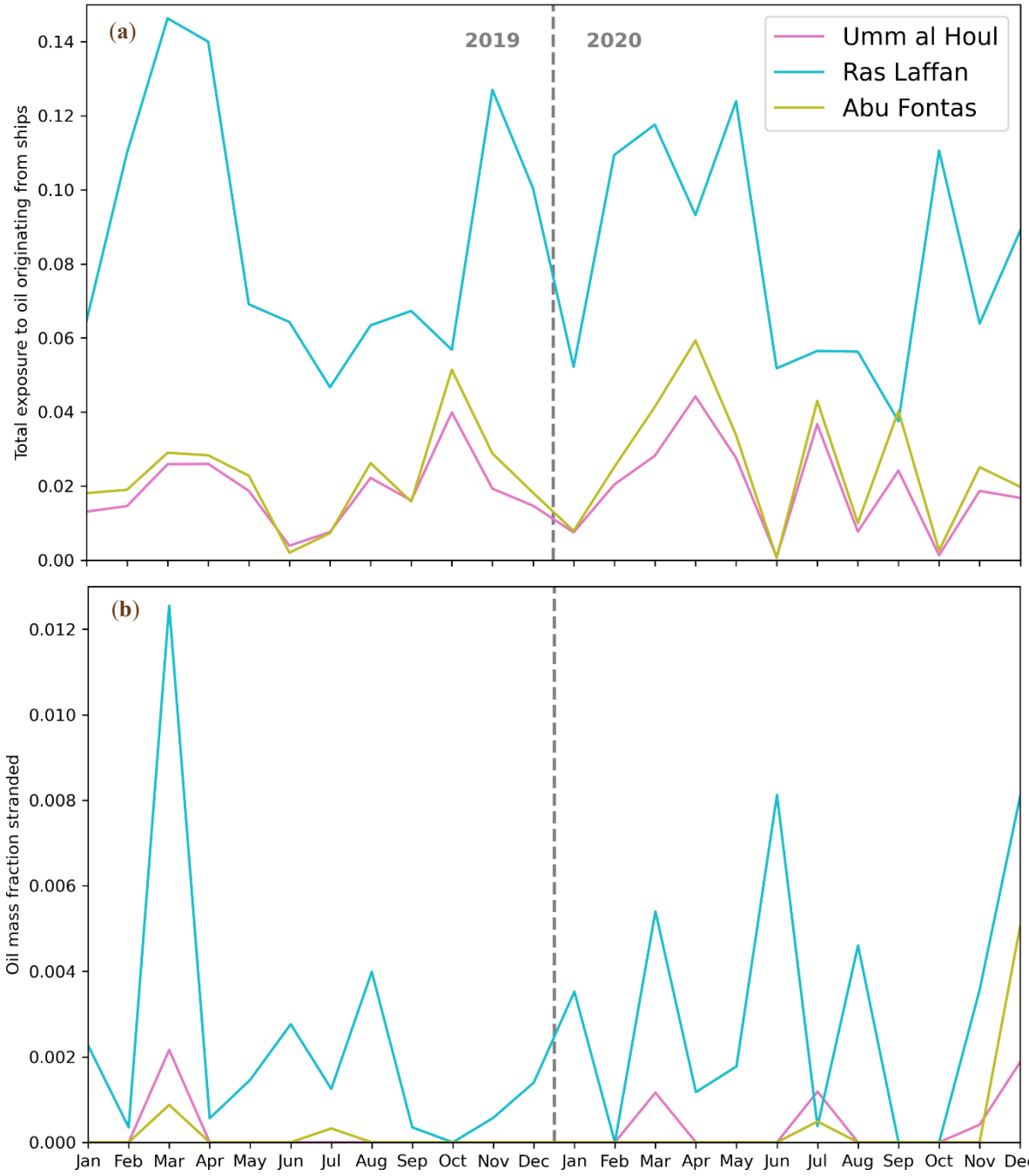


Figure 3.9 : Evolution of Qatari desalination plants exposure to (**a**) ships oil spill and (**b**) oil from oil rigs, in 2019 and 2020

4 Discussion

4.1 Influence of ocean and wind circulation on oil pathways

Oil dispersal is driven by the complex interplay between the atmospheric and oceanic circulation. On the one hand, since oil density is lower than water's, it floats on the sea surface and is directly influenced by the wind. The wind also generates surface waves that contribute as well to oil dispersal through the Stokes drift. The combination of both the direct wind effect and the wind-generated waves effect yields a oil drift velocity of about 3.5% of the wind velocity (C. E. Jones and al. 2016). This is not negligible, especially during the summer and winter months when Shamal winds are frequently blowing at a speed above 10 m/s. On the other hand, heavier oil fractions stay below the surface and vertical mixing in the ocean continuously brings oil particles down in the water column. All these oil particles are transported by the ocean currents, which are influenced by many factors such as wind, density gradients and tides. The combination of a strong vertical stratification and intense northwesterly winds in the summer yields a very directional southeastward circulation (*fig. 3.1c*). Once vertical stratification weakens at the end of summer and winds weaken as well, the circulation becomes more unstable and mesoscale eddies start to dominate (*fig. 3.1d*). The mesoscale eddy activity remains throughout the winter and early spring until temperatures increase again to recreate a stratified vertical density profile (*fig. 3.1a,b*).

The result of this complex interplay is that oil risk areas change throughout the year. In the summer, both the oceanic and atmospheric circulation are southeastward and oil spill risk therefore comes from the North-West (*fig. 3.2c*). In the autumn, winds weaken and mesoscale eddies intensify such that the risk area moves to the East (*fig. 3.2d*). In the winter, mesoscale eddies are still present, but northwesterly Shamal winds intensify such that the risk area becomes again oriented in the NW-SE direction (*fig. 3.2a*). Here tides play a bigger role as the large-scale circulation is weaker than during the summer. Since tidal currents are oriented along the coast and continuously change direction, they yield a more isotropic dispersal in the NW-SE direction (for Ras Laffan) and in the N-S direction (for Umm al Houl and Abu Fontas) (*fig. 3.2a,b* and *fig. 3.3a,b*). In spring, winds tend to weaken again and oil dispersal is again dominated by mesoscale eddies that yield a more isotropic risk areas that extends East again (*fig. 3.2b*). By the end of the spring, temperature increases, water column restratifies and mesoscale activity decreases in favor a stable gyre system that yields again more directional southeastward dispersion.

4.2 Identification of dangerous areas, sensitive stations and risky periods

The risk area for the three desalination plants frequently extends out of Qatar EEZ. Ras Laffan is exposed to oil spills originating from Bahrain and Saudi Arabia's EEZ most of the year except during the autumn (*fig. 3.4*). Umm al Houl and Abu Fontas are exposed to oil spills the UAE EEZ (and to a lesser extend Saudi Arabia's waters between Qatar and UAE) during most of the year except during the summer (*fig. 3.5*). For all three stations, oil spills originating from outside of Qatar EEZ could reach the stations in less than two days. This strongly supports the development of extensive satellite-based monitoring systems that cover Qatar EEZ but also the neighboring countries coastal waters.

The exposure to oil spills originating from ship accidents and intentional oil releases is influenced by three shipping routes that connect the main Gulf-wide shipping route that runs along the long axis of the Gulf to (1) the port of Manama in Bahrain, (2) the port of Ras Laffan and (3) all the ports located between Doha and Mesaieed on the eastern coast of Qatar (*fig. 3.6a*). Ras Laffan desalination plants is obviously mostly exposed to the route going to the port of Ras Laffan but it is also exposed to the shipping route to Bahrain throughout the year except in autumn, and to the shipping route to Doha and Mesaieed in autumn. The desalination plants of Umm al Houl and Abu Fontas are only exposed to the shipping route that connects to all the industrial area between Doha and Mesaieed (*fig. 3.7a*).

Offshore oil platforms present a weaker risk as they are located quite far away from the coast. Qatar O&G offshore fields, such as the major Al Shaheen field, are close to the limits of Qatar EEZ. They are further located East to Northeast of Qatar. They are thus not a threat when the oceanic or atmospheric circulation is oriented southeastward (*fig. 3.8a,b*). However, when Shamal winds are not blowing and mesoscale eddy activity is more intense (such as in autumn and spring), they could then pose a threat to the eastern coast of Qatar and all three desalination plants (*App. 7.20c*). Outside of Qatar EEZ, the oil field of Abu Safah, located between the waters of Bahrain and Saudi Arabia, poses the greatest threat to Qatar in general and to the desalination plant of Ras Laffan in particular. Despite being slightly sheltered by the northern tip of Qatar, Ras Laffan lies about two days downstream Abu Safah when the circulation is northwesterly (*fig. 3.4* and *fig. 3.8*). It should be noted that the Saudi Arabian oil field of Zuluf could also potentially pose a threat to Ras Laffan during the summer months when the large-scale cyclonic gyre is the most intense (*fig. 3.8c*). That threat could however be more easily mitigated as it would take several days for the oil spill to reach the station.

The exposure of Qatar desalination plants to oil spills originating from shipping is the largest in spring and autumn, when winds are weaker and oil dispersal is driven by mesoscale eddies (*fig. 3.6b,d* and *3.7b,d*). When the oceanic and/or the atmospheric circulations are northwesterly, such as during the summer and, to a lesser extent, during winter, desalination plants are more sheltered as oil dispersal is directed in the NW-SE direction and shipping routes are roughly perpendicular to that direction (*fig. 3.6a,c*). Ras Laffan being further North, it is more exposed than the other two stations. It is interesting to note that oil spill risk is further reduced in summer by the higher water temperatures and more intense wave activity that both increase the oil weathering rate (*fig. 4.1*). It is also important to notice that the oil density strongly influence the weathering rate (*fig. 4.2*). In spring and autumn, the circulation is less directional and mesoscale eddies promote a more isotropic dispersal (*fig. 3.2b,d* and *fig. 3.3b,d*). The oil risk therefore shifts to the East, which makes desalination plants more exposed to ships navigating to the different ports along the eastern coast of Qatar (*fig. 3.6b,d* and *3.7b,d*).

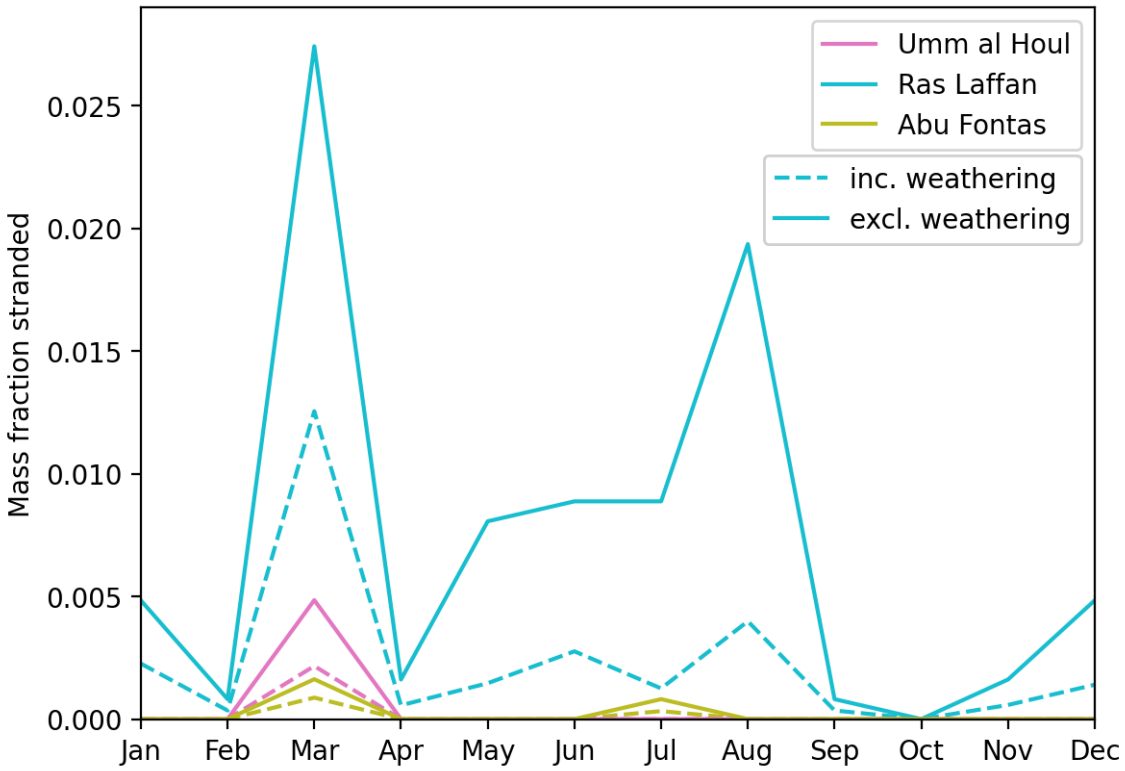


Figure 4.1 : Evolution of Qatari desalination plants exposure to oil from oil rigs in 2019. Dashed lines are real oil mass fraction stranded if the oil weathering are involved. In winter, the weathering approximatively decrease by 50% the oil mass arriving on each station. But in summer and particularly in August, the temperature are on rise leading to a 80% reduction of the oil mass arrived in Ras Laffan

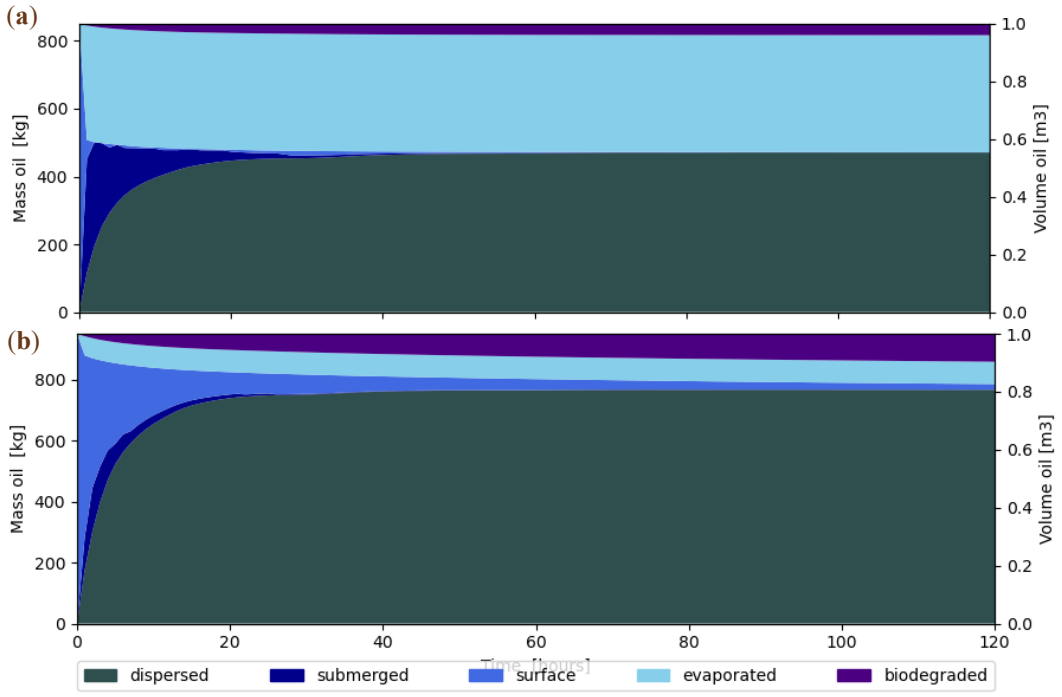


Figure 4.2 : Evolution of oil weathering for (**a**) 'QATAR MARINE' (850.3 kg/m^3) and (**b**) 'Yombo, Amoco' (950.6 kg/m^3). The simulations are performed in March 2019 with 20 oil elements released in the middle of the Arabian Gulf. In the case of 'QATAR MARINE', evaporation and biodegradation reduce the slick mass by 50% in 5 days. If oil has higher density like 'Yombo, Amoco', the oil mass is only reduced by 18%.

Among Qatar's three main desalination plants, Ras Laffan is the one most at risk of being impacted by oil spills and hence the one that requires the most efficient oil spill countermeasures (*fig. 3.6, 3.8* and *3.9*). This is particularly important as Ras Laffan is also home to one of the World's largest petrochemical ports. If a major oil spill were to reach Ras Laffan, it would not only shut off about 20% of Qatar's freshwater production. It would also shut off the largest Liquefied Natural Gas (LNG) terminal in the World and hence substantially destabilize global energy supply. Recent events in Mauritius (MV Wakashio oil spill on 25 July 2020) and Sri Lanka (X-Press Pearl accident on 20 May 2021) have shown that such large-scale pollution events can happen anywhere (BBC News 2021). The X-Press Pearl accident is all the more worrying since the ship caught fire following a nitric acid leakage, which was apparently detected while the ship was trying to stop over at Hamad Port in Qatar.

5 Conclusion

By assessing the oil risk from ships and offshore platforms to the Qatari desalination plants, this thesis intends to provide decision support tools to limit the consequences during an oil spill event and highlight the offshore areas that present the highest risk and which should thus be monitored in priority to reduce the potential risk of an oil spill. Oil drift patterns were simulated with the Lagrangian oil dispersal model OpenOil. We first ran backward oil spill simulations starting from the desalination plants in order to determine which areas could be source of oil spills that would subsequently reach desalination plants. These simulations were performed for every day of both 2019 and 2020 in order to explicitly take into account temporal variability over different time scales. Through this risk assessment, we are able to predict how long it would take for a spill to reach a station and hence evaluate the time available to set up countermeasures. By combining the risk distribution with shipping density maps, we derived an exposure indicator that highlights areas where shipping activities (and accidents) would present the highest risk to desalination plants. As a second step, we ran forward oil spill simulations starting from offshore oil and gas fields in order to build monthly connectivity graphs between these offshore platforms and the Qatari desalination plants. These graphs highlighted which oil and gas field could be a threat to Qatar desalination plants and how that threat evolves through time.

Through this study, we have shown that among the three main desalination plants of Qatar, the one of Ras Laffan is clearly the most at risk of being impacted by an oil spill. Ras Laffan is located in the northern Qatar which makes it more exposed to oil spills, from both ships and offshore platforms. The most hazardous areas are often located near the stations and distributed in the northwest leading to a high exposure originating from the shipping lane going to the Bahrain and the offshore platform of Abu sa Fah. The oil risk distribution changes throughout the year. The summer period, with its strong northwesterly currents, shifts the risk pattern to the West. In contrast, when the mesoscale eddy activity dominates, the risk pattern tends to shift to the East. All of previous conclusions will be adjusted according to the oil weathering processes. We have shown that the mass fraction of oil decrease over time. The major characteristics influencing the weathering extracted in this study are the seawater temperature, the wave activity and the oil density.

As with all modelling study, there are some limitations that are closely related to the modelling assumptions and to the data used to force the model. We have only assessed oil risk over 2 years, which might not be sufficient to completely represent the interannual variability of the atmospheric and oceanic circulation. To produce exposure maps, we only had access to shipping density maps for 2013. However, marine traffic might have changed between 2013 and 2019. Moreover, oil exposure from ships vary along the year (ScanEx 2018). The ships

density should ideally be assessed for 2019 and 2020 year and monthly variability should be taken into account. Besides, the offshore oil field were represented as single points and not as polygons. Better quality information on the spatial extent of oil fields would yield better estimates of the associated risk. Finally, OpenOil does not consider oil weathering processes when the model is run backward in time. It could be interesting to perform the same kind of simulations when oil weathering will take into account. Besides, the OpenOil version used don't regard some weathering processes like sedimentation which could reduce the oil spill risk.

During this study, we have assessed the oil risk represented by an oil spill originating from ships and oil wells. Our results could inform Qatar authorities to better design their oil spill management strategy. The OpenOil model is accurate to predict the drift of an oil particle and it could be the foundation of other studies on oil spill vulnerability in the Gulf. However, as with all models, it remains necessary to thoroughly validate it. This could be done by relying more extensively on previous oil spill observations (both from direct field observations and form satellite imagery). Any full-fledged oil spill monitoring service should combine a broad array of observation sources (from the boat to the aircraft and the satellite) with a quick and accurate modelling interface that would allow rapid estimations of the spill evolution. Qatar is not the only country in the Gulf that relies on seawater desalination. Our study could thus be extended to the entire Gulf, and, potentially, to other areas in the World as well. Finally, the Arabian Gulf is a major crossroad of oil shipping but it is also home to valuable marine ecosystems such as mangroves, coral reefs or seagrass. These ecosystems are threatened by oil spills and the danger could be forecasted through models like the one developed in this study.

Qatar, by having no choice but to produce its water via desalination, makes itself sensitive to oil spills. This thesis was realised to enhance the forecasting and monitoring capacities of oil spills in order to reduce the oil impact on the desalinations plants. We hope that this type of risk assessment will contribute to a stable and safe water production through desalination for countries suffering from water scarcity.

6 References

"Access Data | CMEMS." n.d. Accessed May 16, 2021. https://marine.copernicus.eu/access-data.

Albano, Paolo, Nadezhda Filippova, Jan Steger, Darrell Kaufman, Adam Tomasovych, Michael Stachowitsch, and Martin Zuschin. 2016. "Oil Platforms in the Persian (Arabian) Gulf: Living and Death Assemblages Reveal No Effects." *Continental Shelf Research* 121 (January): 21–34. https://doi.org/10.1016/j.csr.2015.12.007.

Androulidakis, Yannis, Vassiliki Kourafalou, Lars Robert Hole, Matthieu Le Hénaff, and HeeSook Kang. 2020. "Pathways of Oil Spills from Potential Cuban Offshore Exploration: Influence of Ocean Circulation." *Journal of Marine Science and Engineering* 8 (7): 535. https://doi.org/10.3390/jmse8070535.

"AQUASTAT Database Database Query Results." n.d. Accessed May 26, 2021. http://www.fao.org/aquastat/statistics/query/results.html.

Ardhuin, Fabrice, Louis Marié, Nicolas Rascle, Philippe Forget, and Aron Roland. 2009. "Observation and Estimation of Lagrangian, Stokes, and Eulerian Currents Induced by Wind and Waves at the Sea Surface." *Journal of Physical Oceanography* 39 (11): 2820–38. https://doi.org/10.1175/2009JPO4169.1.

BBC News. 2021. "X-Press Pearl: Sri Lanka Braces for Environmental Disaster from Sunken Ship," June 3, 2021, sec. Asia. https://www.bbc.com/news/world-asia-57343139.

Breivik, Øyvind, Jean-Raymond Bidlot, and Peter A. E. M. Janssen. 2016. "A Stokes Drift Approximation Based on the Phillips Spectrum." *Ocean Modelling* 100 (April): 49–56. https://doi.org/10.1016/j.ocemod.2016.01.005.

Ciappa, Achille, and Salvatore Costabile. 2014. "Oil Spill Hazard Assessment Using a Reverse Trajectory Method for the Egadi Marine Protected Area (Central Mediterranean Sea)." *Marine Pollution Bulletin* 84 (1): 44–55. https://doi.org/10.1016/j.marpolbul.2014.05.044.

Dagestad, Knut-Frode, Johannes Röhrs, Øyvind Breivik, and Bjørn Ådlandsvik. 2018. "OpenDrift v1.0: A Generic Framework for Trajectory Modelling." *Geoscientific Model Development* 11 (4): 1405–20. https://doi.org/10.5194/gmd-11-1405-2018.

Daniel, Pierre. 2012. "Modélisation de La Dérive Des Nappes d'hydrocarbures En Mer." *La Météorologie* 8 (April): 6. https://doi.org/10.4267/2042/47021.

"Dessalement de l'Eau de Mer: Bilan Des Dernieres Avancés Technologiques; Bilan Economique; Analyse Critique En Fonction Des Contextes | SSWM - Find Tools for Sustainable Sanitation and Water Management!" n.d. Accessed June 1, 2021. https://sswm.info/node/3972.

"ERA5 Hourly Data on Single Levels from 1979 to Present." n.d. Accessed May 16, 2021. https://cds.climate.copernicus.eu/cdsapp#!/dataset/reanalysis-era5-single-levels?tab=overview.

"Food and Water Security in Qatar: Part 2 - Water Resources." 2015. *Future Directions International* (blog). July 23, 2015. https://www.futuredirections.org.au/publication/food-and-water-security-in-qatar-part-2-water-resources/.

"Global Water Crisis - Water Scarcity Facts & How To Help | World Vision Australia." n.d. Accessed May 26, 2021. https://www.worldvision.com.au/global-water-crisis-facts.

Halpern, Benjamin, Melanie Frazier, John Potapenko, Kenneth Casey, Kellee Koenig, Catherine Longo, Julia Lowndes, et al. 2015. "Cumulative Human Impacts: Raw

Stressor Data (2008 and 2013)." Text/xml. KNB Data Repository. https://doi.org/10.5063/F1S180FS.

Hofste, Rutger Willem, Paul Reig, and Leah Schleifer. 2019. "17 Countries, Home to One-Quarter of the World's Population, Face Extremely High Water Stress," August. https://www.wri.org/insights/17-countries-home-one-quarter-worlds-population-face-extremely-high-water-stress.

Hussein, H., and L. Lambert. 2020. "A Rentier State under Blockade: Qatar's Water-Energy-Food Predicament from Energy Abundance and Food Insecurity to a Silent Water Crisis." *Water* 12 (4). https://ora.ox.ac.uk/objects/uuid:53424dbc-fb40-405a-a164-cc577ef146e9.

Johns, W.E., Fengchao Yao, Donald Olson, Simon Josey, J.P. Grist, and David Smeed. 2003. "Observations of Seasonal Exchange through the Straits of Hormuz and the Inferred Heat and Freshwater Budgets of the Persian Gulf." *J Geophys Res* 108 (December). https://doi.org/10.1029/2003JC001881.

Jones, Cathleen E., Knut-Frode Dagestad, Øyvind Breivik, Benjamin Holt, Johannes Röhrs, Kai Håkon Christensen, Martine Espeseth, Camilla Brekke, and Stine Skrunes. 2016. "Measurement and Modeling of Oil Slick Transport." *Journal of Geophysical Research: Oceans* 121 (10): 7759–75. https://doi.org/10.1002/2016JC012113.

Jones, Edward, Manzoor Qadir, Michelle van Vliet, Vladimir Smakhtin, and Seong-mu Kang. 2019. "The State of Desalination and Brine Production: A Global Outlook." *Science of The Total Environment* 657 (March). https://doi.org/10.1016/j.scitotenv.2018.12.076.

Kaempf, Jochen, and Masoud Sadrinasab. 2006. "The Circulation of the Persian Gulf: A Numerical Study." *Ocean Science (OS)* 2 (July). https://doi.org/10.5194/osd-2-129-2005.

Khonkar, Hussameldin I., and K. Abdulaziz. 2009. "Complete Survey of Wind Behavior over the Arabian Gulf." In . https://doi.org/10.4197/MAR.20-1.3.

Le Grand Atlas 13ème Édition de Boeck. n.d.

Lee, Kenneth, Michel Boufadel, Bing Chen, Julia Foght, Peter Hodson, Stella Swanson, and Albert Venosa. 2016. *High-Priority Research Needs for Oil Spills in Canada: Summary of a Royal Society Expert Panel Report on the Behaviour and Environmental Impacts of Crude Oil Released into Aqueous Environments*.

Mekonnen, Mesfin M., and Arjen Y. Hoekstra. 2016. "Four Billion People Facing Severe Water Scarcity." *Science Advances* 2 (2): e1500323. https://doi.org/10.1126/sciadv.1500323.

"Middle East Oil and Gas Field Map by CIA." n.d. Accessed February 12, 2021. https://www.arcgis.com/home/item.html?id=4a99caf63d6b4d3290ed27290e261a07.

Mishra, Aditya Kumar, and G. Suresh Kumar. 2015. "Weathering of Oil Spill: Modeling and Analysis." *Aquatic Procedia*, INTERNATIONAL CONFERENCE ON WATER RESOURCES, COASTAL AND OCEAN ENGINEERING (ICWRCOE'15), 4 (January): 435–42. https://doi.org/10.1016/j.aqpro.2015.02.058.

Mohamed A. Dawouda, Saleh O. Alaswadb, Hatem A. Eweac, Rokia M. Dawoudd. 2020. "Towards Sustainable Desalination Industry in Arab Region: Challenges and Opportunities."

Name. 2015. ""Doha Has Just Three Days' Supply": Are Water Shortages the Biggest Threat to the Middle East?" *City Monitor* (blog). July 16, 2015. https://citymonitor.ai/horizons/doha-has-just-three-days-supply-are-water-shortages-biggest-threat-middle-east-1234.

"Petrole." n.d. Accessed April 16, 2021. https://www.cesbc.org/basededonnees/petrole/accueil_page_petrole.htm.

"Qatar | History, Population, Flag, Language, & Facts." n.d. Encyclopedia Britannica. Accessed May 27, 2021. https://www.britannica.com/place/Qatar.

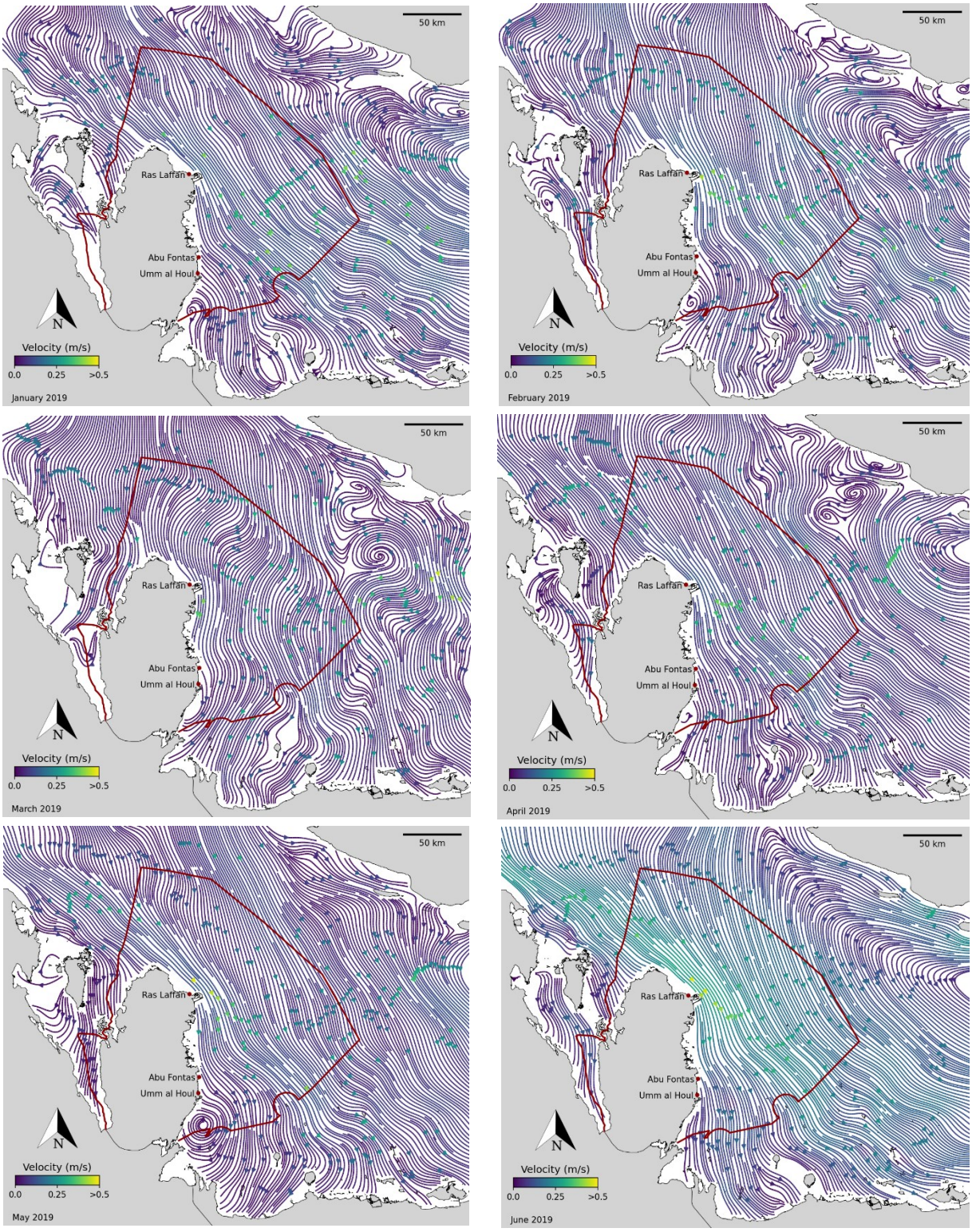
"Qatar - The World Factbook." n.d. Accessed June 1, 2021. https://www.cia.gov/the-world-factbook/countries/qatar/#economy.
"Qatar Population (2021) - Worldometer." n.d. Accessed May 31, 2021. https://www.worldometers.info/world-population/qatar-population/.
"Qatar Population 2021 (Demographics, Maps, Graphs)." n.d. Accessed May 31, 2021. https://worldpopulationreview.com/countries/qatar-population.
Rahman, Hammadur, and Syed Javaid Zaidi. 2018. "Desalination in Qatar: Present Status and Future Prospects." *Civil Engineering Research Journal* 6 (5): 1–7. https://doi.org/10.19080/CERJ.2018.06.555700.
Reed, Mark, Oistein Johansen, Per Brandvik, Per Daling, Alun Lewis, Robert Fiocco, Don Mackay, and Richard Prentki. 1999. "Oil Spill Modeling towards the Close of the 20th Century: Overview of the State of the Art." *Spill Science & Technology Bulletin* 5 (April): 3–16. https://doi.org/10.1016/S1353-2561(98)00029-2.
"Reimagining WASH." n.d. Accessed May 26, 2021. https://www.unicef.org/reports/reimagining-wash-water-security-for-all.
Reynolds, R. M. 1993. "Physical Oceanography of the Gulf, Strait of Hormuz, and the Gulf of Oman—Results from the Mt Mitchell Expedition." https://doi.org/10.1016/0025-326X(93)90007-7.
Röhrs, Johannes, Knut-Frode Dagestad, Helene Asbjørnsen, Tor Nordam, Jørgen Skancke, Cathleen E. Jones, and Camilla Brekke. 2018. "The Effect of Vertical Mixing on the Horizontal Drift of Oil Spills." *Ocean Science* 14 (6): 1581–1601. https://doi.org/10.5194/os-14-1581-2018.
SAS, Des Clics Nomades. n.d. "Température de l'eau du golfe Persique - Carte en temps réel et températures mois par mois." ÇaBaigne.net. Accessed May 5, 2021. https://www.cabaigne.net/mers/golfe-persique/.
"Satellite Monitoring of Oil Pollution in the Persian Gulf — ScanEx." n.d. Accessed May 13, 2021. https://www.scanex.ru/en/company/news/satellite-monitoring-of-oil-pollution-in-the-persian-gulf/.
Schleifer, Leah. 2017. "7 Reasons We're Facing a Global Water Crisis," August. https://www.wri.org/insights/7-reasons-were-facing-global-water-crisis.
"Summary Progress Update 2021: SDG 6 — Water and Sanitation for All." n.d. *UN-Water* (blog). Accessed May 26, 2021. https://www.unwater.org/publications/summary-progress-update-2021-sdg-6-water-and-sanitation-for-all/.
Tarr, Matthew, Pheobe Zito, Edward Overton, Gregory Olson, Puspa Adkikari, and Christopher Reddy. 2016. "Weathering of Oil Spilled in the Marine Environment." *Oceanography* 29 (3): 126–35. https://doi.org/10.5670/oceanog.2016.77.
Tkalich, Pavlo, and Eng Soon Chan. 2002. "Vertical Mixing of Oil Droplets by Breaking Waves." *Marine Pollution Bulletin* 44 (11): 1219–29. https://doi.org/10.1016/S0025-326X(02)00178-9.
Tzanakakis, Vasileios A., Nikolaos V. Paranychianakis, and Andreas N. Angelakis. 2020. "Water Supply and Water Scarcity." *Water* 12 (9): 2347. https://doi.org/10.3390/w12092347.
Vaughan, Grace O., Noura Al-Mansoori, and John A. Burt. 2019. "Chapter 1 - The Arabian Gulf." In *World Seas: An Environmental Evaluation (Second Edition)*, edited by Charles Sheppard, 1–23. Academic Press. https://doi.org/10.1016/B978-0-08-100853-9.00001-4.
"Water Scarcity | Threats | WWF." n.d. World Wildlife Fund. Accessed May 26, 2021. https://www.worldwildlife.org/threats/water-scarcity.

"Water Worries: The Future of Desalination in the UAE." 2020. *Arab Gulf States Institute in Washington* (blog). March 4, 2020. https://agsiw.org/water-worries-the-future-of-desalination-in-the-uae/.

Zhang, Baiyu, Ethan J. Matchinski, Bing Chen, Xudong Ye, Liang Jing, and Kenneth Lee. 2019. "Chapter 21 - Marine Oil Spills—Oil Pollution, Sources and Effects." In *World Seas: An Environmental Evaluation (Second Edition)*, edited by Charles Sheppard, 391–406. Academic Press. https://doi.org/10.1016/B978-0-12-805052-1.00024-3.

7 Appendices

A. Circulation pattern in the Arabian Gulf



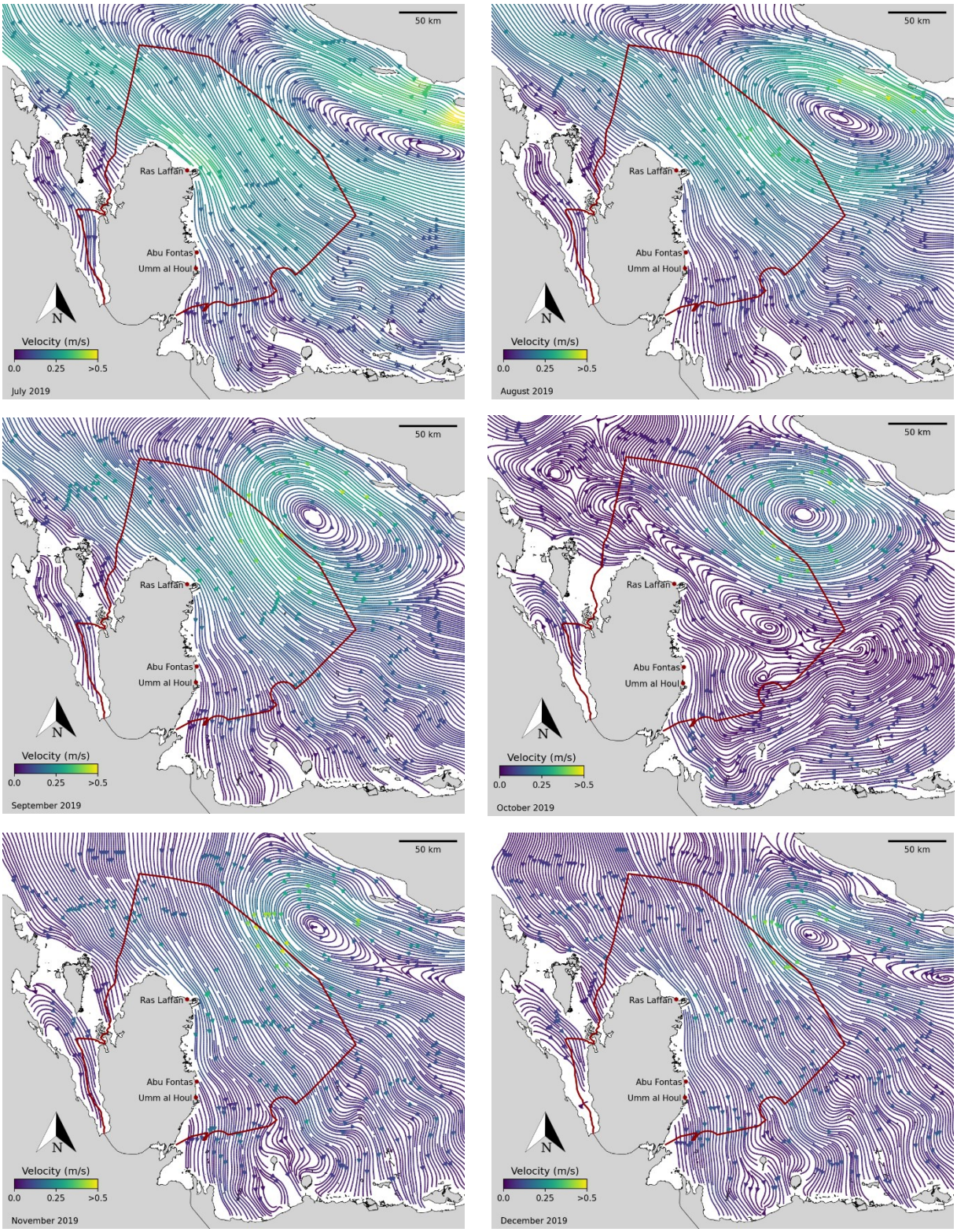
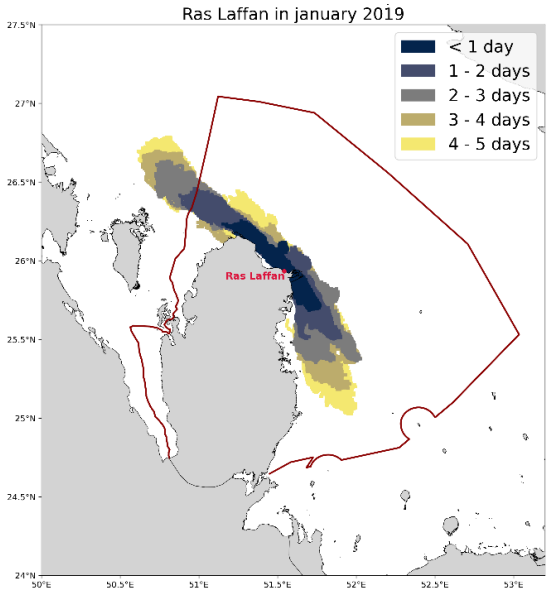
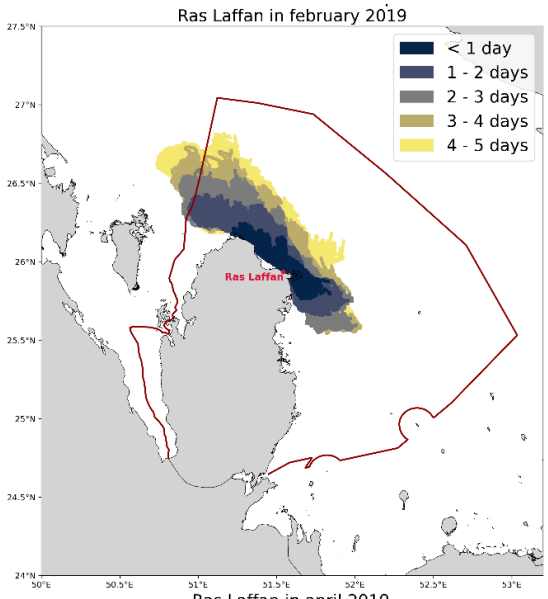
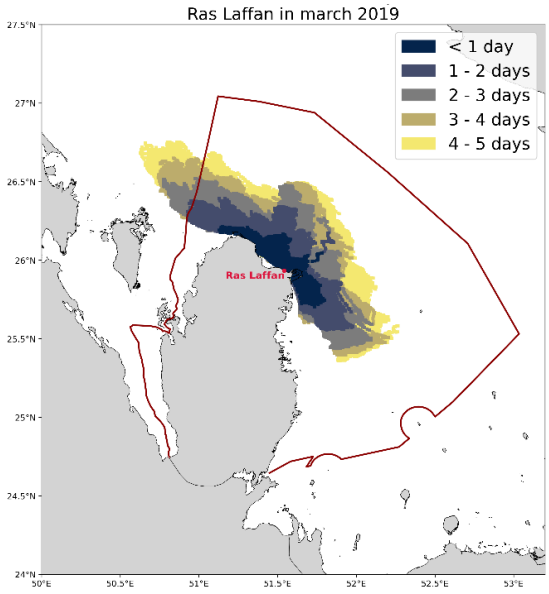


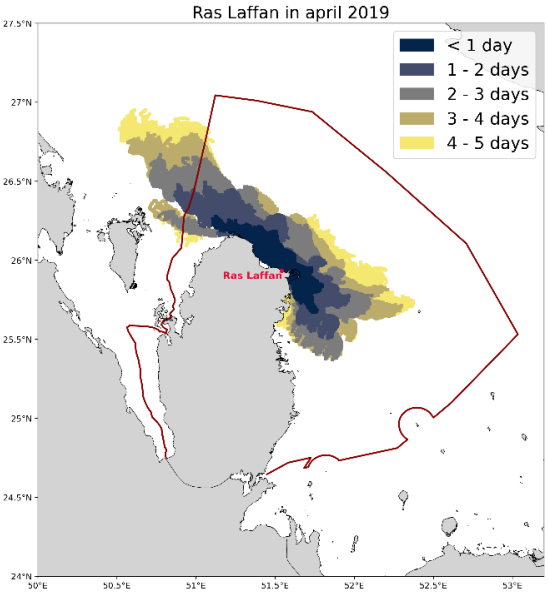
Figure 7.1 : Seasonal variability of the monthly-averaged ocean circulation around Qatar as simulated by the ocean model NEMO in 2019

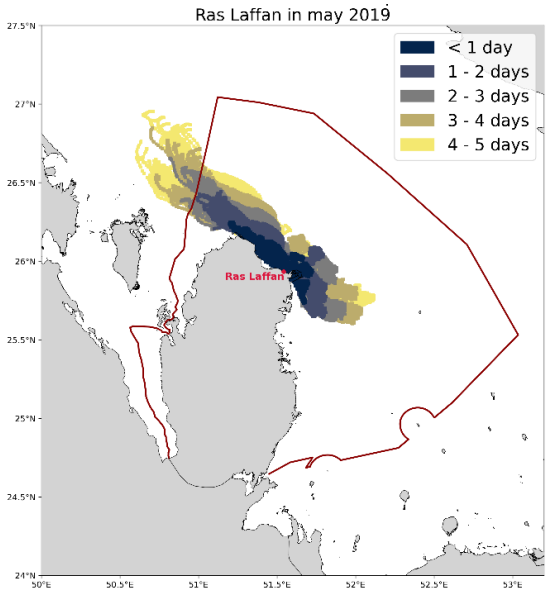
B. Minimum arrival time maps

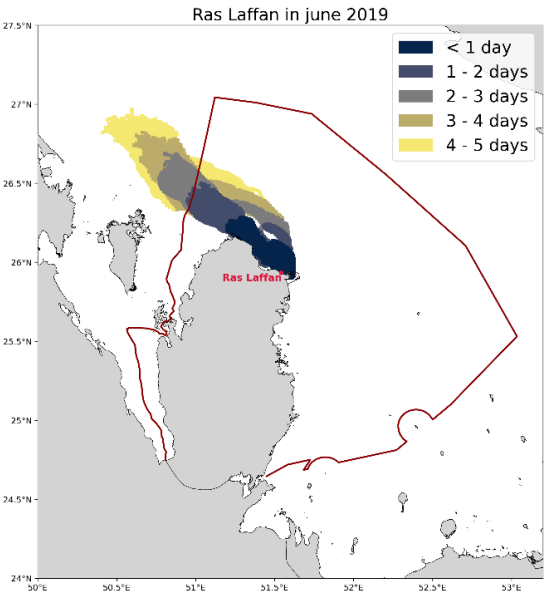












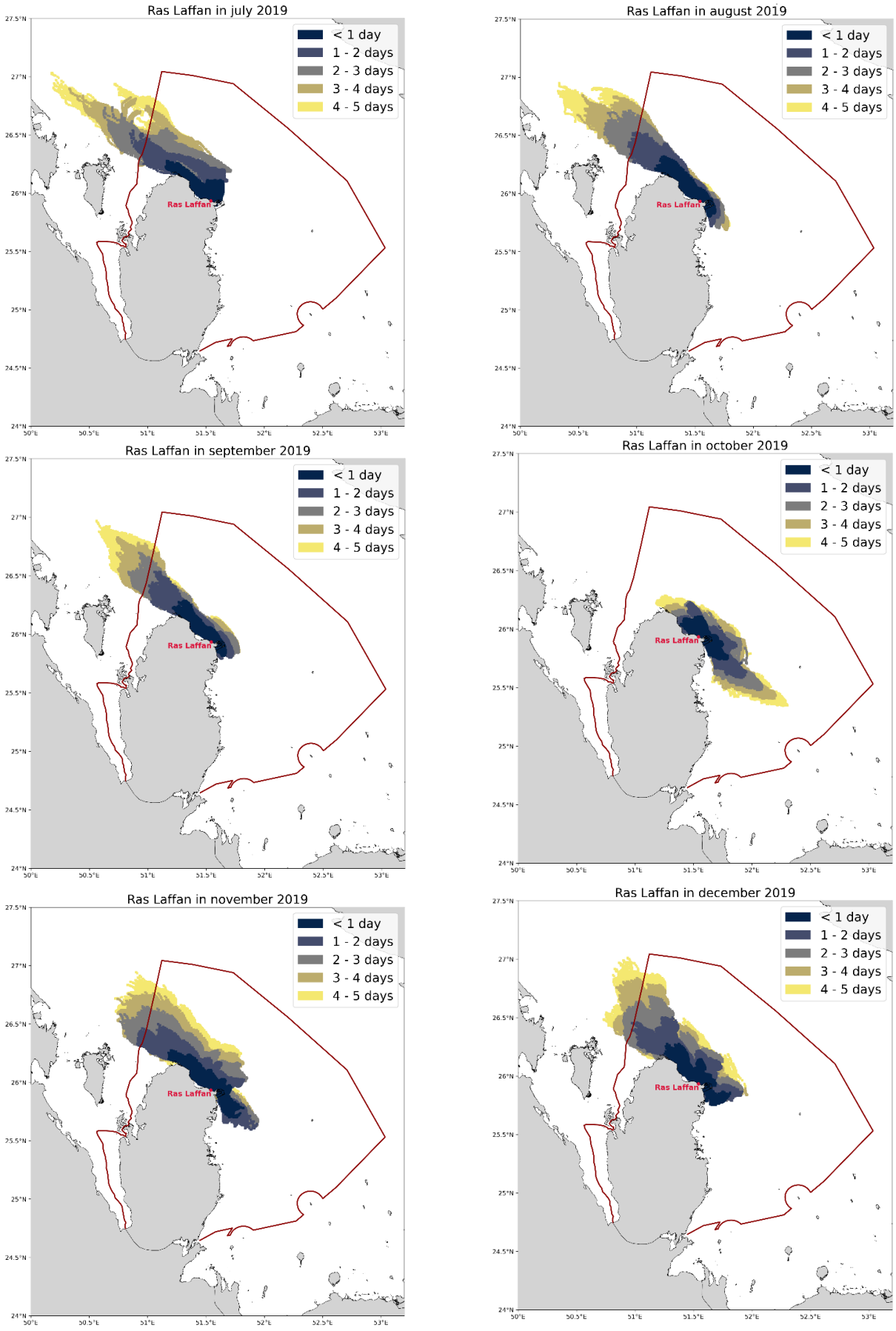
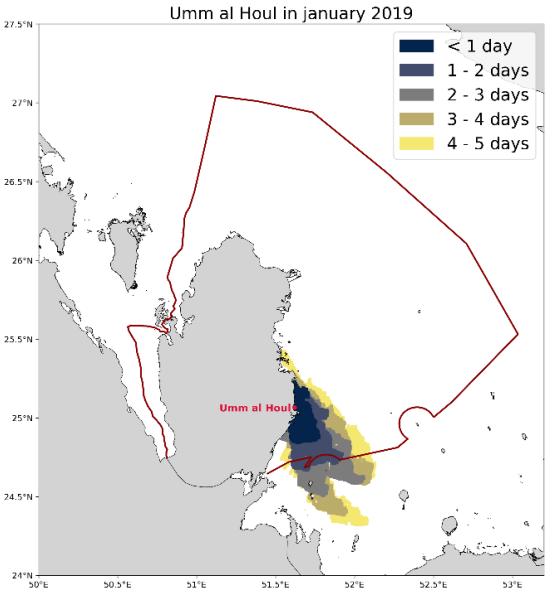
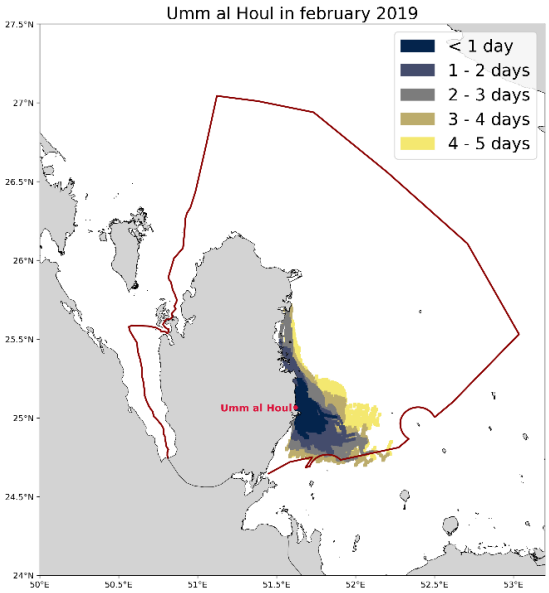
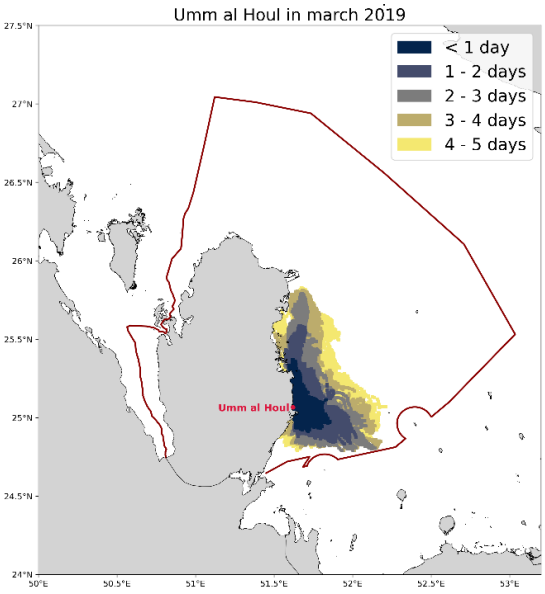
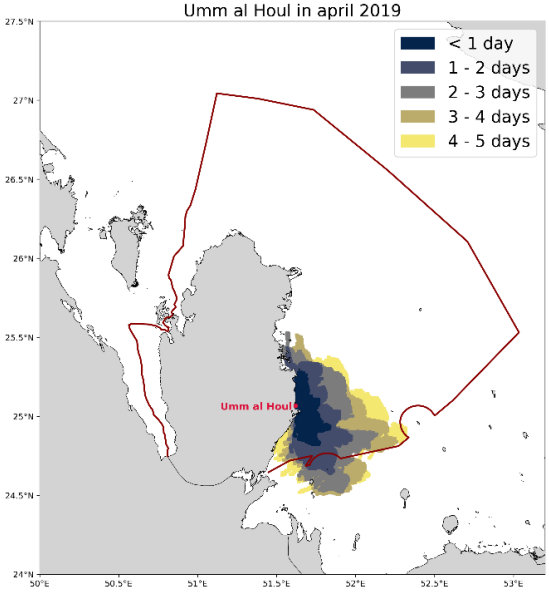


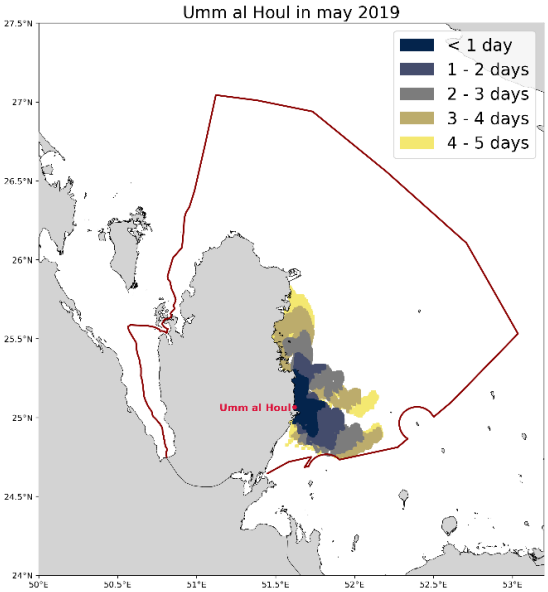
Figure 7.2 : Minimum arrival time of oil spill for Ras Laffan in 2019

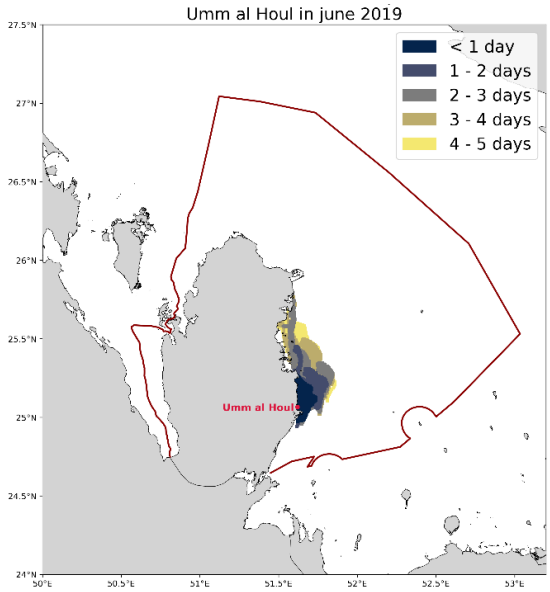

Umm al Houl in january 2019
< 1 day
1 - 2 days
2 - 3 days
3 - 4 days
4 - 5 days
Umm al Houl


Umm al Houl in february 2019
< 1 day
1 - 2 days
2 - 3 days
3 - 4 days
4 - 5 days
Umm al Houl


Umm al Houl in march 2019
< 1 day
1 - 2 days
2 - 3 days
3 - 4 days
4 - 5 days
Umm al Houl


Umm al Houl in april 2019
< 1 day
1 - 2 days
2 - 3 days
3 - 4 days
4 - 5 days
Umm al Houl


Umm al Houl in may 2019
< 1 day
1 - 2 days
2 - 3 days
3 - 4 days
4 - 5 days
Umm al Houl


Umm al Houl in june 2019
< 1 day
1 - 2 days
2 - 3 days
3 - 4 days
4 - 5 days
Umm al Houl

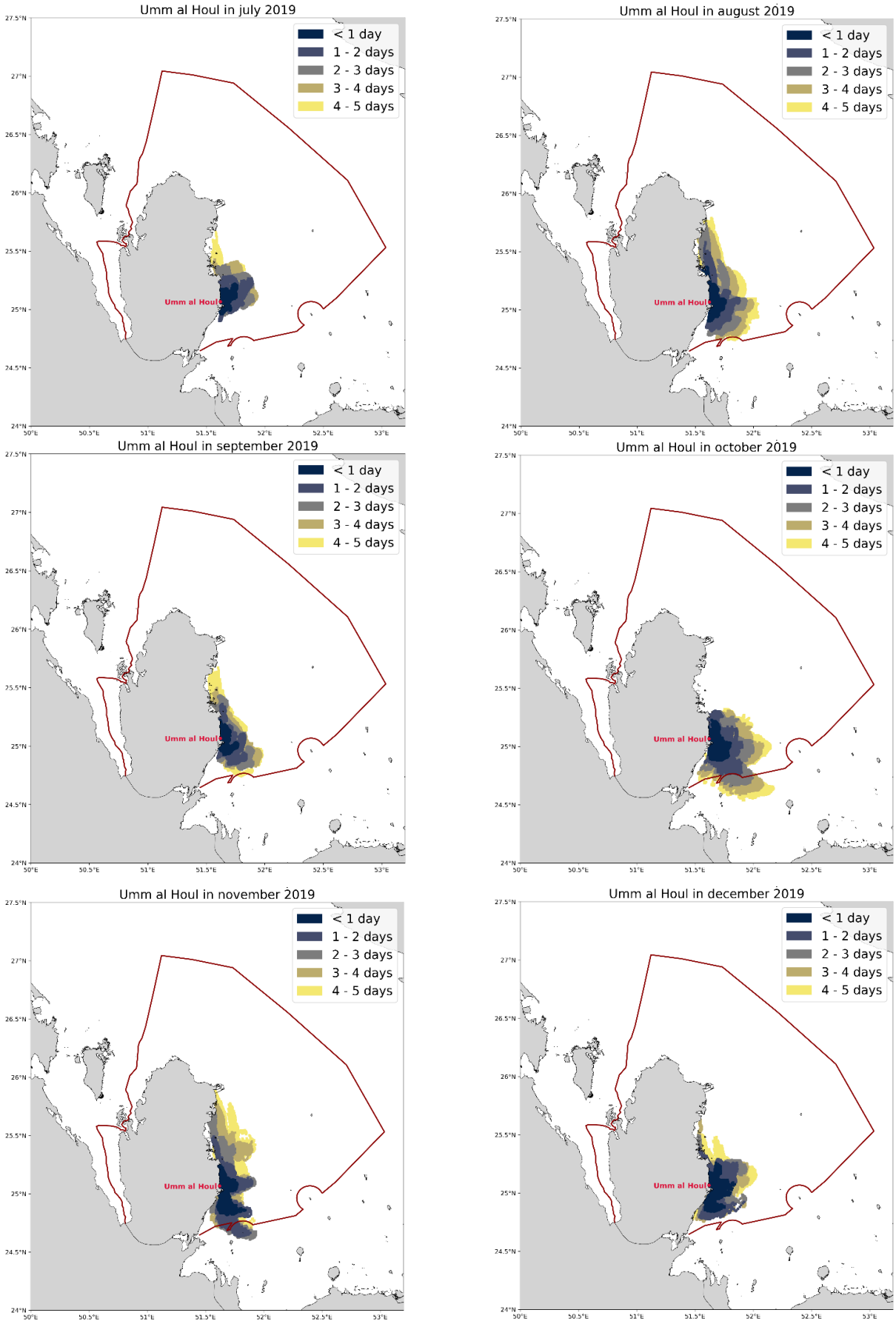
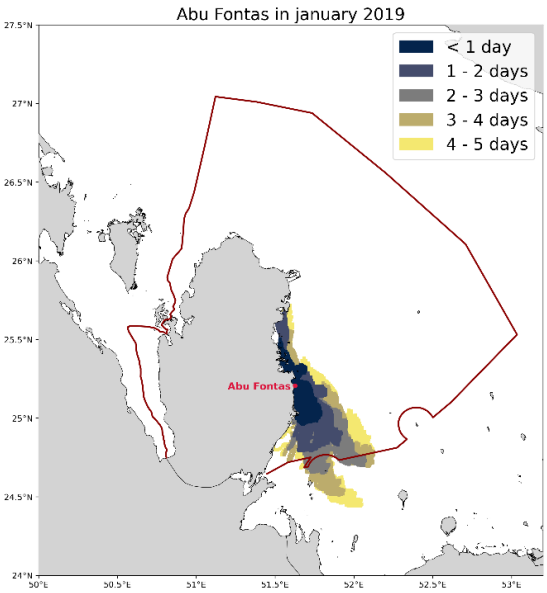
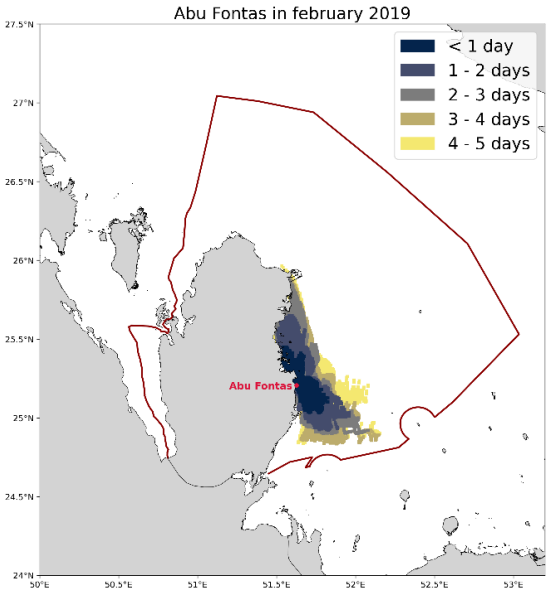
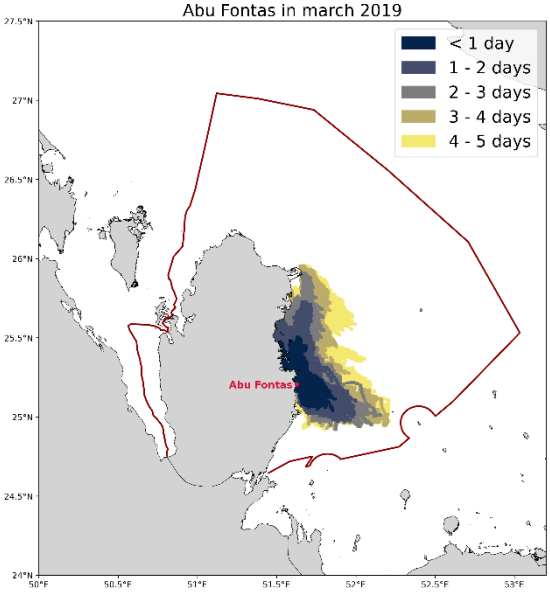
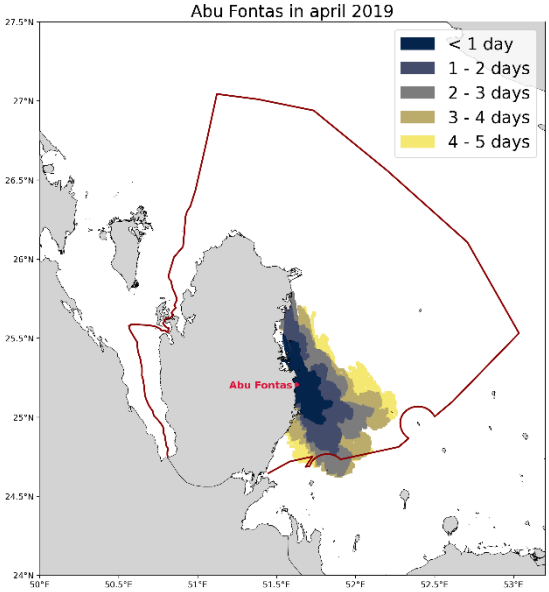


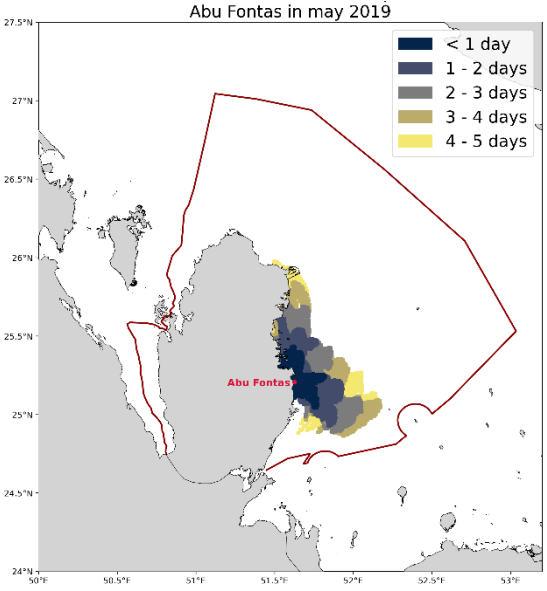
Figure 7.3 : Minimum arrival time of oil spill for Umm al Houl in 2019

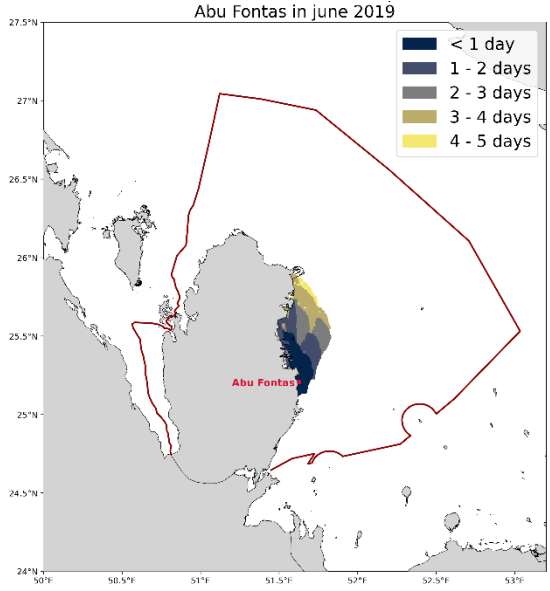

Abu Fontas in january 2019
< 1 day
1 - 2 days
2 - 3 days
3 - 4 days
4 - 5 days
Abu Fontas


Abu Fontas in february 2019
< 1 day
1 - 2 days
2 - 3 days
3 - 4 days
4 - 5 days
Abu Fontas


Abu Fontas in march 2019
< 1 day
1 - 2 days
2 - 3 days
3 - 4 days
4 - 5 days
Abu Fontas


Abu Fontas in april 2019
< 1 day
1 - 2 days
2 - 3 days
3 - 4 days
4 - 5 days
Abu Fontas


Abu Fontas in may 2019
< 1 day
1 - 2 days
2 - 3 days
3 - 4 days
4 - 5 days
Abu Fontas


Abu Fontas in june 2019
< 1 day
1 - 2 days
2 - 3 days
3 - 4 days
4 - 5 days
Abu Fontas

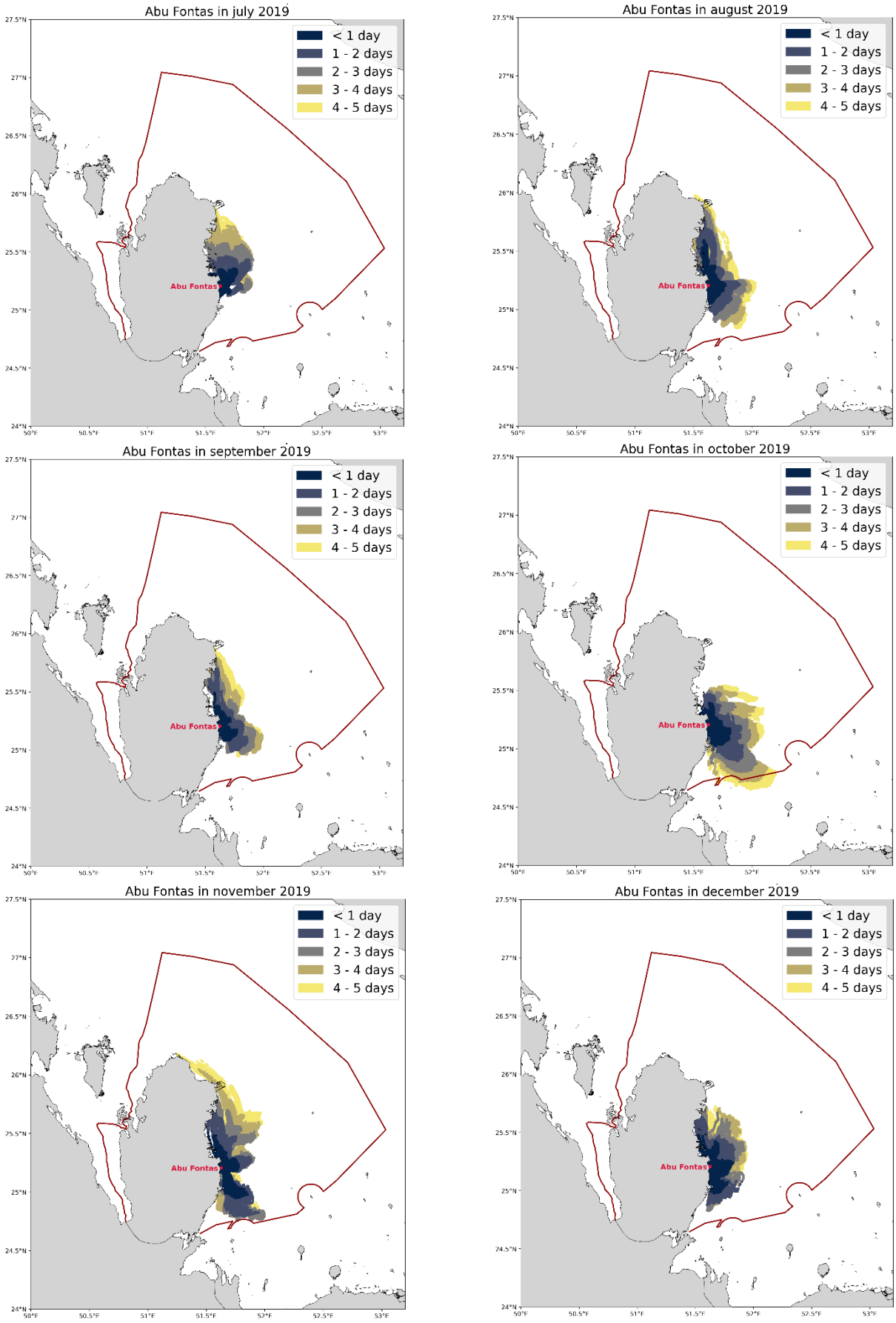
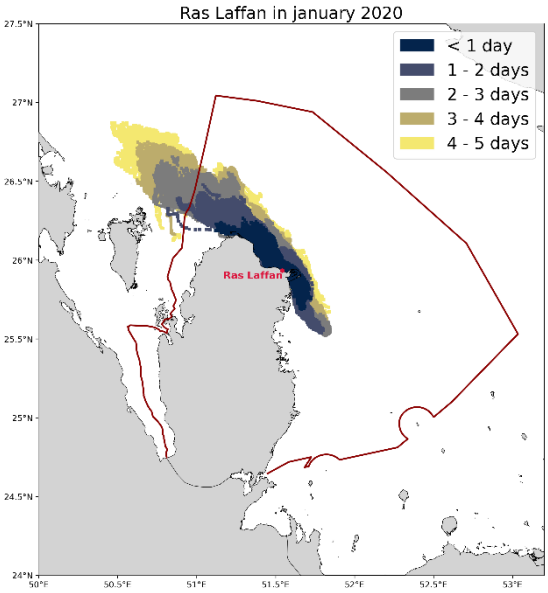
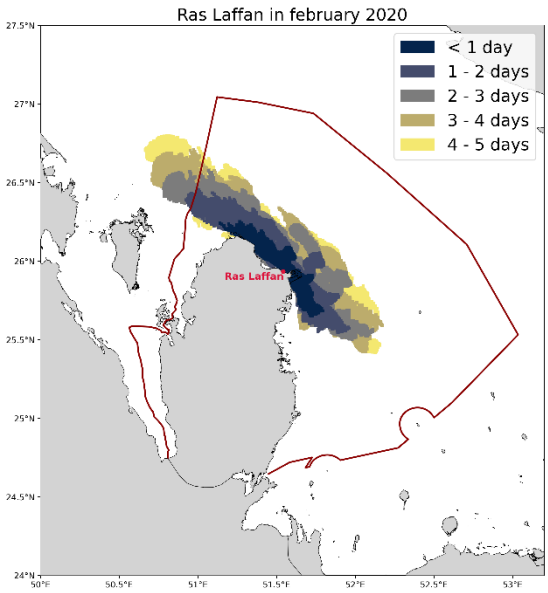
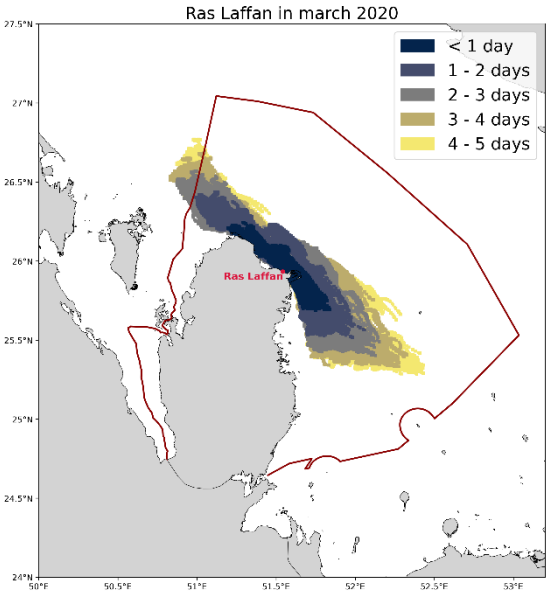
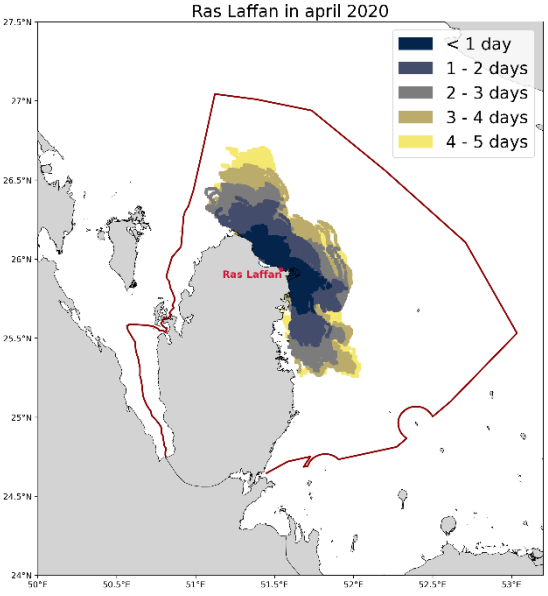


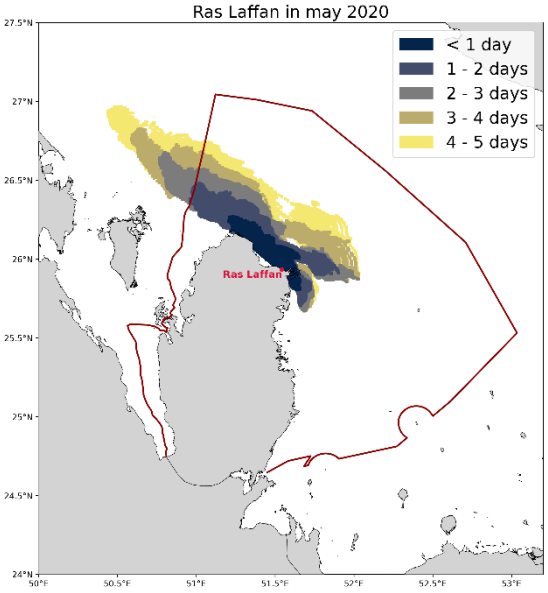
Figure 7.4 : Minimum arrival time of oil spill for Abu Fontas in 2019

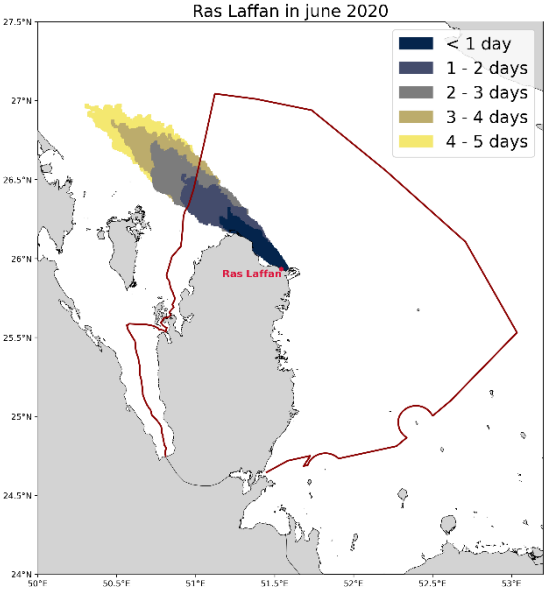

Ras Laffan in january 2020
< 1 day
1 - 2 days
2 - 3 days
3 - 4 days
4 - 5 days
Ras Laffan


Ras Laffan in february 2020
< 1 day
1 - 2 days
2 - 3 days
3 - 4 days
4 - 5 days
Ras Laffan


Ras Laffan in march 2020
< 1 day
1 - 2 days
2 - 3 days
3 - 4 days
4 - 5 days
Ras Laffan


Ras Laffan in april 2020
< 1 day
1 - 2 days
2 - 3 days
3 - 4 days
4 - 5 days
Ras Laffan


Ras Laffan in may 2020
< 1 day
1 - 2 days
2 - 3 days
3 - 4 days
4 - 5 days
Ras Laffan


Ras Laffan in june 2020
< 1 day
1 - 2 days
2 - 3 days
3 - 4 days
4 - 5 days
Ras Laffan

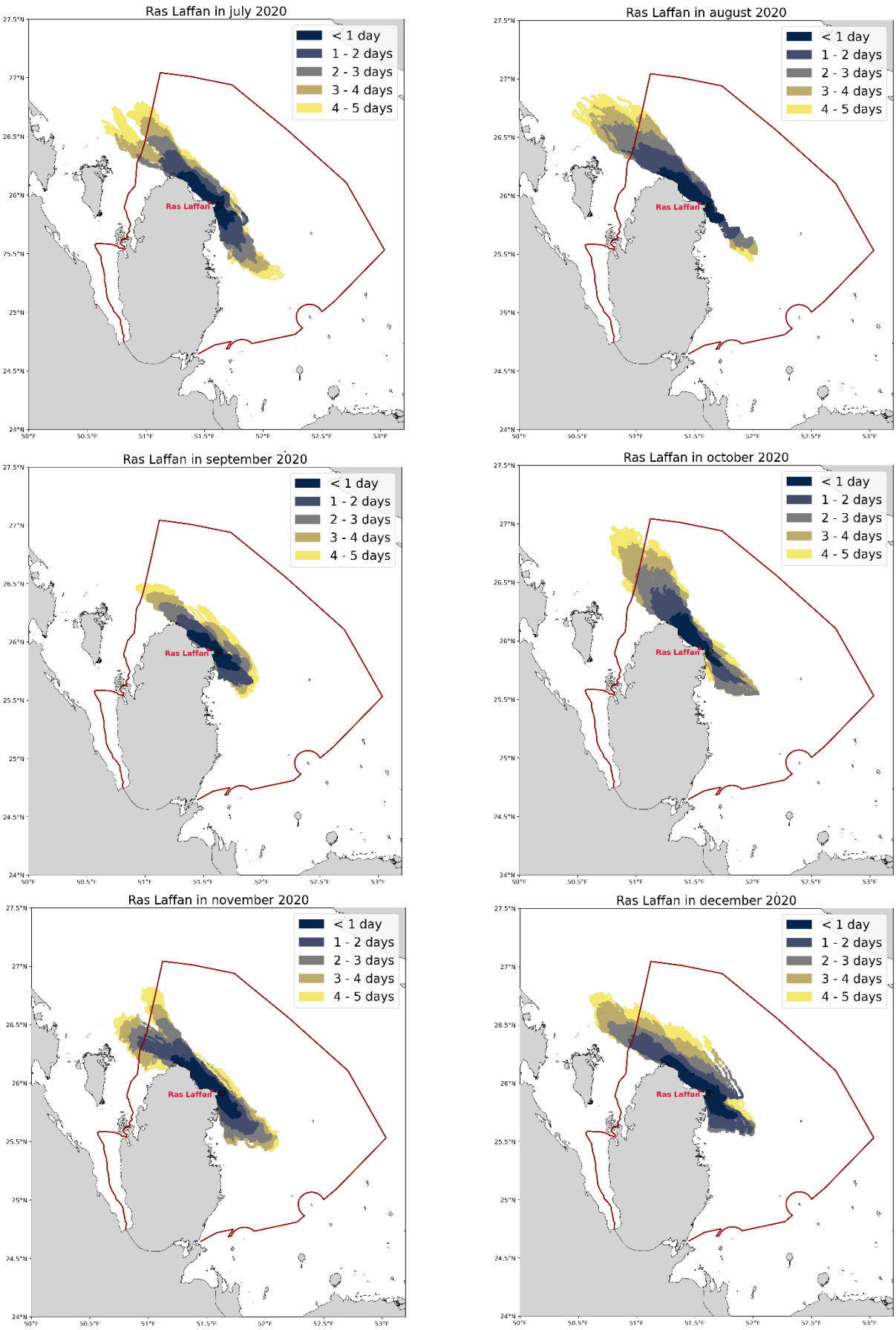
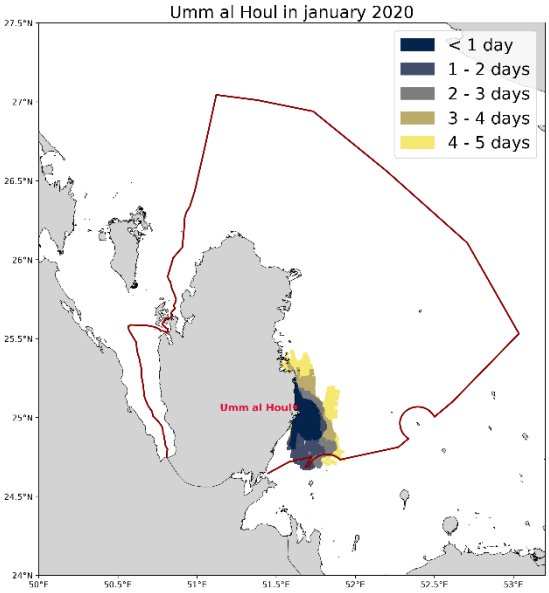
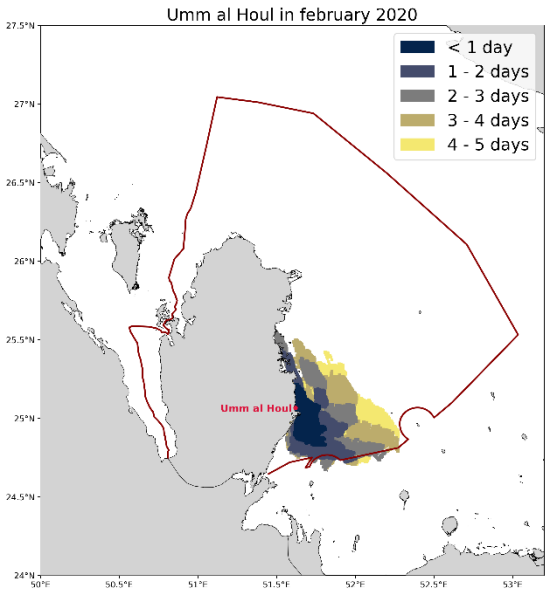
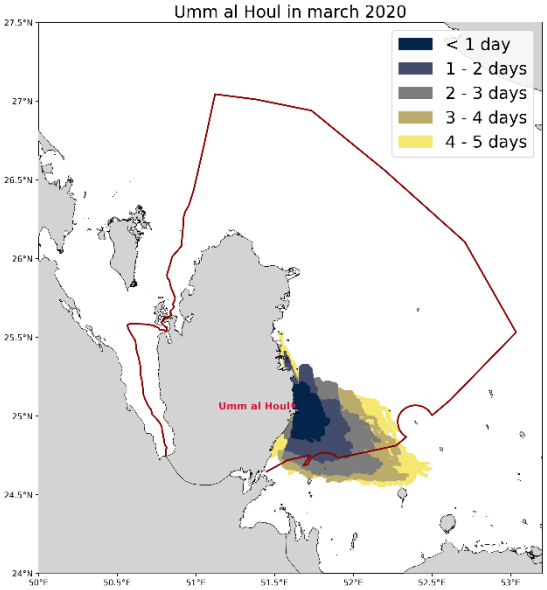
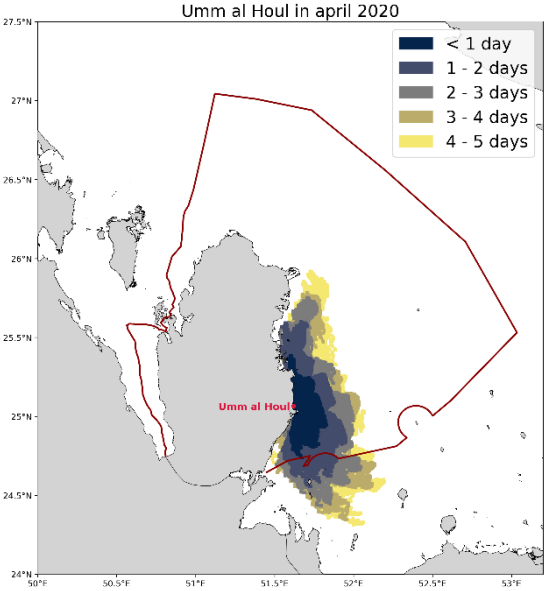


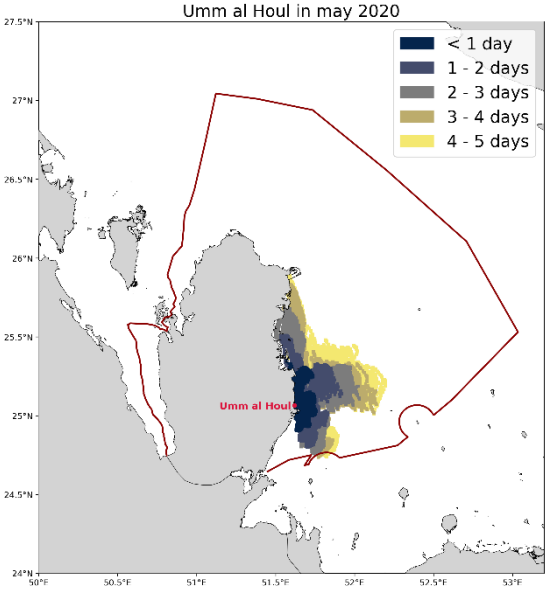
Figure 7.5 : Minimum arrival time of oil spill for Ras Laffan in 2020

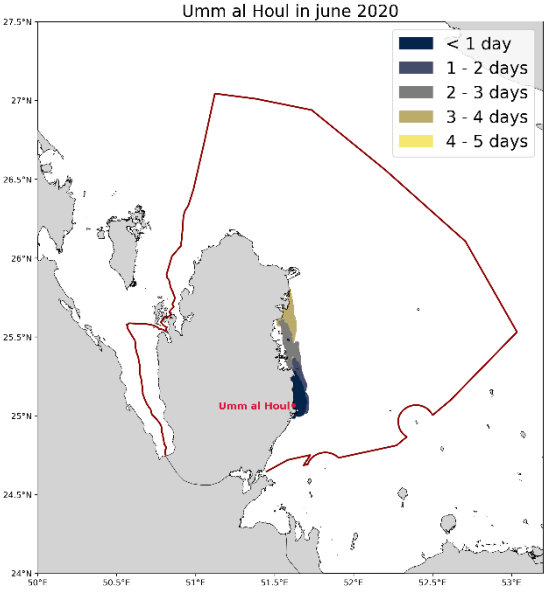

Umm al Houl in january 2020
< 1 day
1 - 2 days
2 - 3 days
3 - 4 days
4 - 5 days
Umm al Houl


Umm al Houl in february 2020
< 1 day
1 - 2 days
2 - 3 days
3 - 4 days
4 - 5 days
Umm al Houl


Umm al Houl in march 2020
< 1 day
1 - 2 days
2 - 3 days
3 - 4 days
4 - 5 days
Umm al Houl


Umm al Houl in april 2020
< 1 day
1 - 2 days
2 - 3 days
3 - 4 days
4 - 5 days
Umm al Houl


Umm al Houl in may 2020
< 1 day
1 - 2 days
2 - 3 days
3 - 4 days
4 - 5 days
Umm al Houl


Umm al Houl in june 2020
< 1 day
1 - 2 days
2 - 3 days
3 - 4 days
4 - 5 days
Umm al Houl

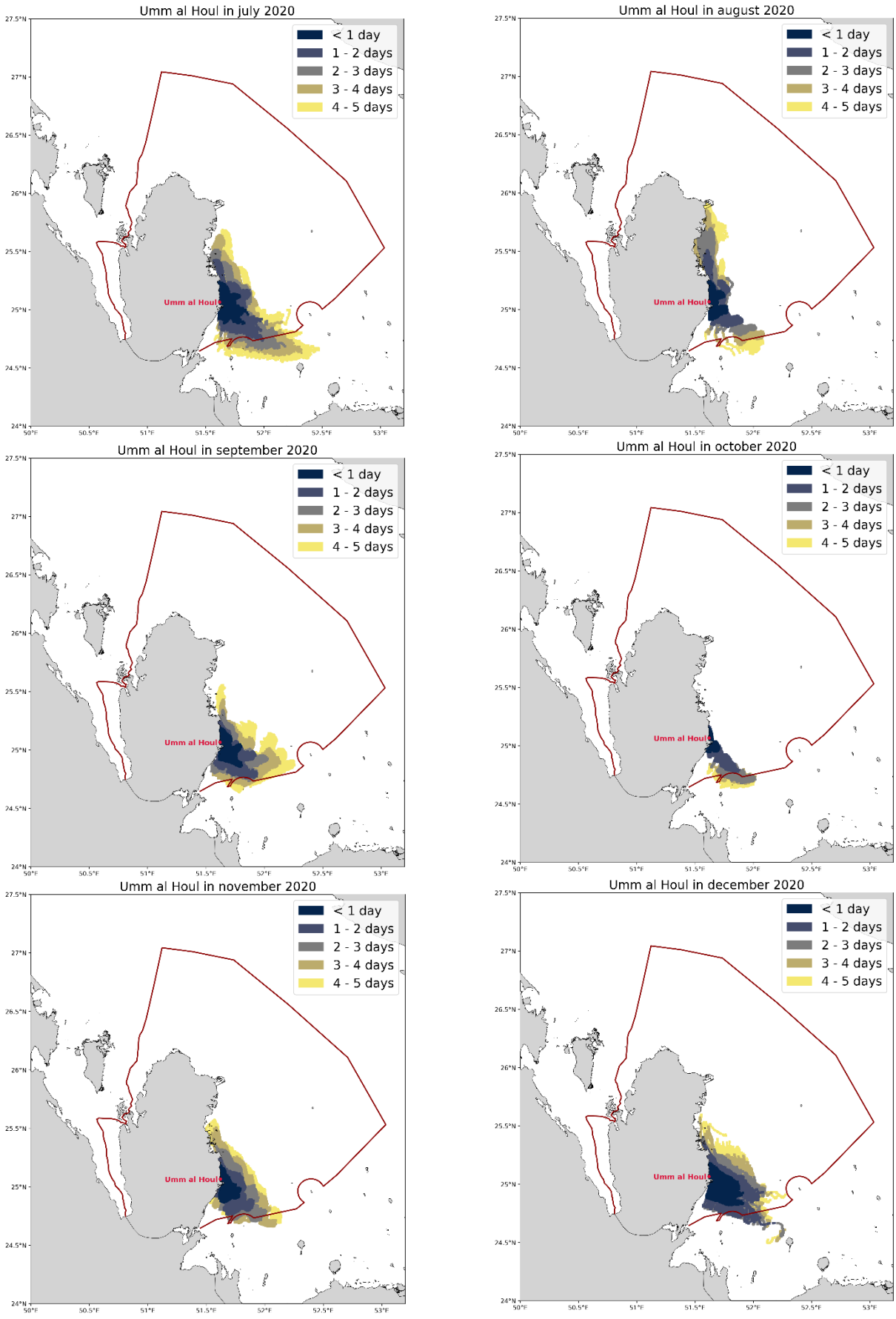
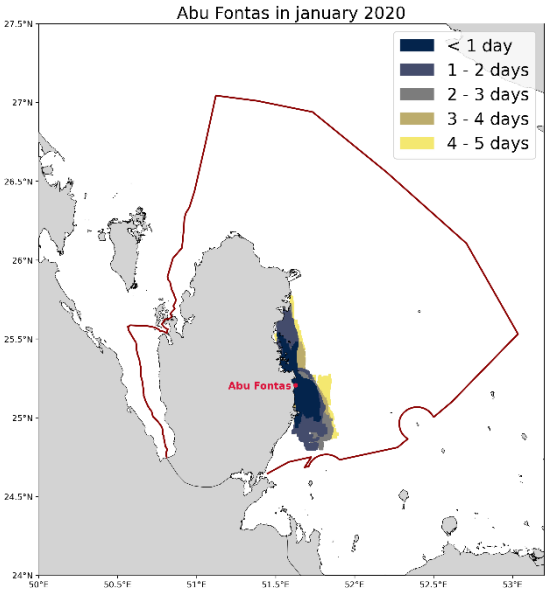
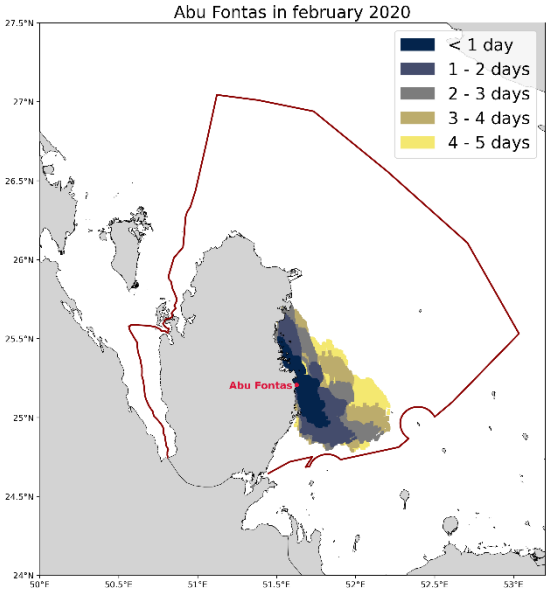
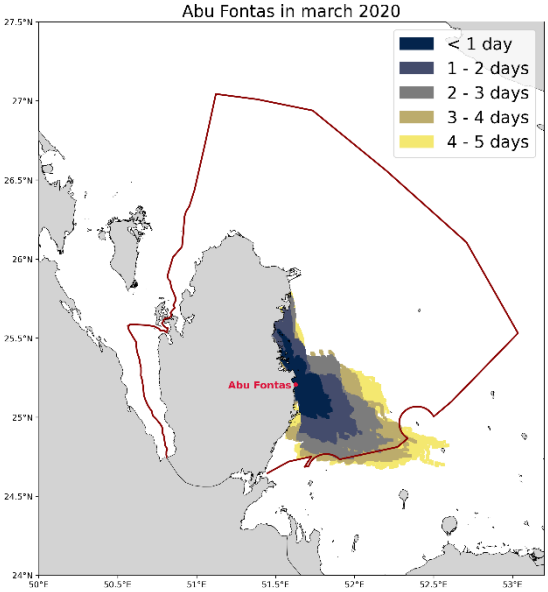
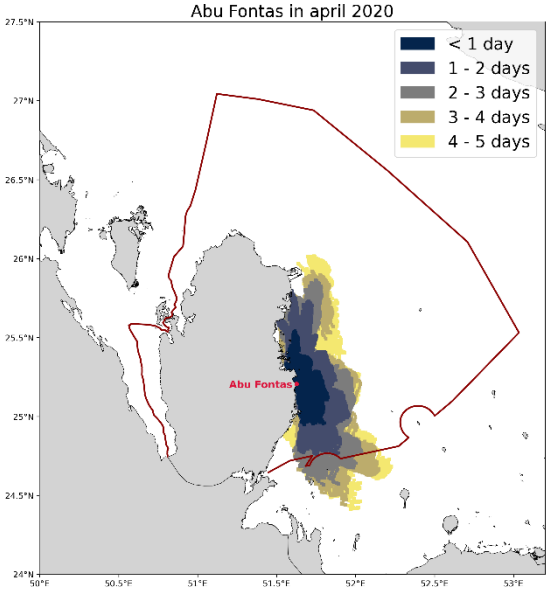


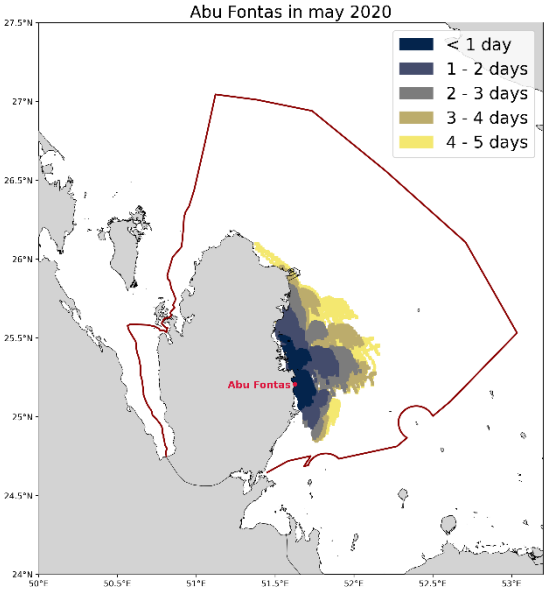
Figure 7.6 : Minimum arrival time of oil spill for Umm al Houl in 2020

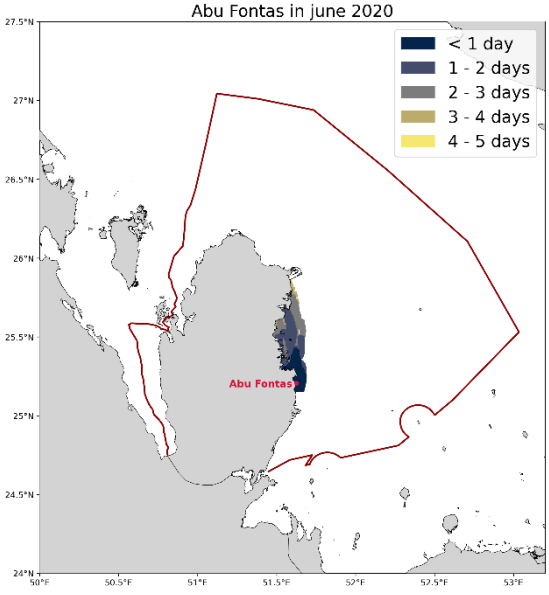

Abu Fontas in january 2020
< 1 day
1 - 2 days
2 - 3 days
3 - 4 days
4 - 5 days
Abu Fontas


Abu Fontas in february 2020
< 1 day
1 - 2 days
2 - 3 days
3 - 4 days
4 - 5 days
Abu Fontas


Abu Fontas in march 2020
< 1 day
1 - 2 days
2 - 3 days
3 - 4 days
4 - 5 days
Abu Fontas


Abu Fontas in april 2020
< 1 day
1 - 2 days
2 - 3 days
3 - 4 days
4 - 5 days
Abu Fontas


Abu Fontas in may 2020
< 1 day
1 - 2 days
2 - 3 days
3 - 4 days
4 - 5 days
Abu Fontas


Abu Fontas in june 2020
< 1 day
1 - 2 days
2 - 3 days
3 - 4 days
4 - 5 days
Abu Fontas

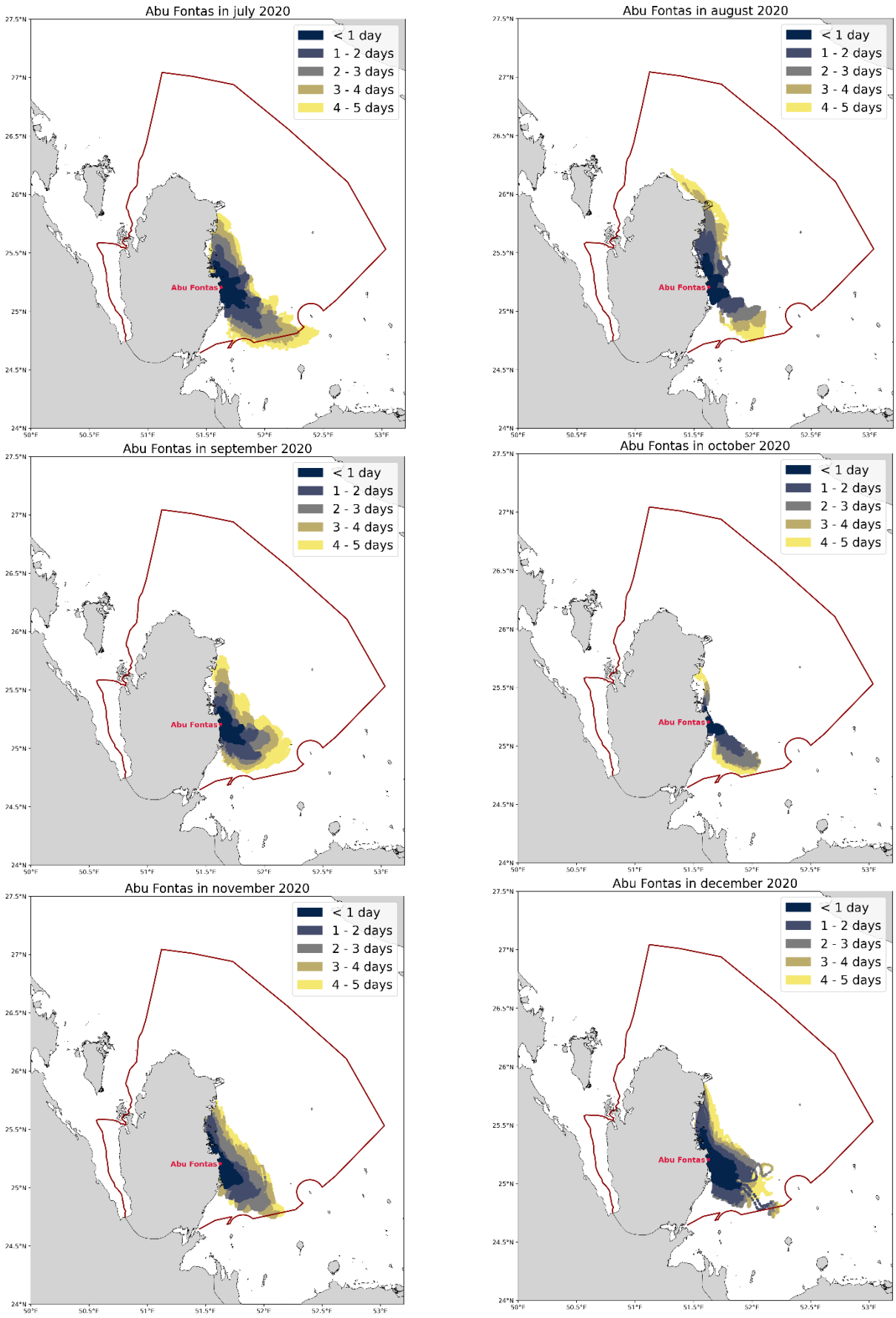
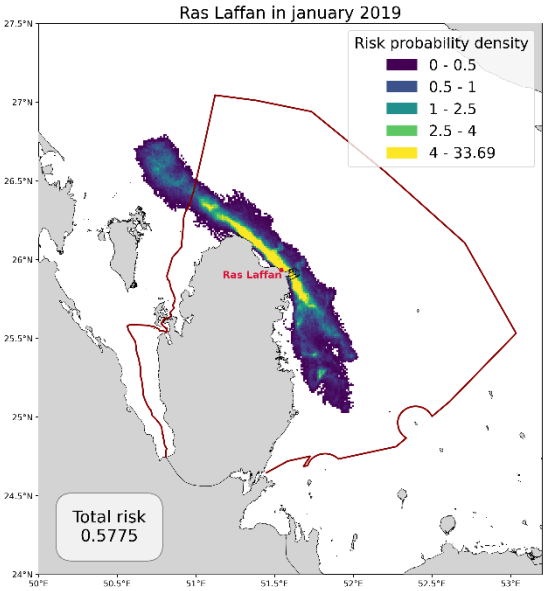
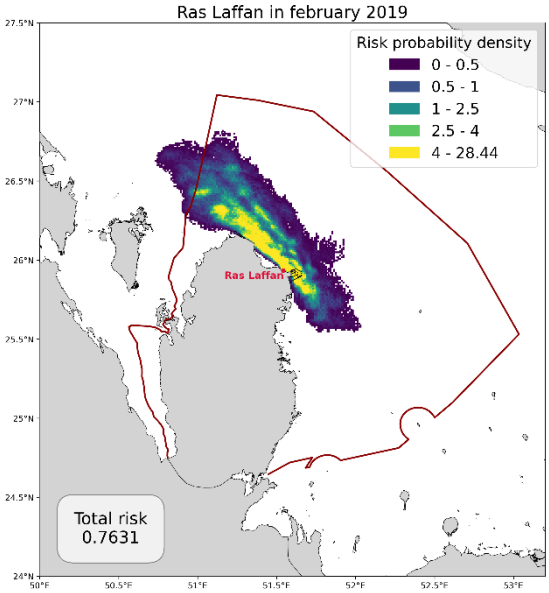
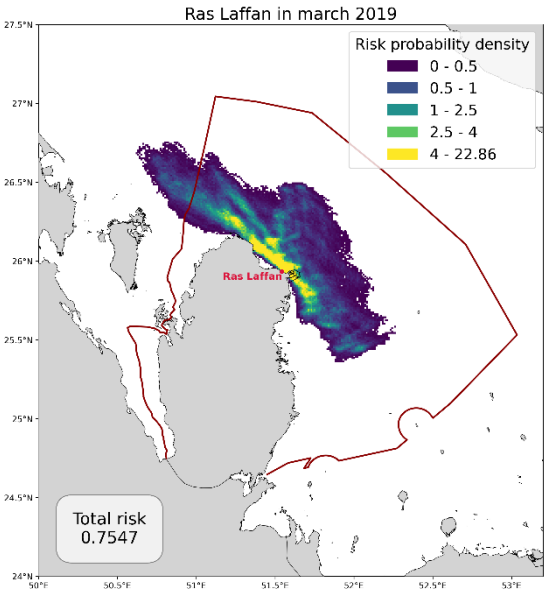


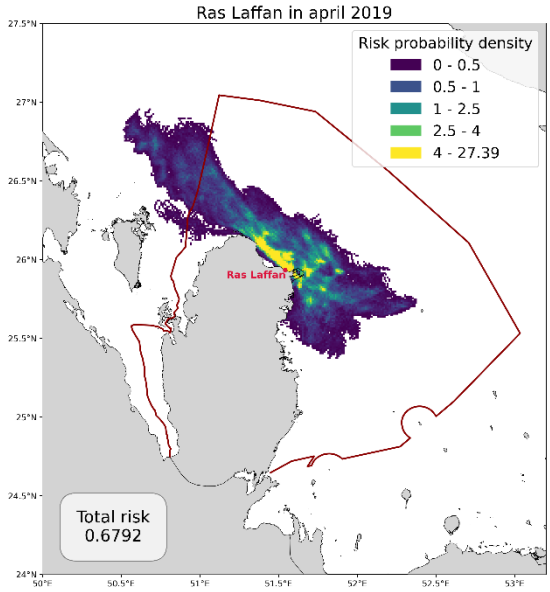
Figure 7.7 : Minimum arrival time of oil spill for Abu Fontas in 2020

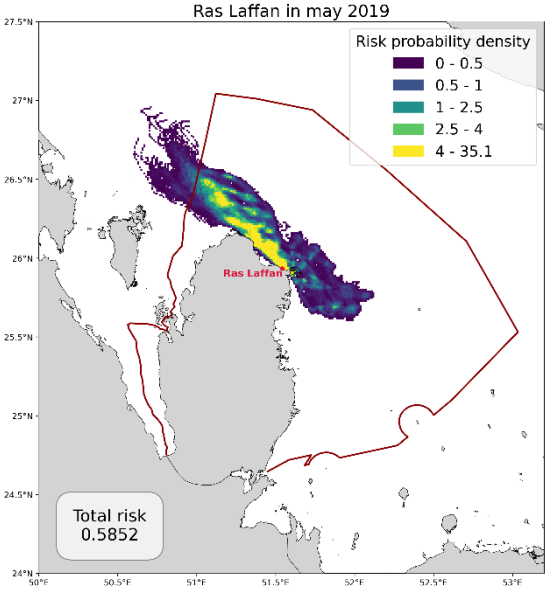
C. Oil risk density maps

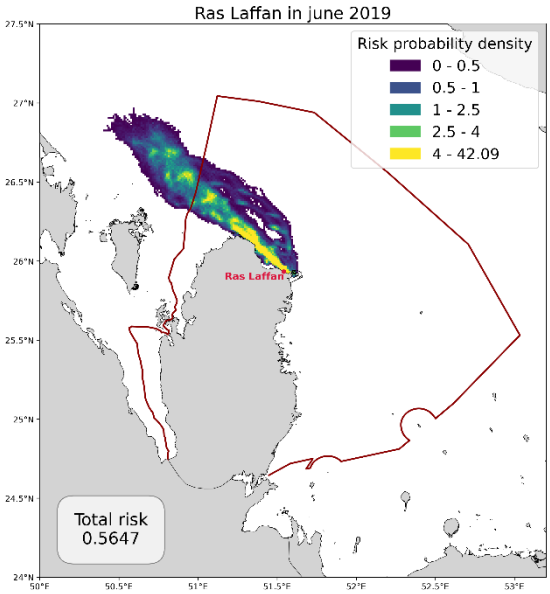












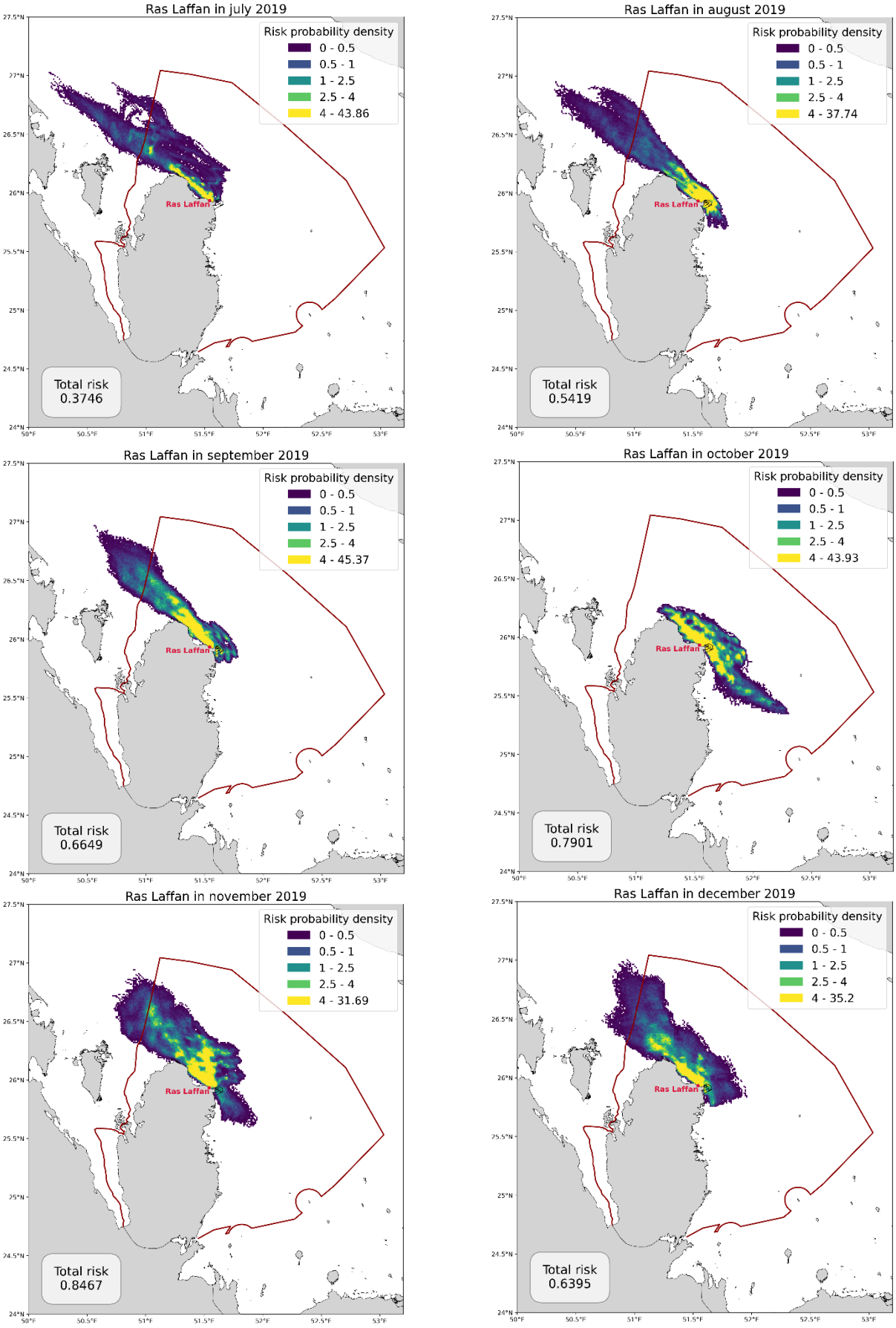
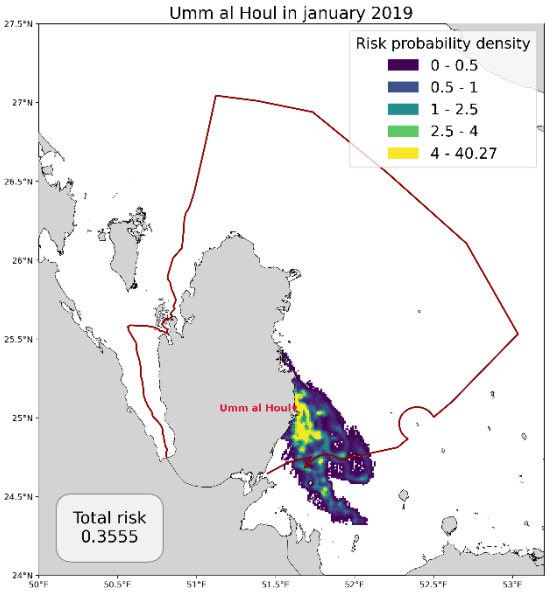
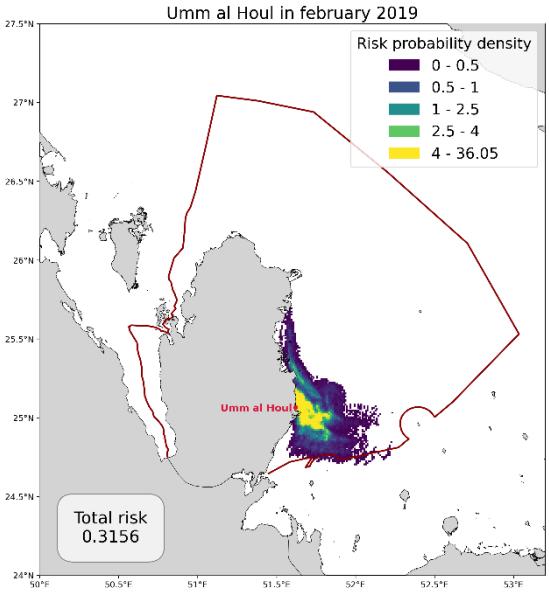
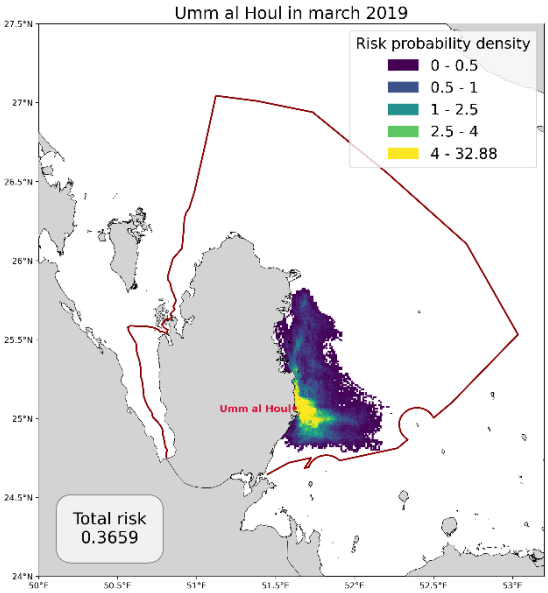
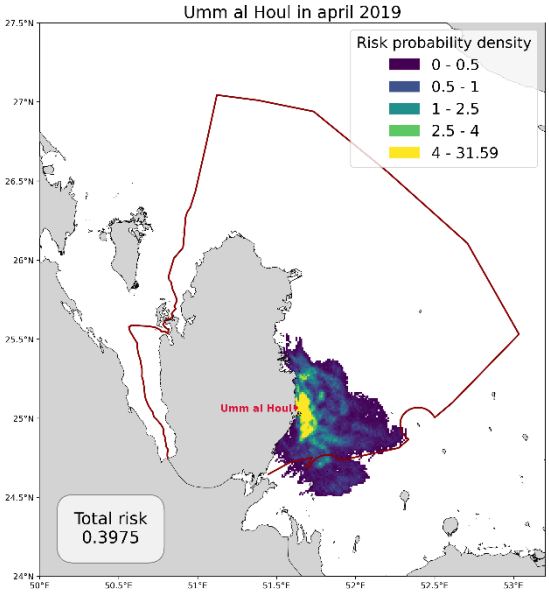


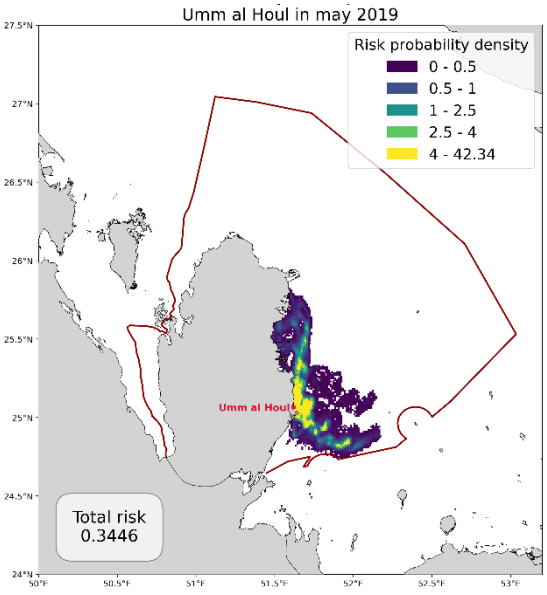
Figure 7.8 : Maps of oil risk probability density for Ras Laffan in 2019

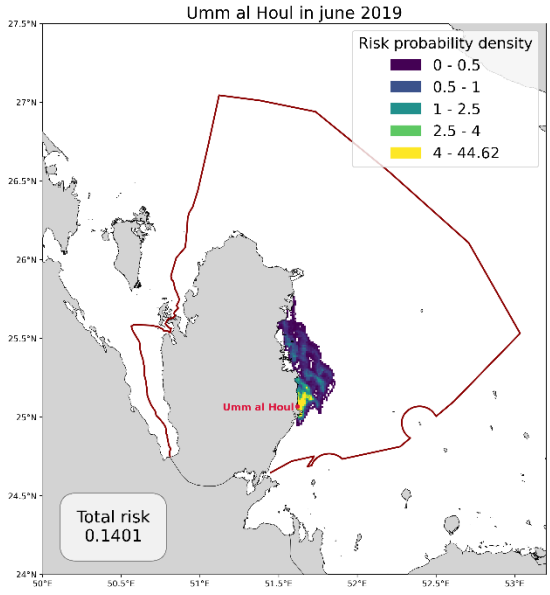

Umm al Houl in january 2019
Risk probability density
0 - 0.5
0.5 - 1
1 - 2.5
2.5 - 4
4 - 40.27
Umm al Houl
Total risk
0.3555


Umm al Houl in february 2019
Risk probability density
0 - 0.5
0.5 - 1
1 - 2.5
2.5 - 4
4 - 36.05
Umm al Houl
Total risk
0.3156


Umm al Houl in march 2019
Risk probability density
0 - 0.5
0.5 - 1
1 - 2.5
2.5 - 4
4 - 32.88
Umm al Houl
Total risk
0.3659


Umm al Houl in april 2019
Risk probability density
0 - 0.5
0.5 - 1
1 - 2.5
2.5 - 4
4 - 31.59
Umm al Houl
Total risk
0.3975


Umm al Houl in may 2019
Risk probability density
0 - 0.5
0.5 - 1
1 - 2.5
2.5 - 4
4 - 42.34
Umm al Houl
Total risk
0.3446


Umm al Houl in june 2019
Risk probability density
0 - 0.5
0.5 - 1
1 - 2.5
2.5 - 4
4 - 44.62
Umm al Houl
Total risk
0.1401

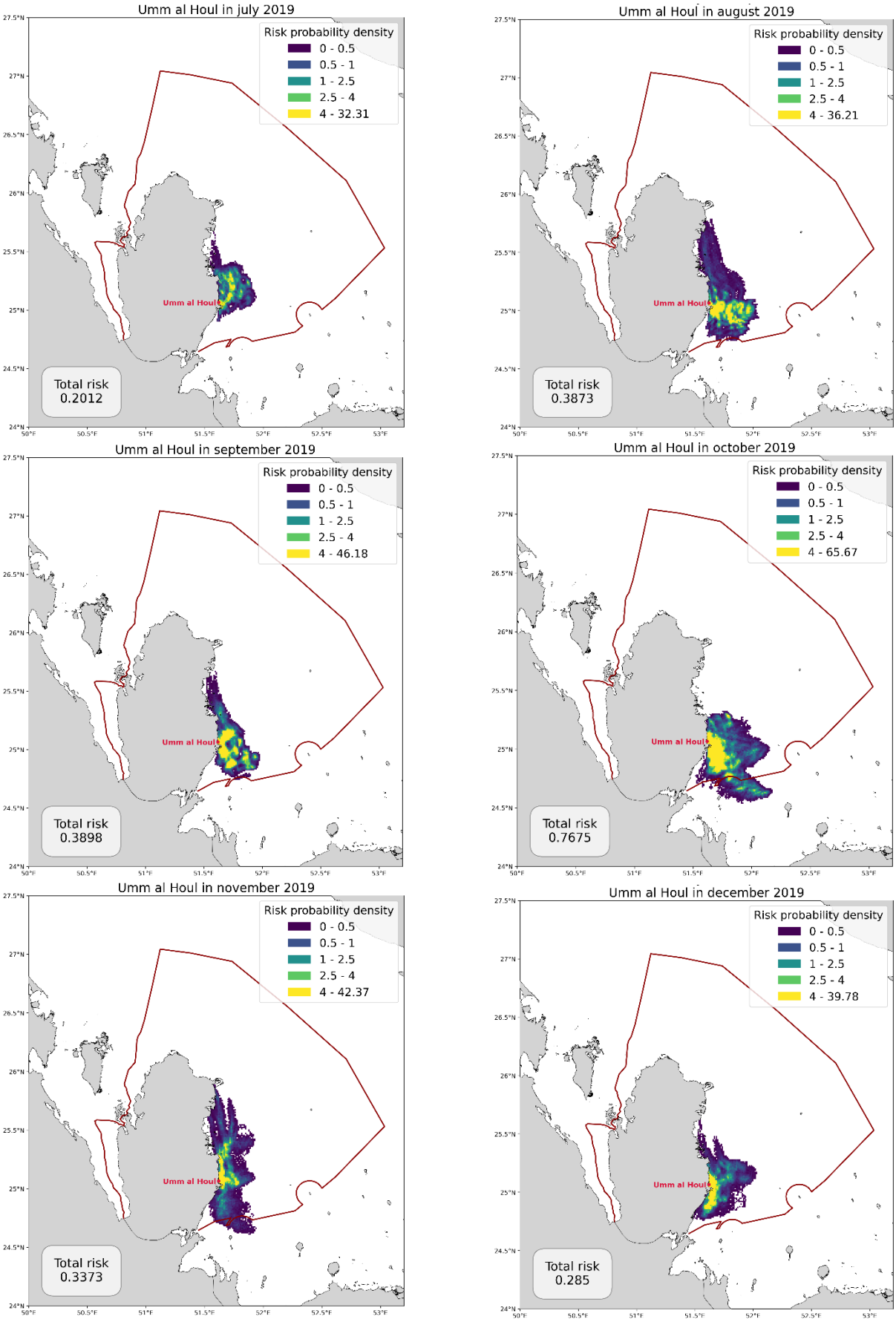
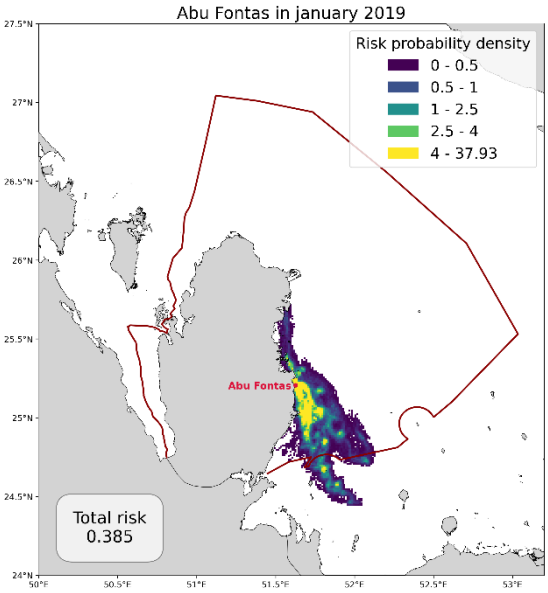
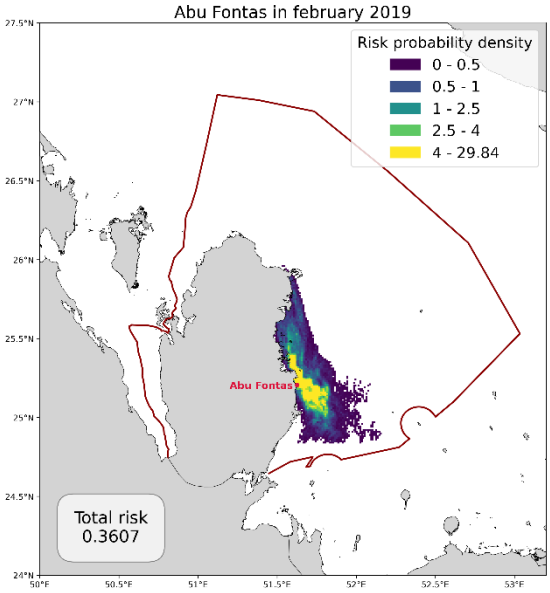
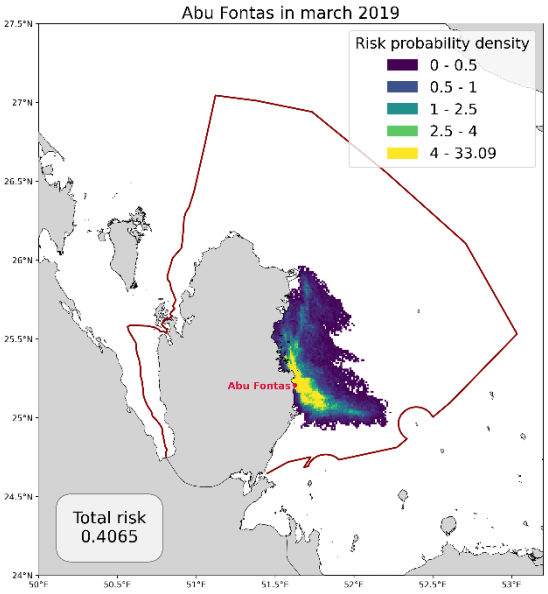
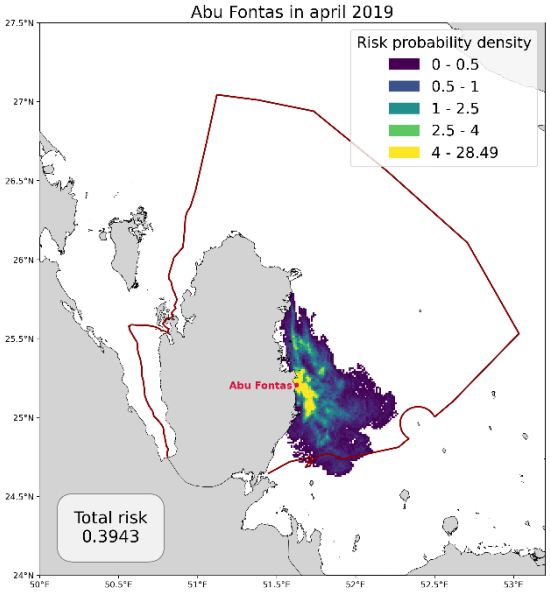


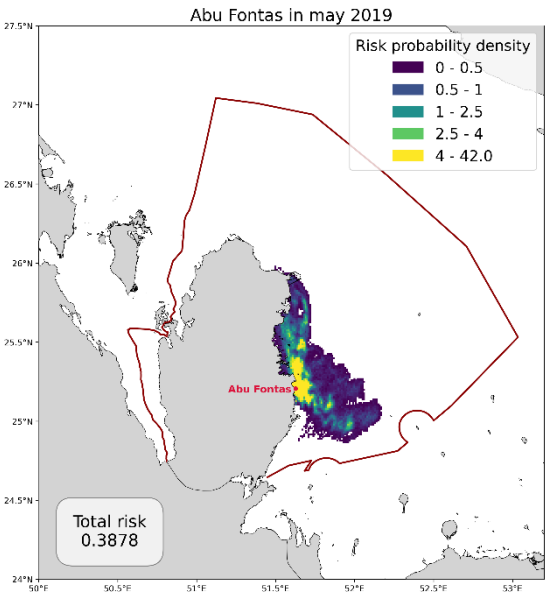
Figure 7.9 : Maps of oil risk probability density for Umm al Houl in 2019

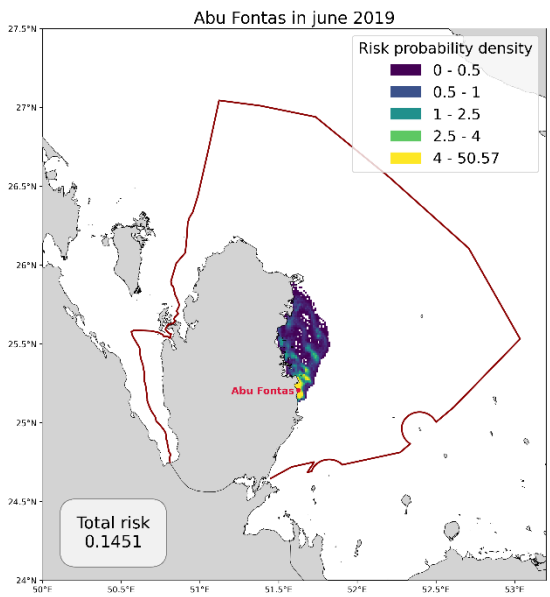

Abu Fontas in january 2019
Risk probability density
0 - 0.5
0.5 - 1
1 - 2.5
2.5 - 4
4 - 37.93
Abu Fontas
Total risk
0.385


Abu Fontas in february 2019
Risk probability density
0 - 0.5
0.5 - 1
1 - 2.5
2.5 - 4
4 - 29.84
Abu Fontas
Total risk
0.3607


Abu Fontas in march 2019
Risk probability density
0 - 0.5
0.5 - 1
1 - 2.5
2.5 - 4
4 - 33.09
Abu Fontas
Total risk
0.4065


Abu Fontas in april 2019
Risk probability density
0 - 0.5
0.5 - 1
1 - 2.5
2.5 - 4
4 - 28.49
Abu Fontas
Total risk
0.3943


Abu Fontas in may 2019
Risk probability density
0 - 0.5
0.5 - 1
1 - 2.5
2.5 - 4
4 - 42.0
Abu Fontas
Total risk
0.3878


Abu Fontas in june 2019
Risk probability density
0 - 0.5
0.5 - 1
1 - 2.5
2.5 - 4
4 - 50.57
Abu Fontas
Total risk
0.1451

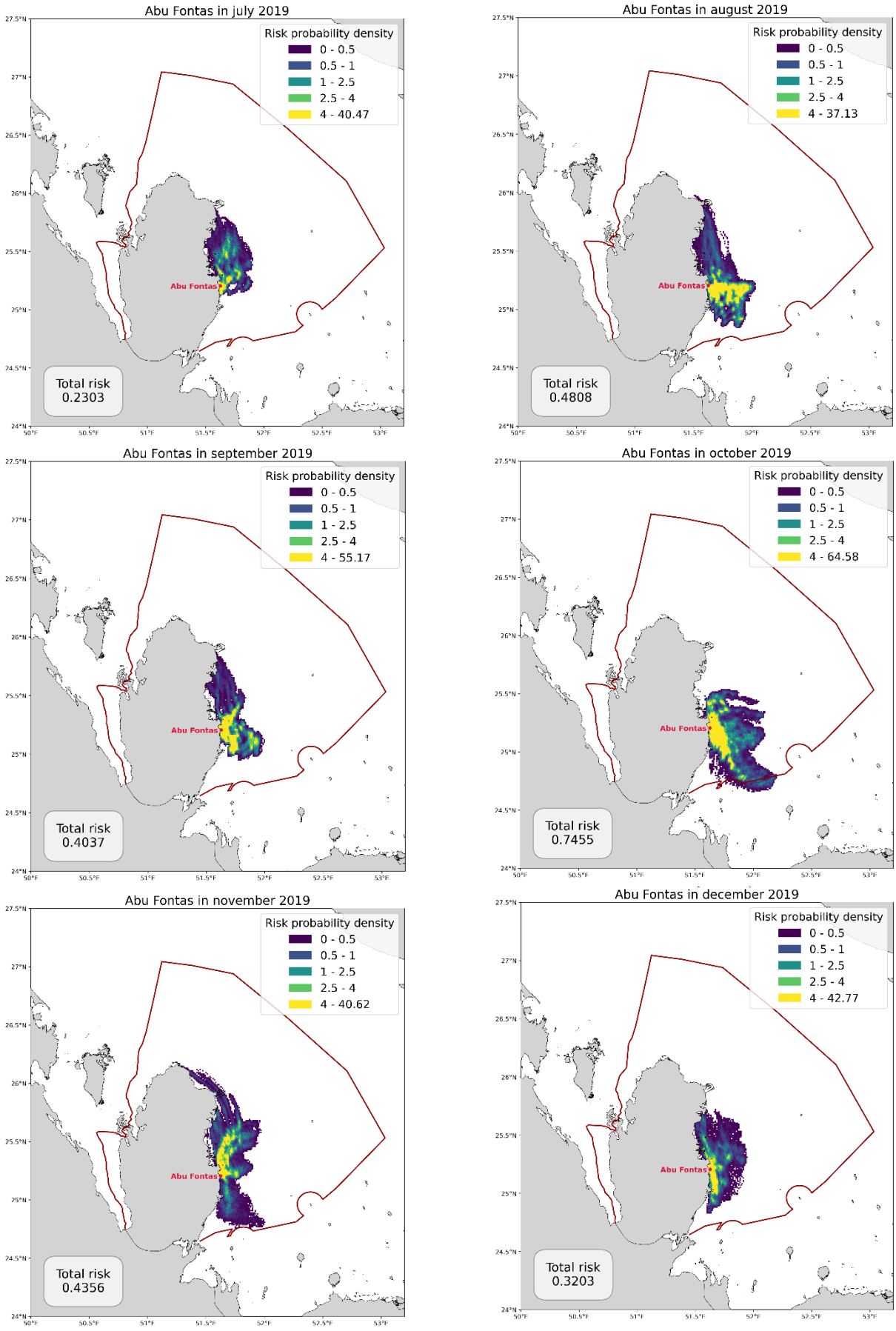
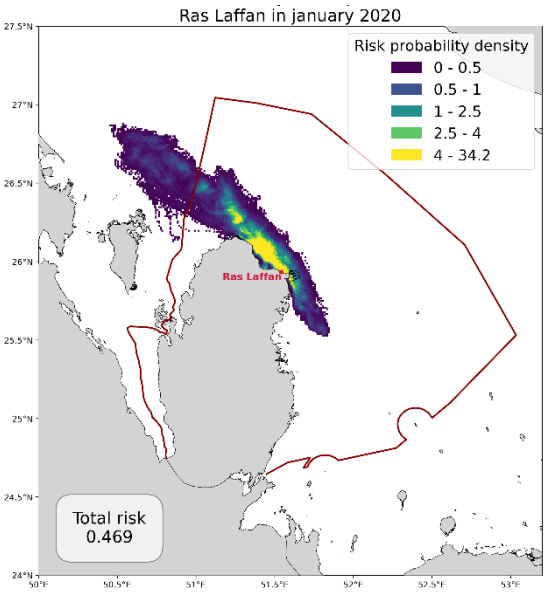
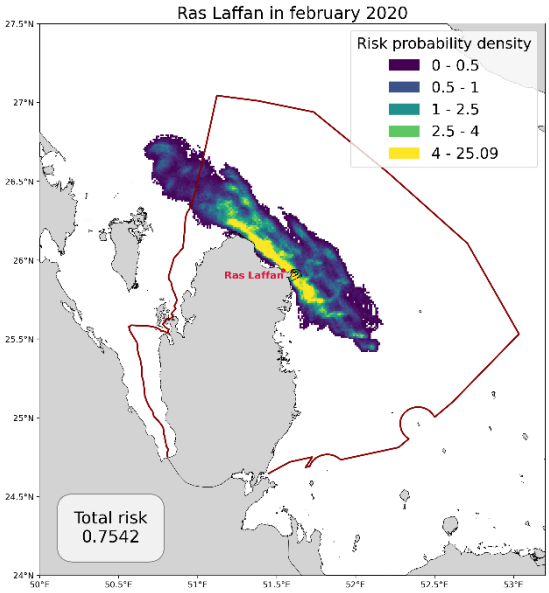
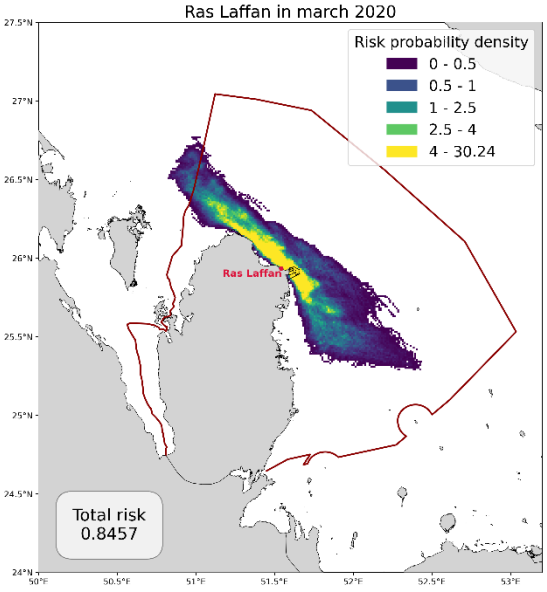
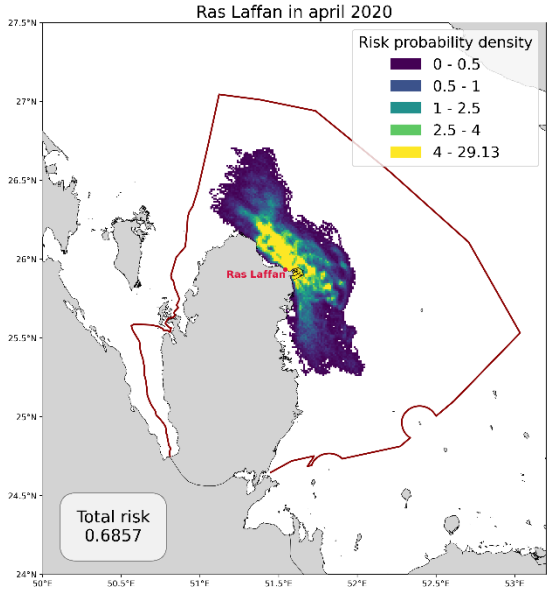


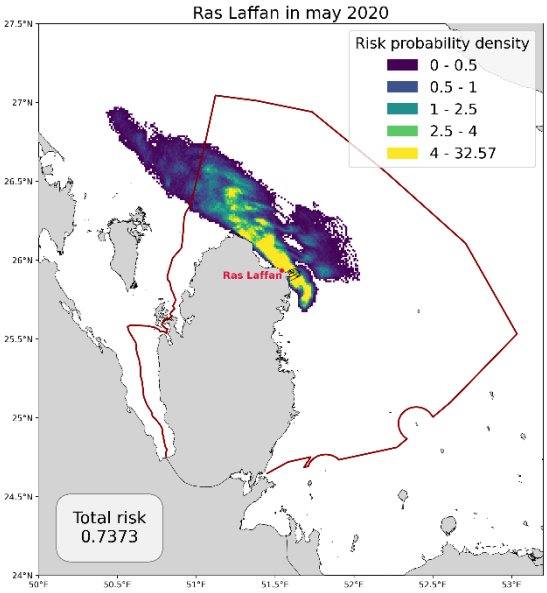
Figure 7.10 : Maps of oil risk probability density for Abu Fontas in 2019

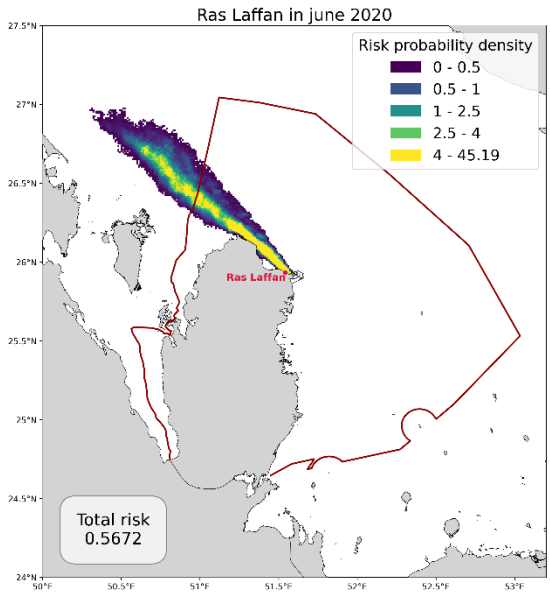

Ras Laffan in january 2020
Risk probability density
0 - 0.5
0.5 - 1
1 - 2.5
2.5 - 4
4 - 34.2
Ras Laffan
Total risk
0.469


Ras Laffan in february 2020
Risk probability density
0 - 0.5
0.5 - 1
1 - 2.5
2.5 - 4
4 - 25.09
Ras Laffan
Total risk
0.7542


Ras Laffan in march 2020
Risk probability density
0 - 0.5
0.5 - 1
1 - 2.5
2.5 - 4
4 - 30.24
Ras Laffan
Total risk
0.8457


Ras Laffan in april 2020
Risk probability density
0 - 0.5
0.5 - 1
1 - 2.5
2.5 - 4
4 - 29.13
Ras Laffan
Total risk
0.6857


Ras Laffan in may 2020
Risk probability density
0 - 0.5
0.5 - 1
1 - 2.5
2.5 - 4
4 - 32.57
Ras Laffan
Total risk
0.7373


Ras Laffan in june 2020
Risk probability density
0 - 0.5
0.5 - 1
1 - 2.5
2.5 - 4
4 - 45.19
Ras Laffan
Total risk
0.5672

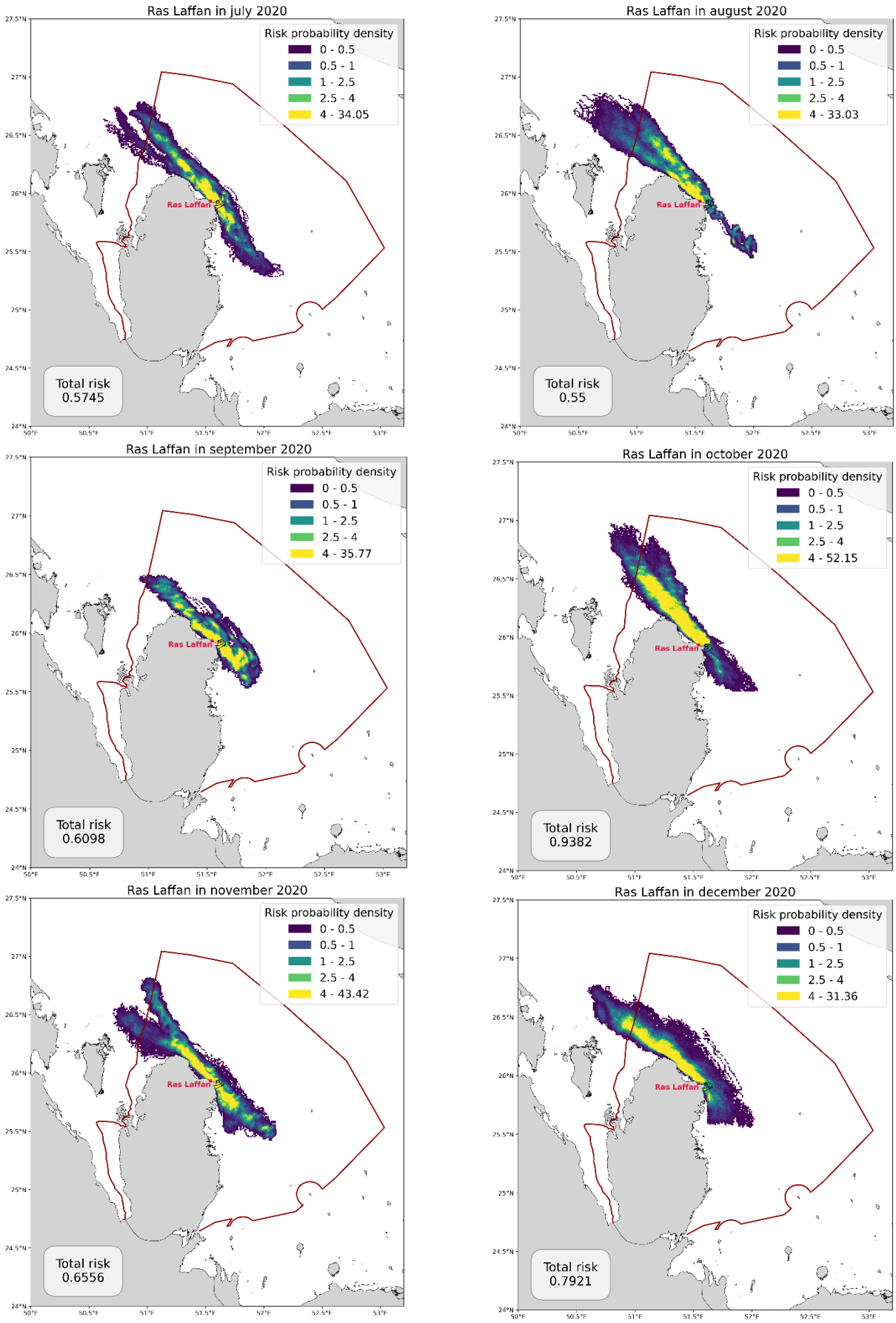
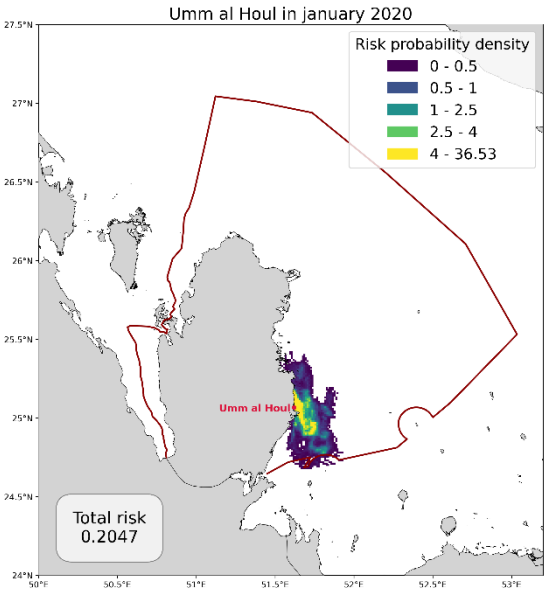
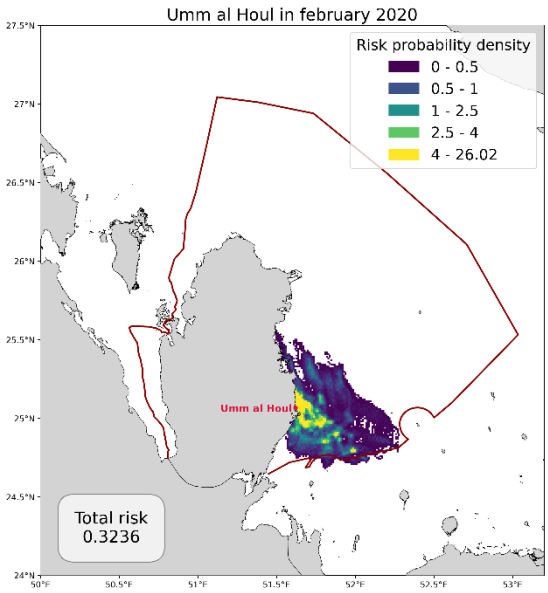
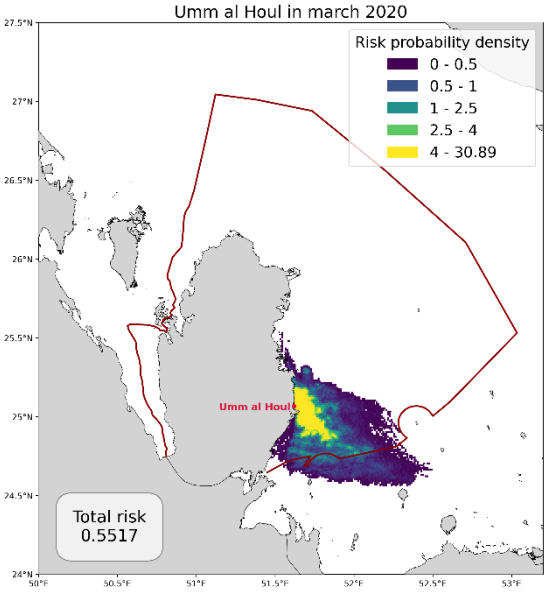
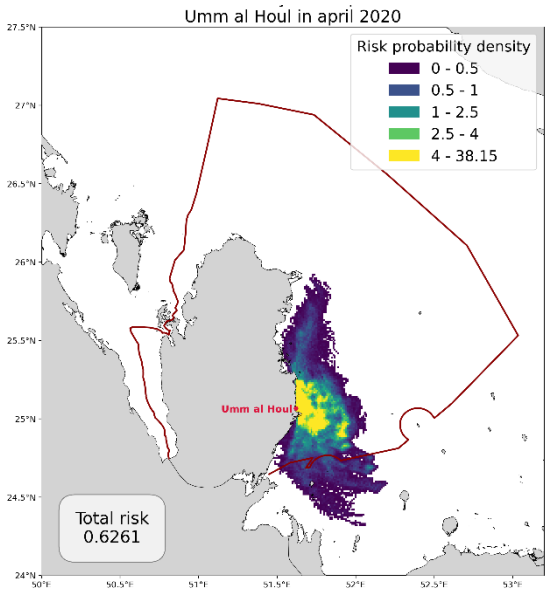


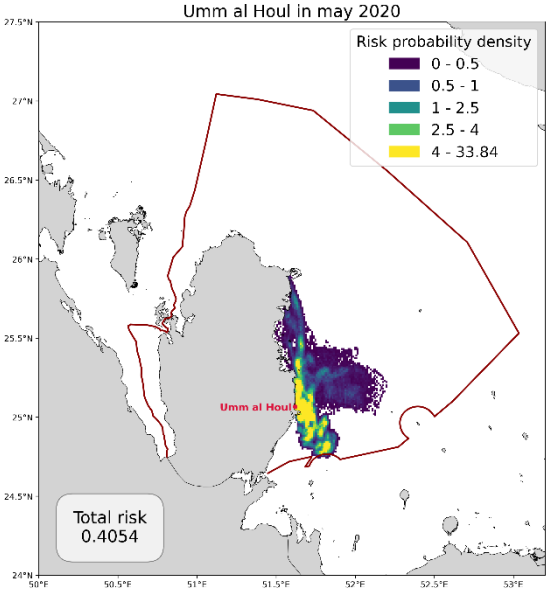
Figure 7.11 : Maps of oil risk probability density for Ras Laffan in 2020

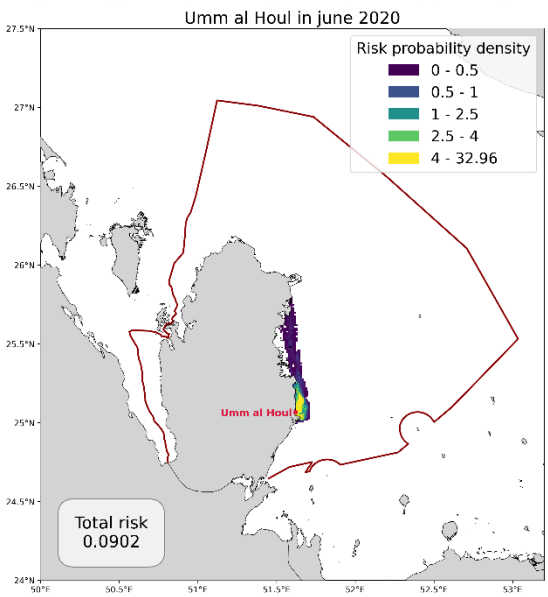

Umm al Houl in january 2020
Risk probability density
0 - 0.5
0.5 - 1
1 - 2.5
2.5 - 4
4 - 36.53
Umm al Houl
Total risk
0.2047


Umm al Houl in february 2020
Risk probability density
0 - 0.5
0.5 - 1
1 - 2.5
2.5 - 4
4 - 26.02
Umm al Houl
Total risk
0.3236


Umm al Houl in march 2020
Risk probability density
0 - 0.5
0.5 - 1
1 - 2.5
2.5 - 4
4 - 30.89
Umm al Houl
Total risk
0.5517


Umm al Houl in april 2020
Risk probability density
0 - 0.5
0.5 - 1
1 - 2.5
2.5 - 4
4 - 38.15
Umm al Houl
Total risk
0.6261


Umm al Houl in may 2020
Risk probability density
0 - 0.5
0.5 - 1
1 - 2.5
2.5 - 4
4 - 33.84
Umm al Houl
Total risk
0.4054


Umm al Houl in june 2020
Risk probability density
0 - 0.5
0.5 - 1
1 - 2.5
2.5 - 4
4 - 32.96
Umm al Houl
Total risk
0.0902

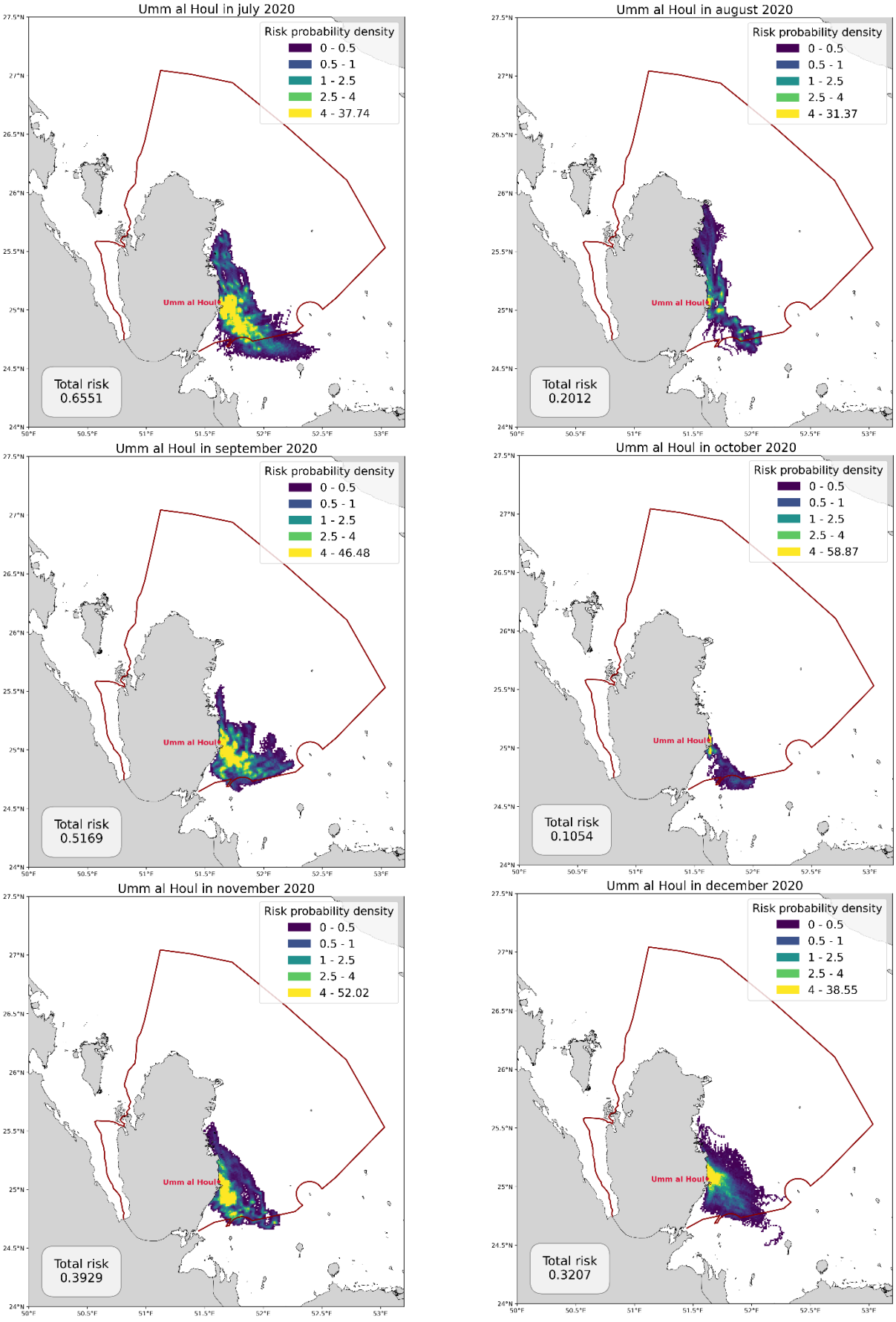
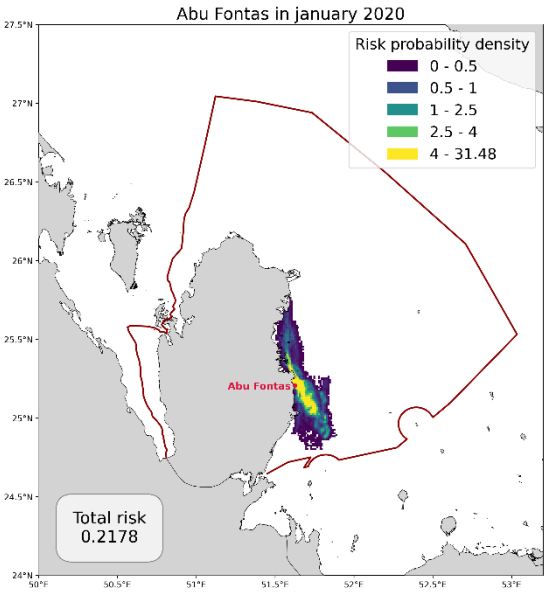
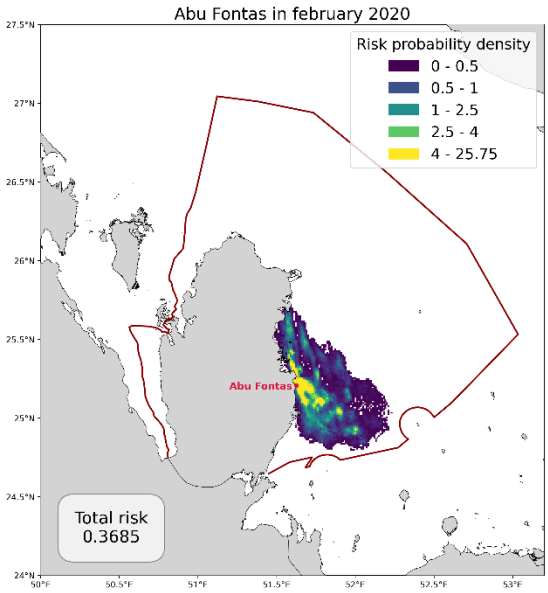
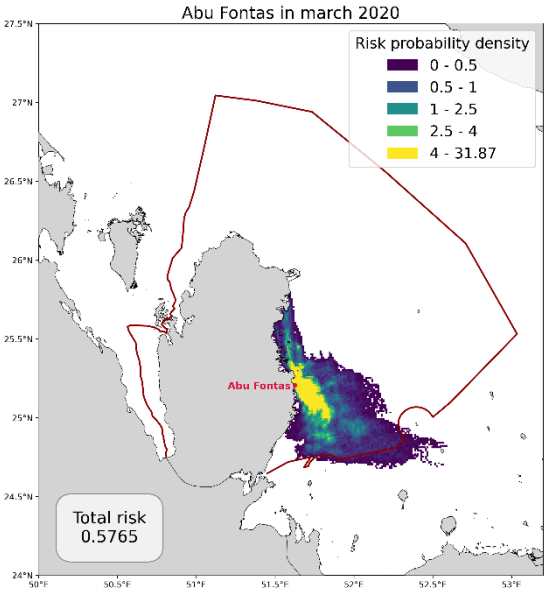
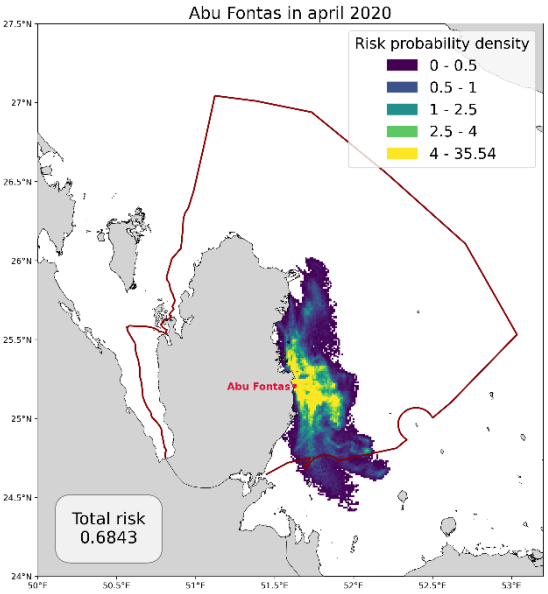


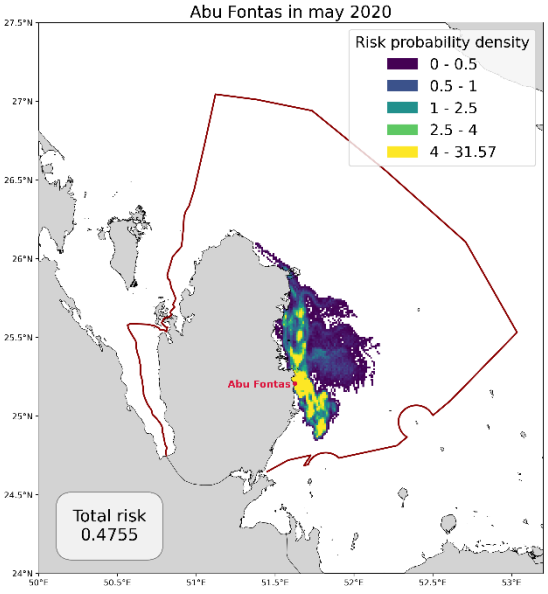
Figure 7.12 : Maps of oil risk probability density for Umm al Houl in 2020

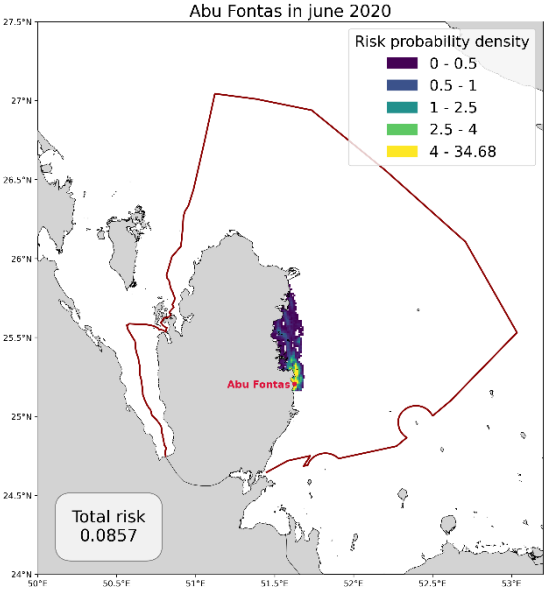

Abu Fontas in january 2020
Risk probability density
0 - 0.5
0.5 - 1
1 - 2.5
2.5 - 4
4 - 31.48
Abu Fontas
Total risk
0.2178


Abu Fontas in february 2020
Risk probability density
0 - 0.5
0.5 - 1
1 - 2.5
2.5 - 4
4 - 25.75
Abu Fontas
Total risk
0.3685


Abu Fontas in march 2020
Risk probability density
0 - 0.5
0.5 - 1
1 - 2.5
2.5 - 4
4 - 31.87
Abu Fontas
Total risk
0.5765


Abu Fontas in april 2020
Risk probability density
0 - 0.5
0.5 - 1
1 - 2.5
2.5 - 4
4 - 35.54
Abu Fontas
Total risk
0.6843


Abu Fontas in may 2020
Risk probability density
0 - 0.5
0.5 - 1
1 - 2.5
2.5 - 4
4 - 31.57
Abu Fontas
Total risk
0.4755


Abu Fontas in june 2020
Risk probability density
0 - 0.5
0.5 - 1
1 - 2.5
2.5 - 4
4 - 34.68
Abu Fontas
Total risk
0.0857

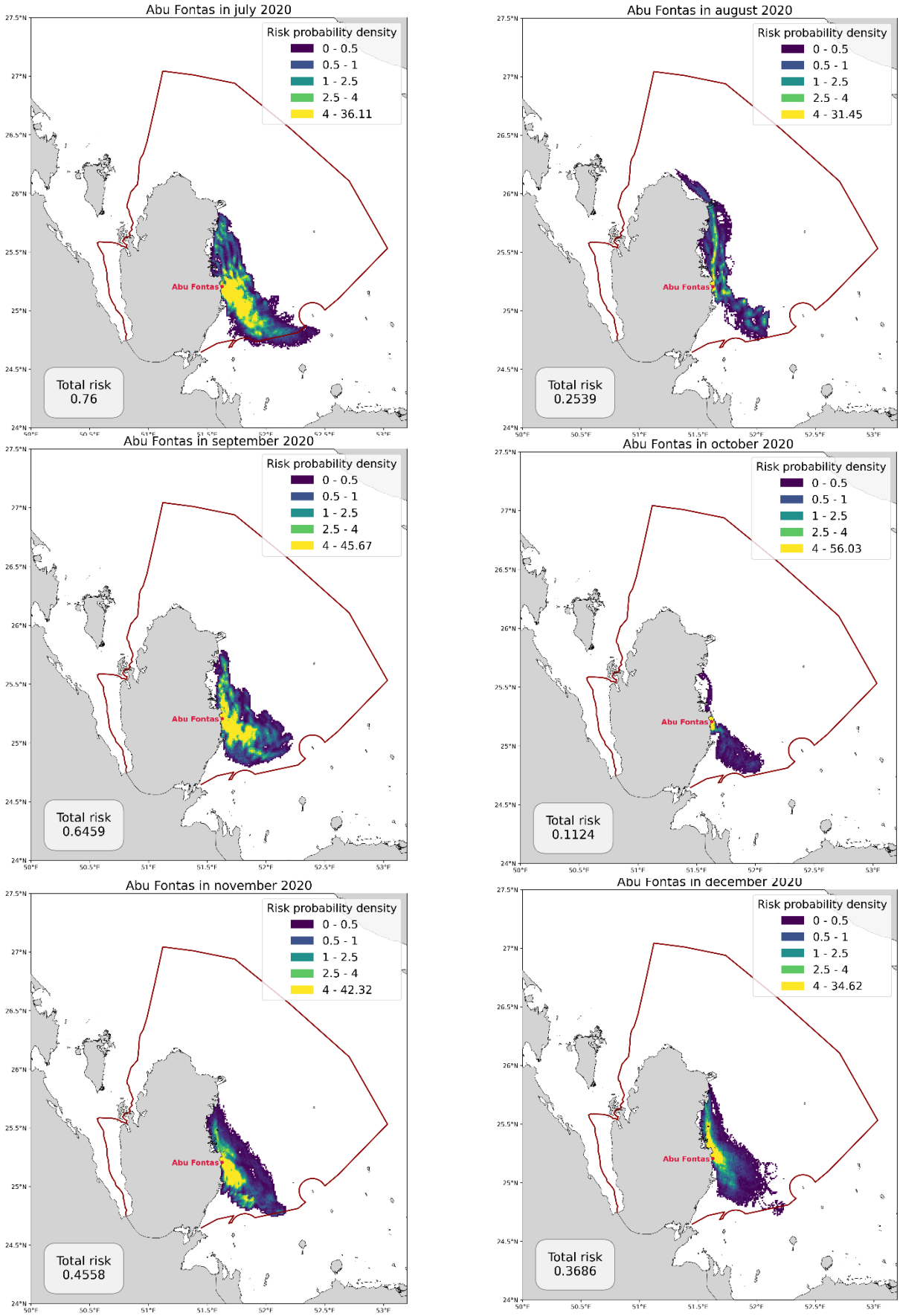
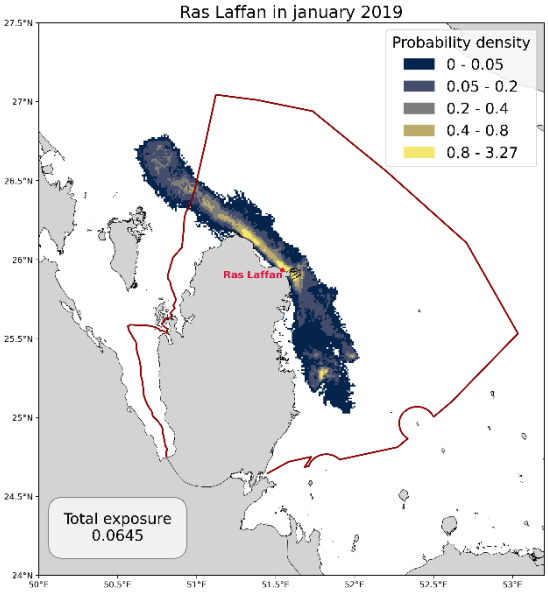
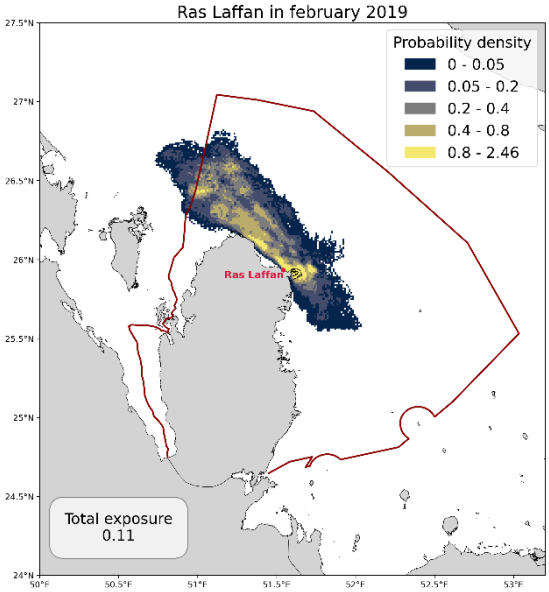
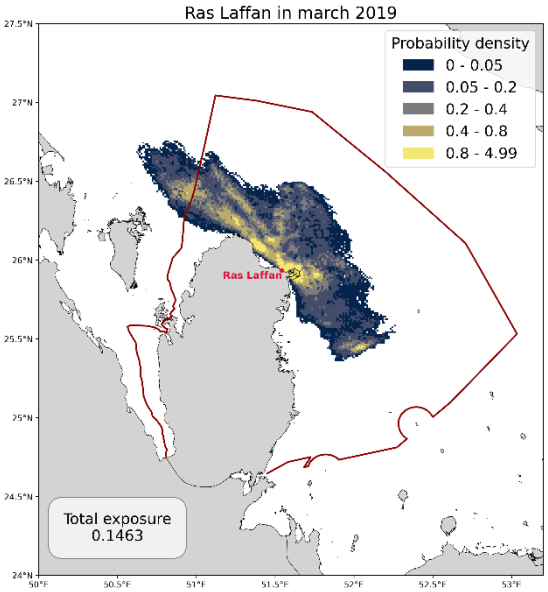


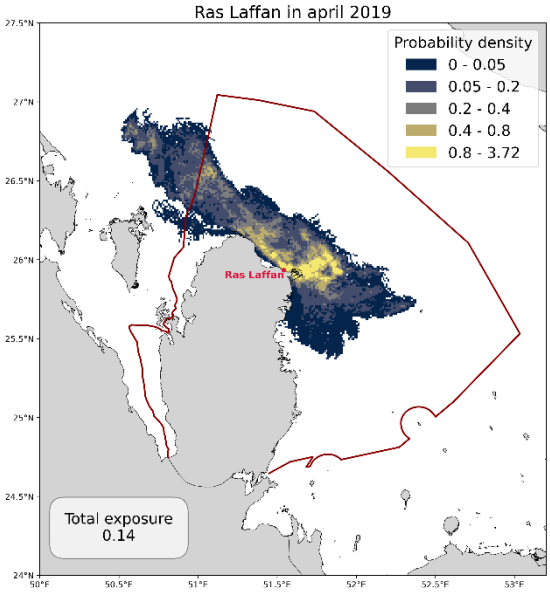
Figure 7.13 : Maps of oil risk probability density for Abu Fontas in 2020

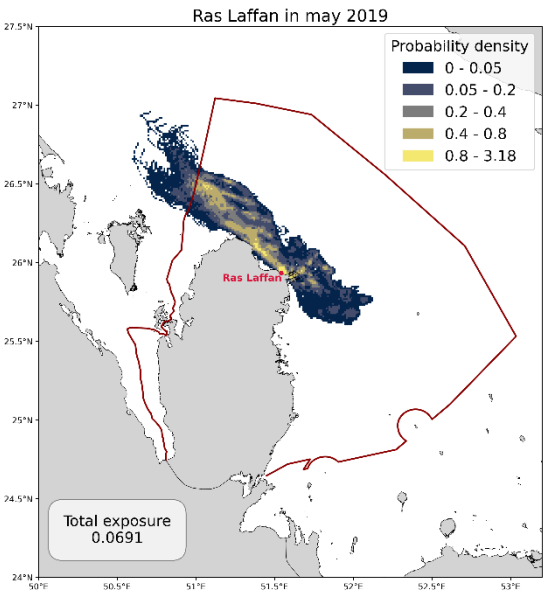
D. Oil exposure maps from ships

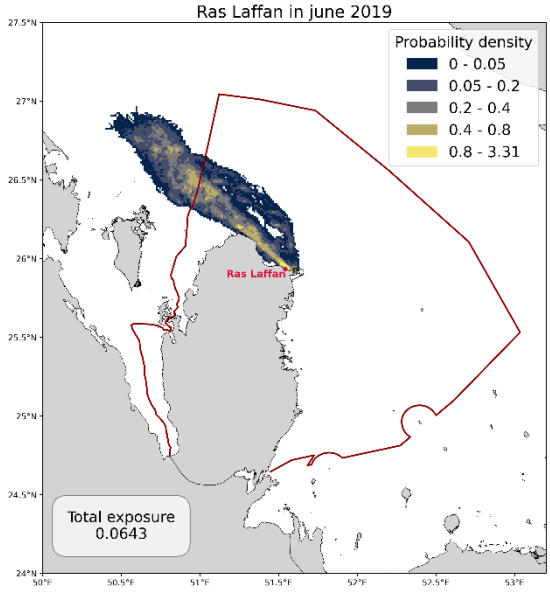












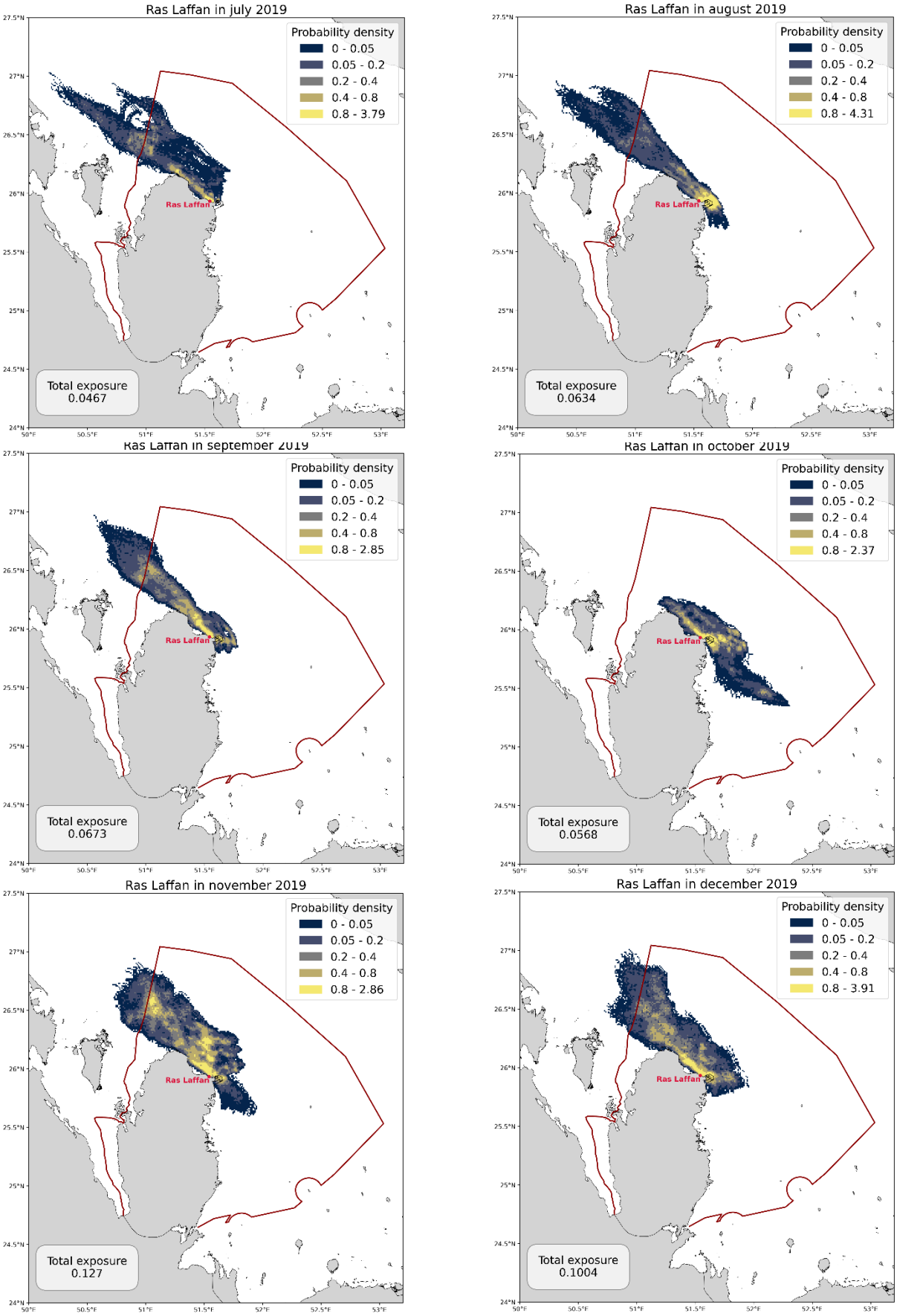
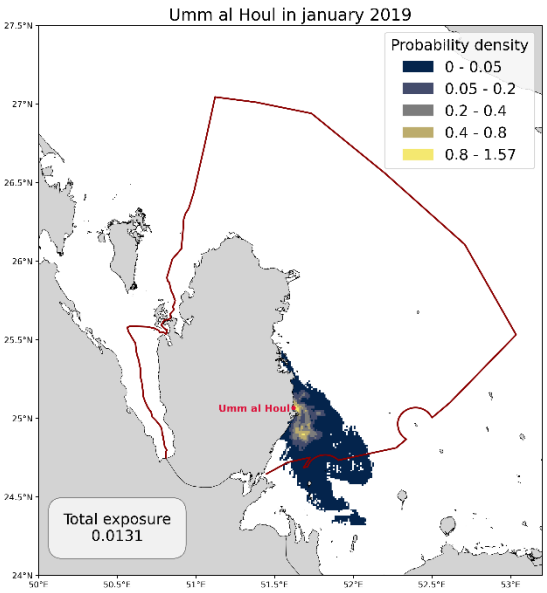
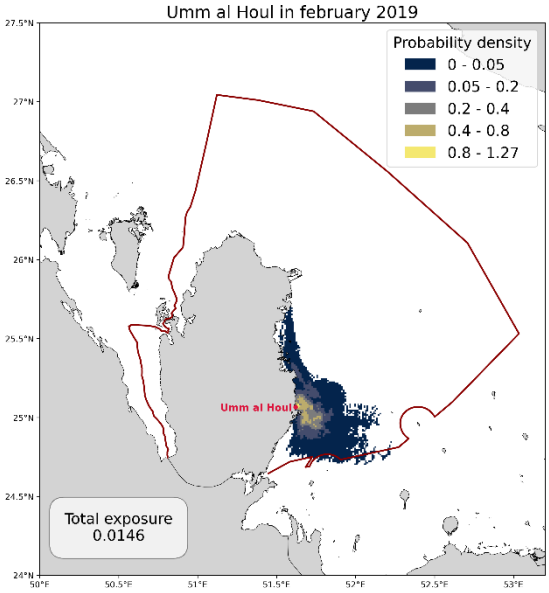
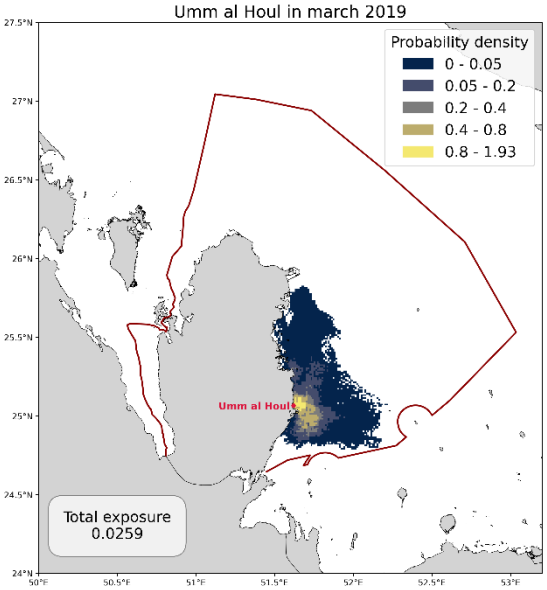
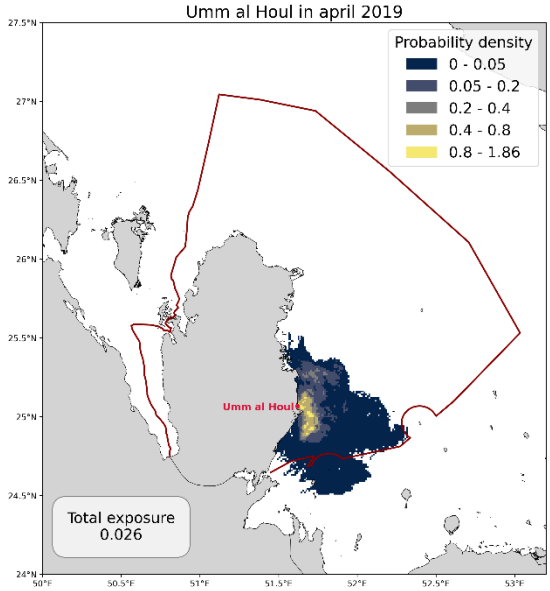


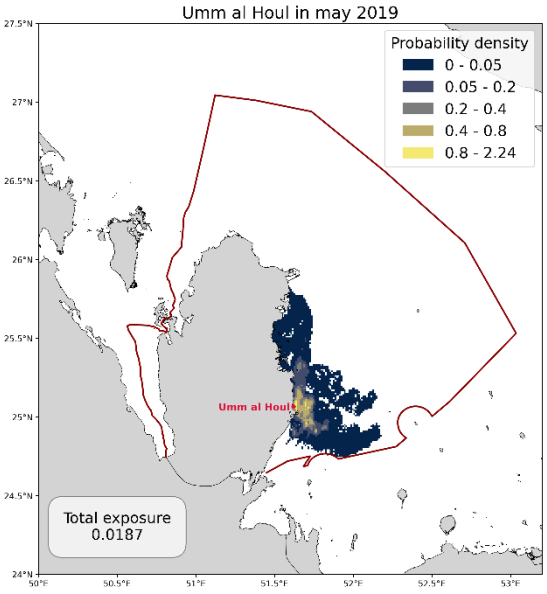
Figure 7.14 : Exposure to ships oil spill for Ras Laffan in 2019

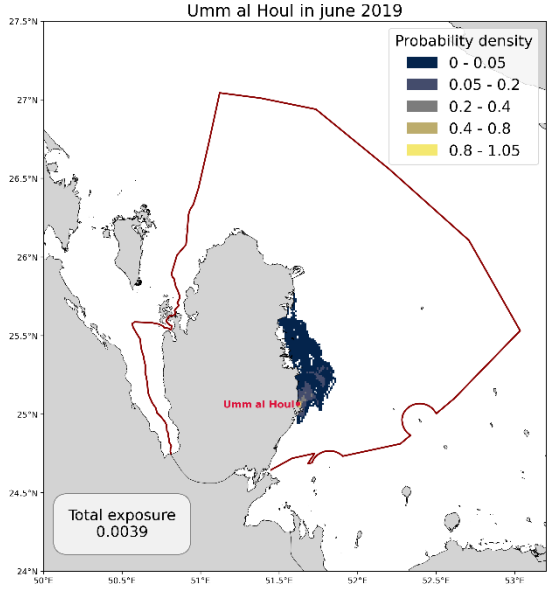

Umm al Houl in january 2019
Probability density
0 - 0.05
0.05 - 0.2
0.2 - 0.4
0.4 - 0.8
0.8 - 1.57
Umm al Houl
Total exposure
0.0131


Umm al Houl in february 2019
Probability density
0 - 0.05
0.05 - 0.2
0.2 - 0.4
0.4 - 0.8
0.8 - 1.27
Umm al Houl
Total exposure
0.0146


Umm al Houl in march 2019
Probability density
0 - 0.05
0.05 - 0.2
0.2 - 0.4
0.4 - 0.8
0.8 - 1.93
Umm al Houl
Total exposure
0.0259


Umm al Houl in april 2019
Probability density
0 - 0.05
0.05 - 0.2
0.2 - 0.4
0.4 - 0.8
0.8 - 1.86
Umm al Houl
Total exposure
0.026


Umm al Houl in may 2019
Probability density
0 - 0.05
0.05 - 0.2
0.2 - 0.4
0.4 - 0.8
0.8 - 2.24
Umm al Houl
Total exposure
0.0187


Umm al Houl in june 2019
Probability density
0 - 0.05
0.05 - 0.2
0.2 - 0.4
0.4 - 0.8
0.8 - 1.05
Umm al Houl
Total exposure
0.0039

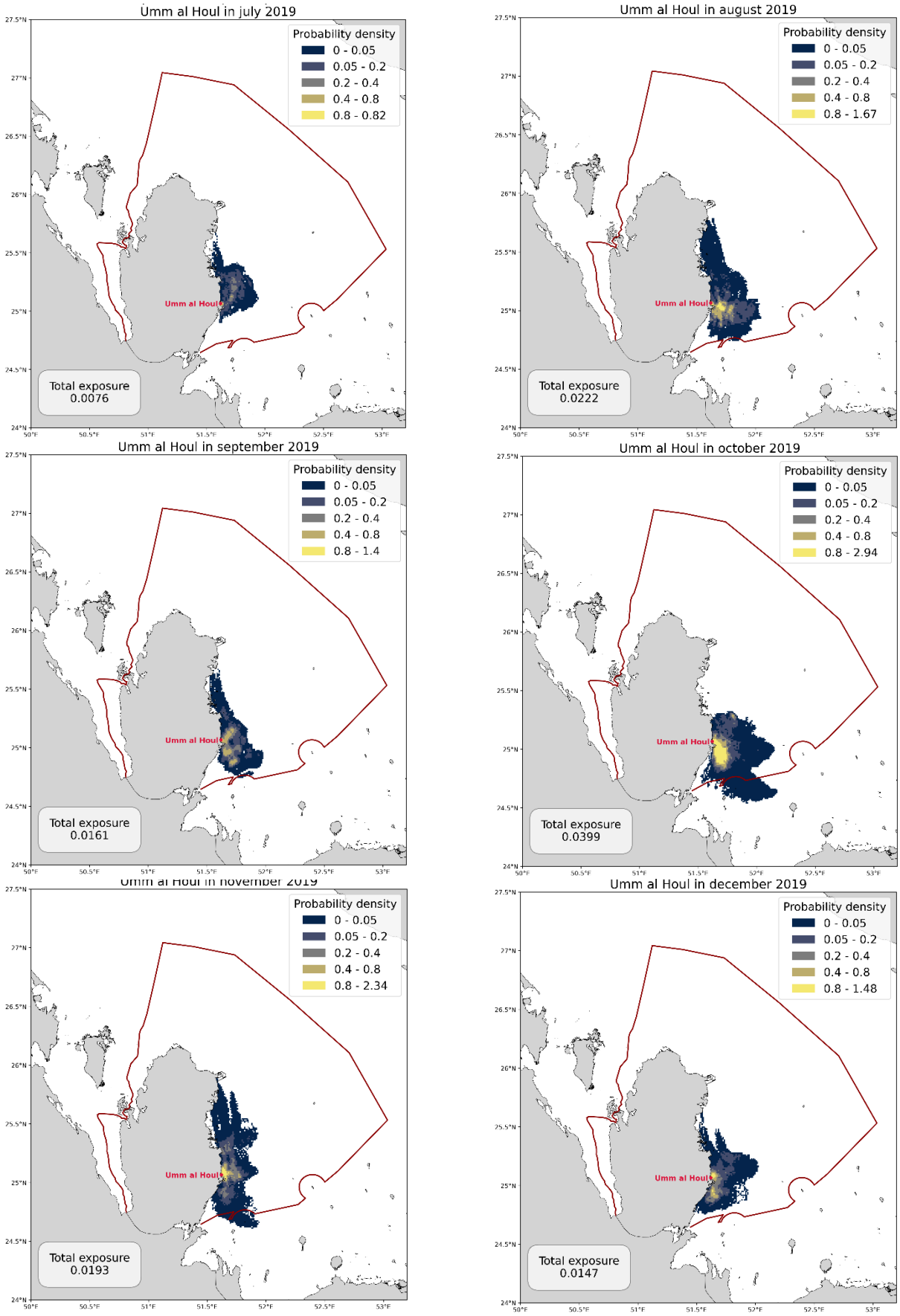
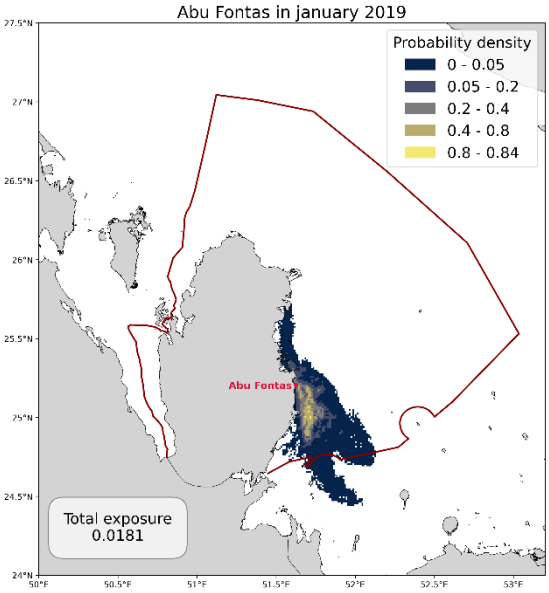
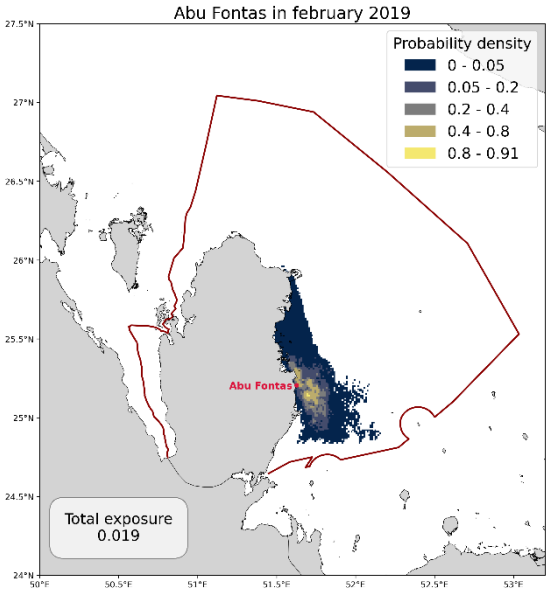
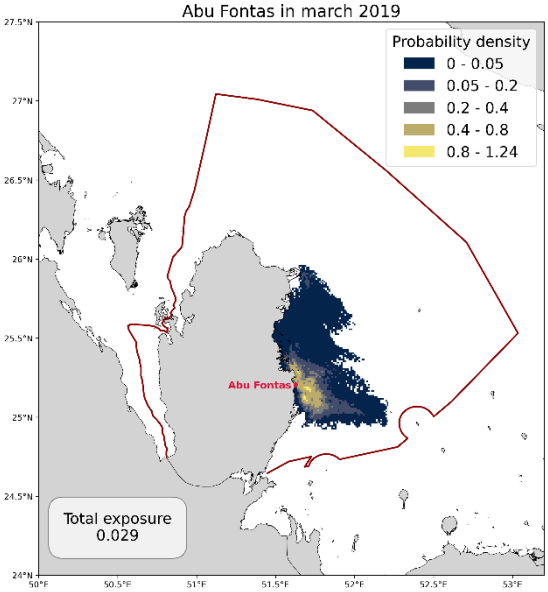
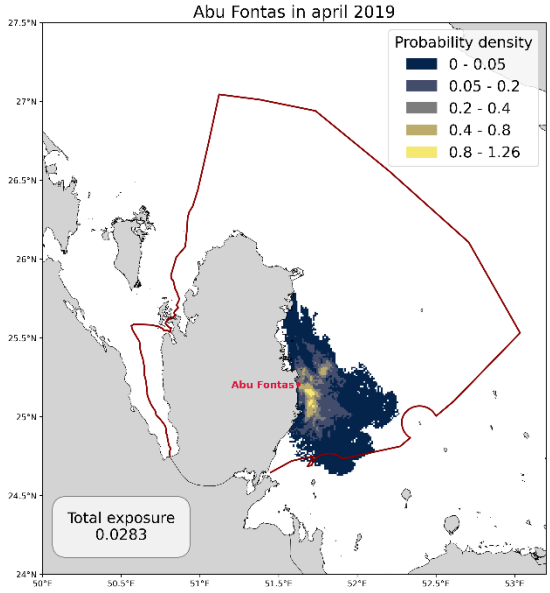


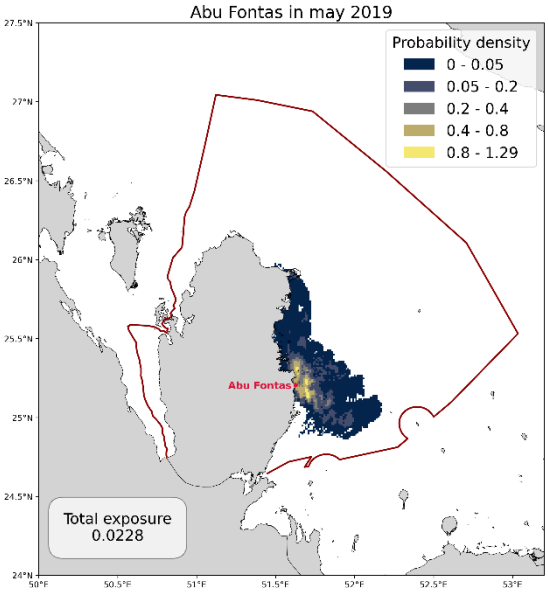
Figure 7.15 : Exposure to ships oil spills for Umm al Houl in 2019

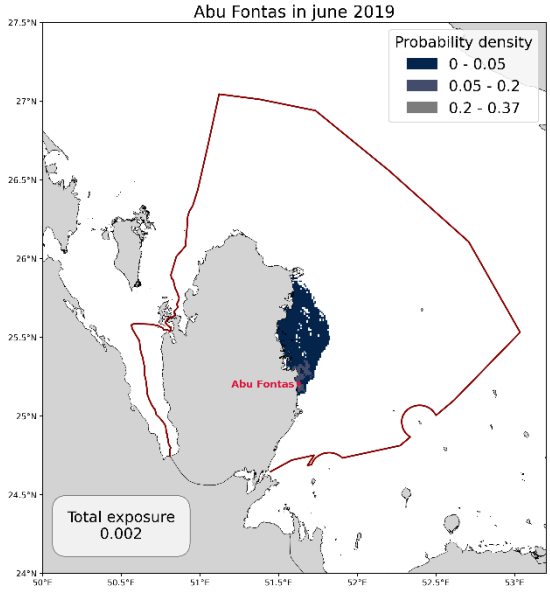

Abu Fontas in january 2019
Probability density
0 - 0.05
0.05 - 0.2
0.2 - 0.4
0.4 - 0.8
0.8 - 0.84
Abu Fontas
Total exposure
0.0181


Abu Fontas in february 2019
Probability density
0 - 0.05
0.05 - 0.2
0.2 - 0.4
0.4 - 0.8
0.8 - 0.91
Abu Fontas
Total exposure
0.019


Abu Fontas in march 2019
Probability density
0 - 0.05
0.05 - 0.2
0.2 - 0.4
0.4 - 0.8
0.8 - 1.24
Abu Fontas
Total exposure
0.029


Abu Fontas in april 2019
Probability density
0 - 0.05
0.05 - 0.2
0.2 - 0.4
0.4 - 0.8
0.8 - 1.26
Abu Fontas
Total exposure
0.0283


Abu Fontas in may 2019
Probability density
0 - 0.05
0.05 - 0.2
0.2 - 0.4
0.4 - 0.8
0.8 - 1.29
Abu Fontas
Total exposure
0.0228


Abu Fontas in june 2019
Probability density
0 - 0.05
0.05 - 0.2
0.2 - 0.37
Abu Fontas
Total exposure
0.002

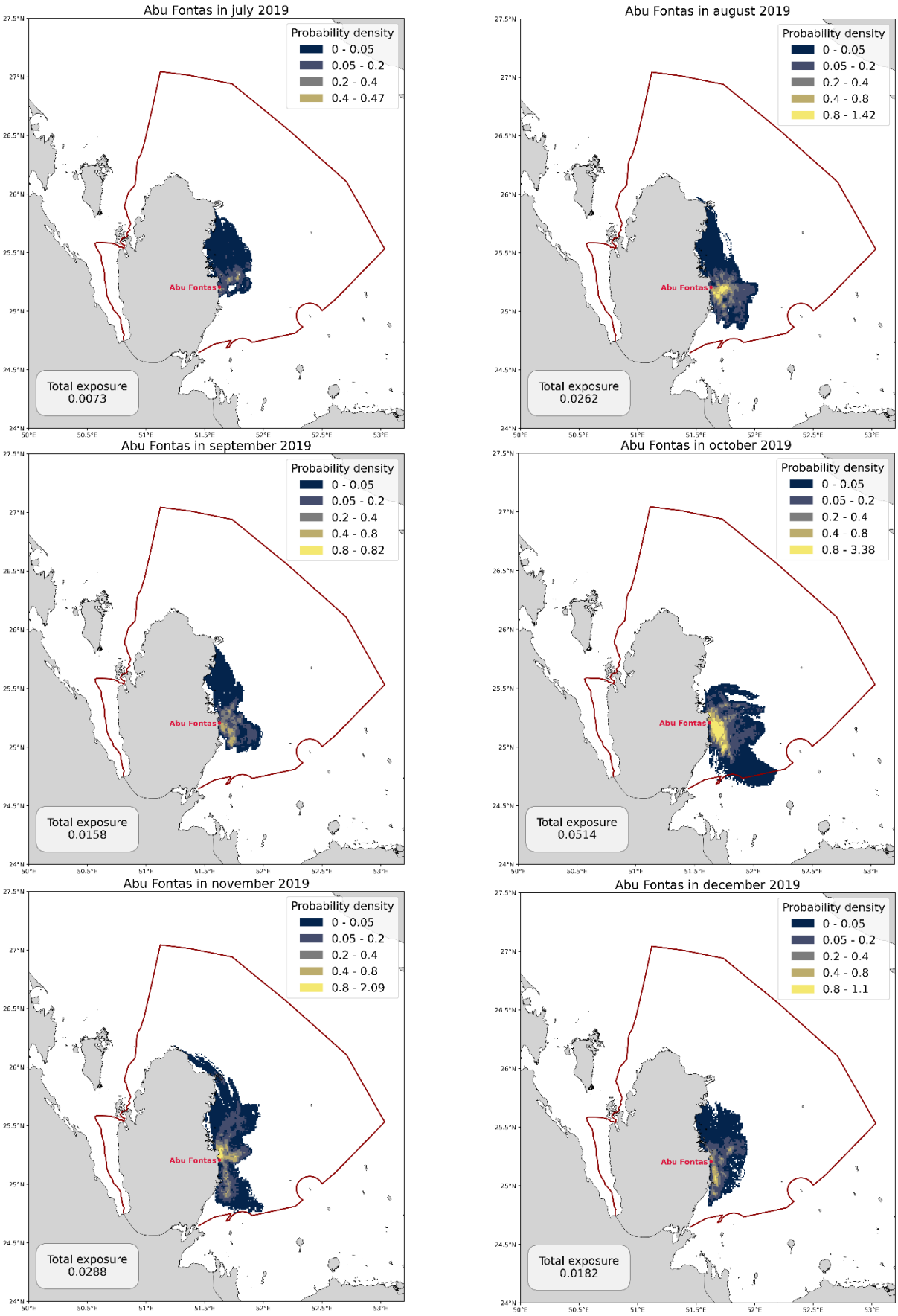
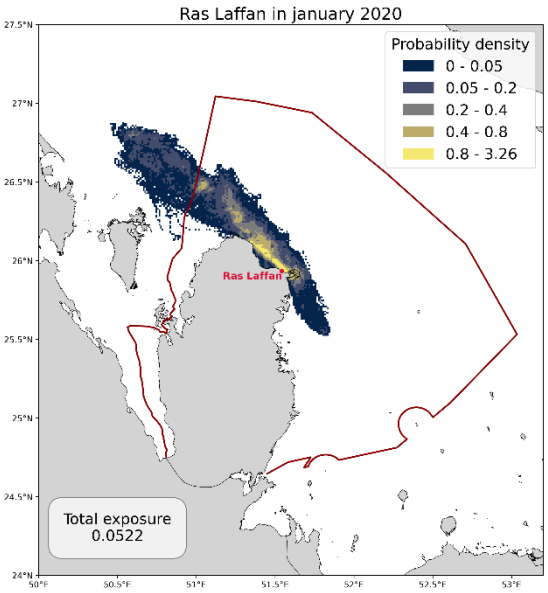
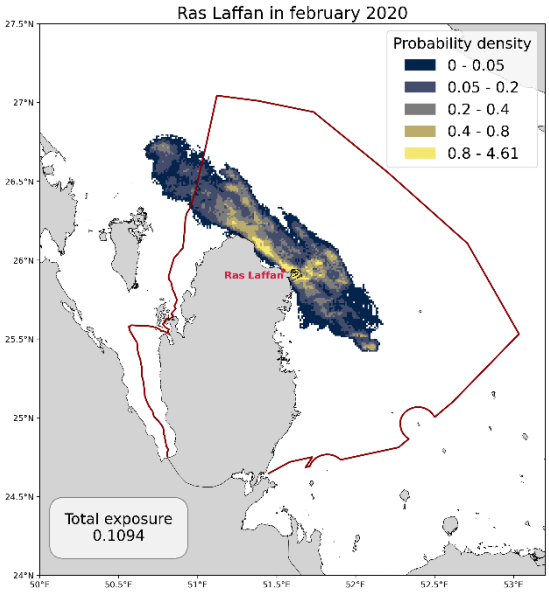
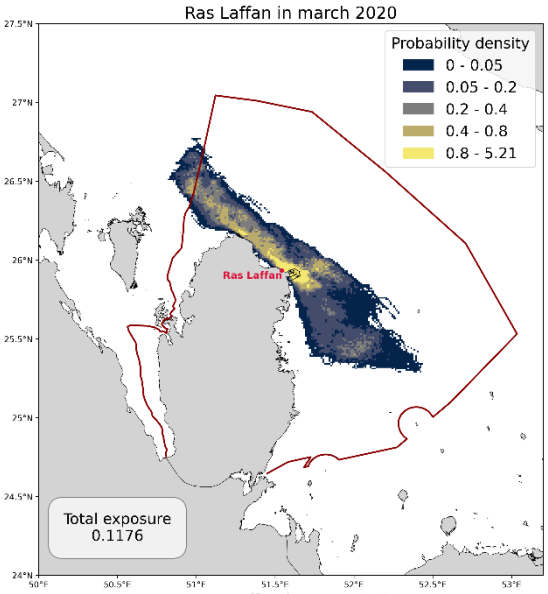
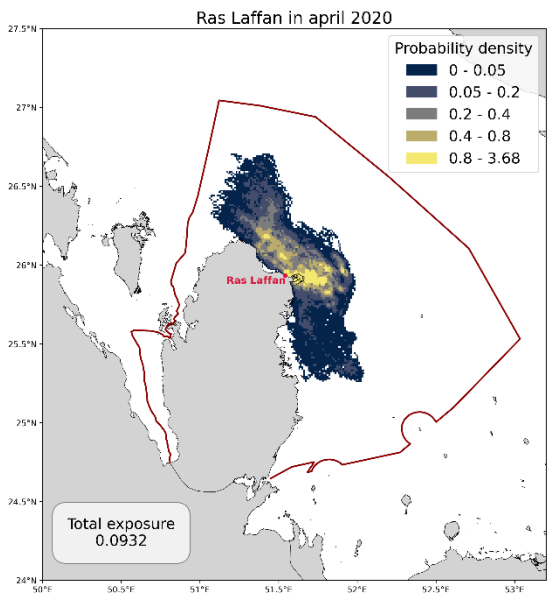


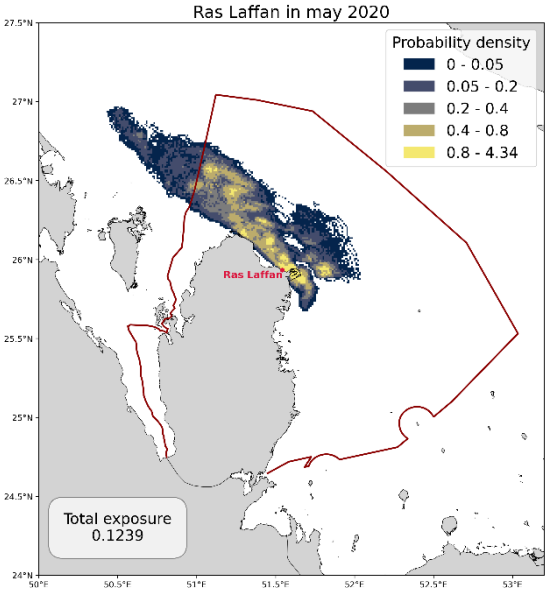
Figure 7.16 : Exposure to ships oil spills for Abu Fontas in 2019

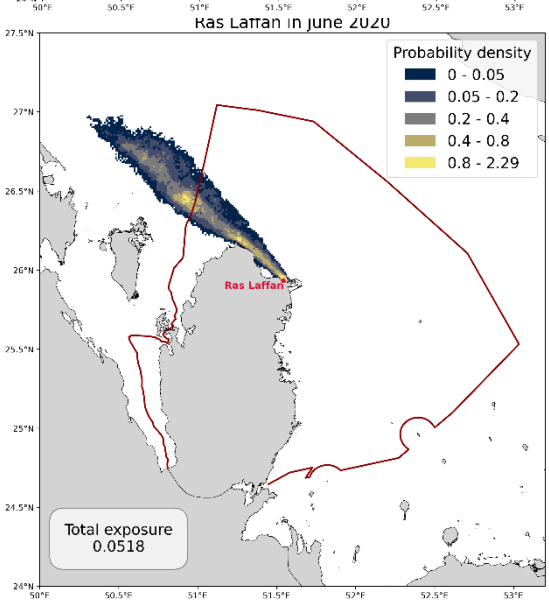

Ras Laffan in january 2020
Probability density
0 - 0.05
0.05 - 0.2
0.2 - 0.4
0.4 - 0.8
0.8 - 3.26
Ras Laffan
Total exposure
0.0522


Ras Laffan in february 2020
Probability density
0 - 0.05
0.05 - 0.2
0.2 - 0.4
0.4 - 0.8
0.8 - 4.61
Ras Laffan
Total exposure
0.1094


Ras Laffan in march 2020
Probability density
0 - 0.05
0.05 - 0.2
0.2 - 0.4
0.4 - 0.8
0.8 - 5.21
Ras Laffan
Total exposure
0.1176


Ras Laffan in april 2020
Probability density
0 - 0.05
0.05 - 0.2
0.2 - 0.4
0.4 - 0.8
0.8 - 3.68
Ras Laffan
Total exposure
0.0932


Ras Laffan in may 2020
Probability density
0 - 0.05
0.05 - 0.2
0.2 - 0.4
0.4 - 0.8
0.8 - 4.34
Ras Laffan
Total exposure
0.1239


Ras Laffan in june 2020
Probability density
0 - 0.05
0.05 - 0.2
0.2 - 0.4
0.4 - 0.8
0.8 - 2.29
Ras Laffan
Total exposure
0.0518

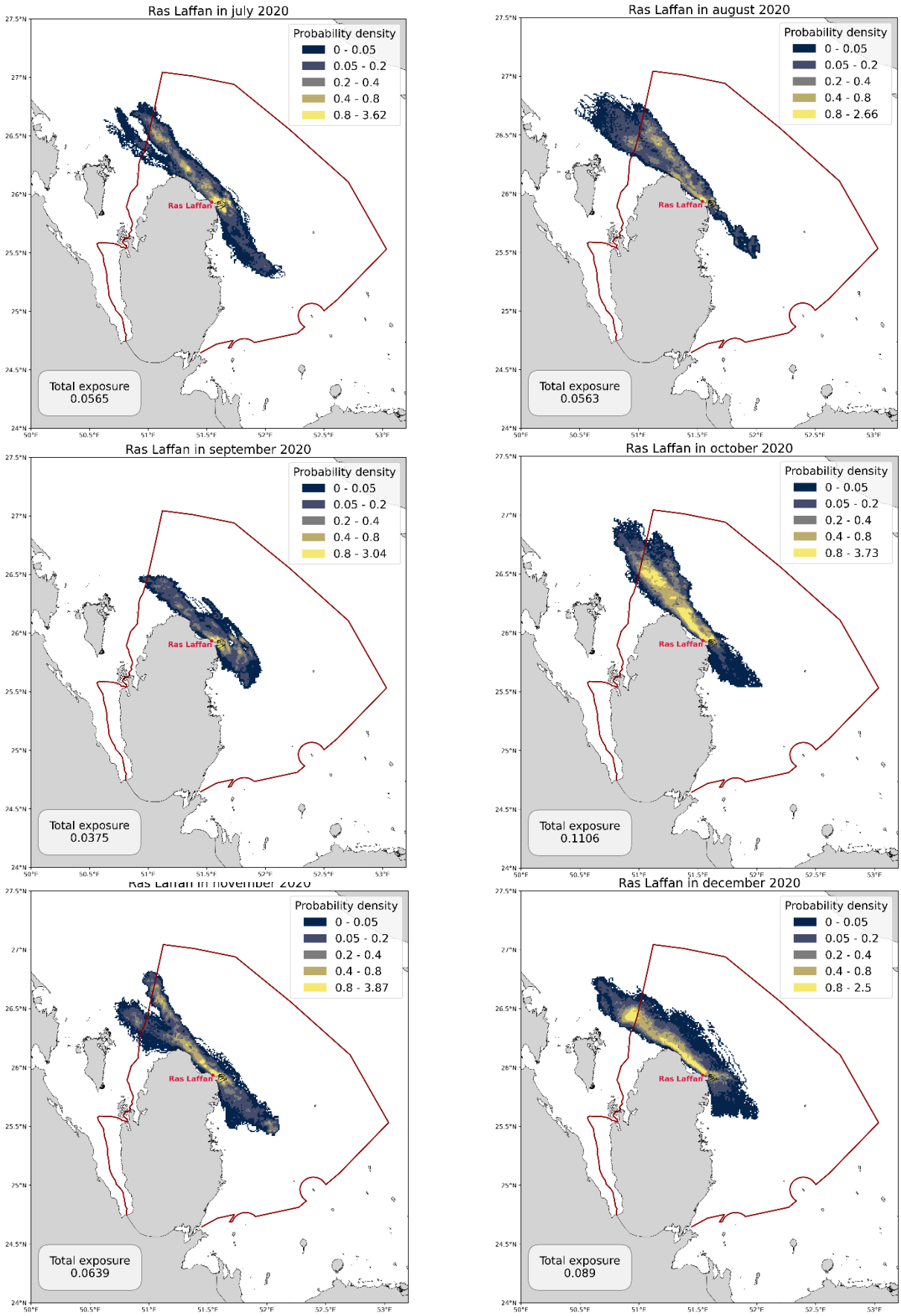
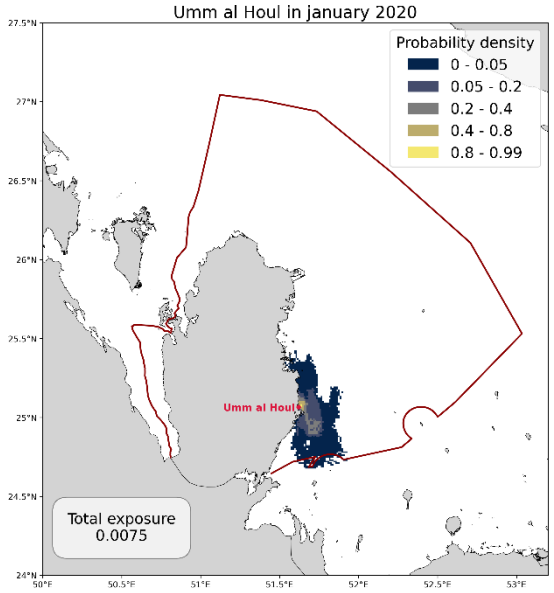
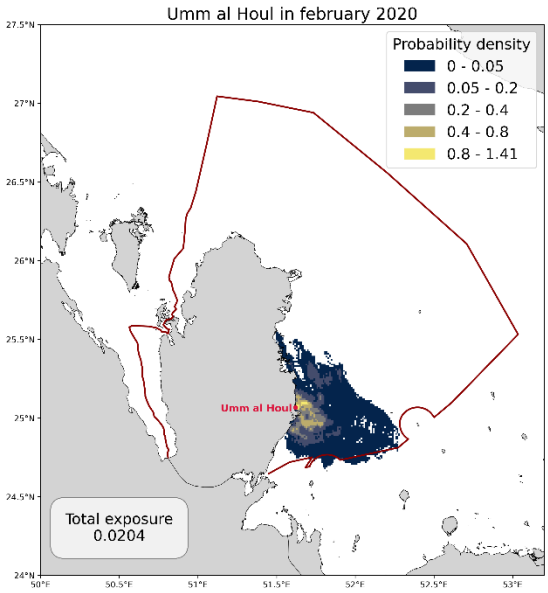
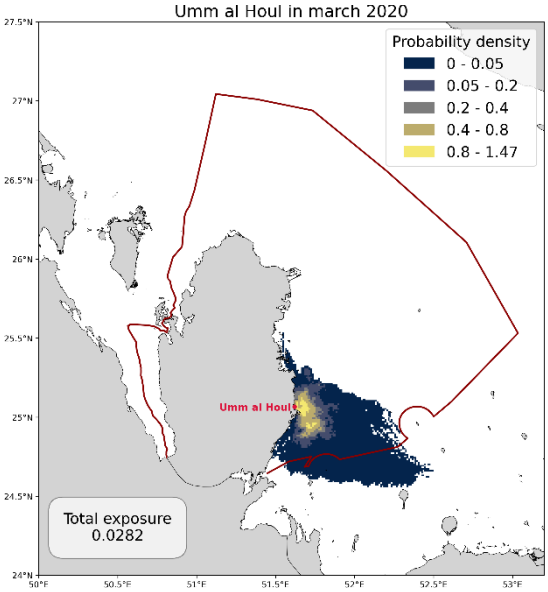
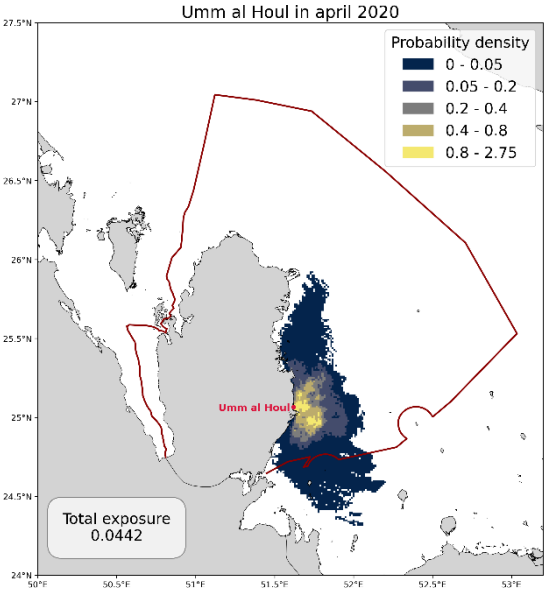


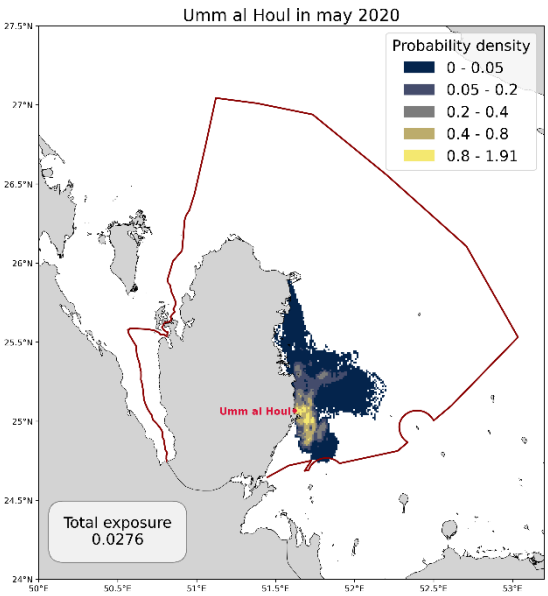
Figure 7.17 : Exposure to ships oil spills for Ras Laffan in 2020

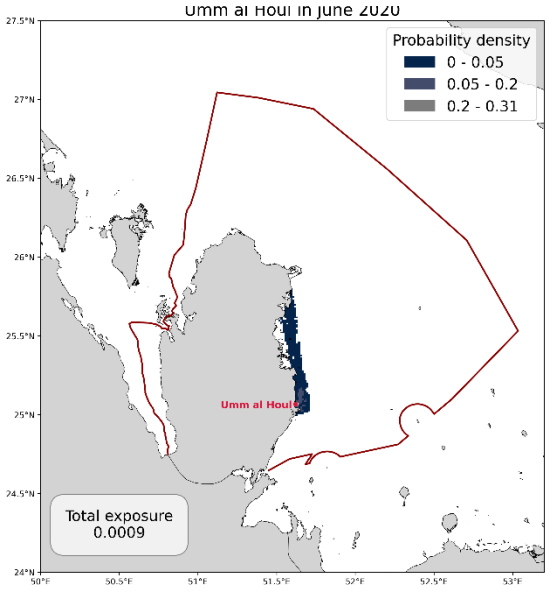

Umm al Houl in january 2020
Probability density
0 - 0.05
0.05 - 0.2
0.2 - 0.4
0.4 - 0.8
0.8 - 0.99
Umm al Houl
Total exposure
0.0075


Umm al Houl in february 2020
Probability density
0 - 0.05
0.05 - 0.2
0.2 - 0.4
0.4 - 0.8
0.8 - 1.41
Umm al Houl
Total exposure
0.0204


Umm al Houl in march 2020
Probability density
0 - 0.05
0.05 - 0.2
0.2 - 0.4
0.4 - 0.8
0.8 - 1.47
Umm al Houl
Total exposure
0.0282


Umm al Houl in april 2020
Probability density
0 - 0.05
0.05 - 0.2
0.2 - 0.4
0.4 - 0.8
0.8 - 2.75
Umm al Houl
Total exposure
0.0442


Umm al Houl in may 2020
Probability density
0 - 0.05
0.05 - 0.2
0.2 - 0.4
0.4 - 0.8
0.8 - 1.91
Umm al Houl
Total exposure
0.0276


Umm al Houl in june 2020
Probability density
0 - 0.05
0.05 - 0.2
0.2 - 0.31
Umm al Houl
Total exposure
0.0009

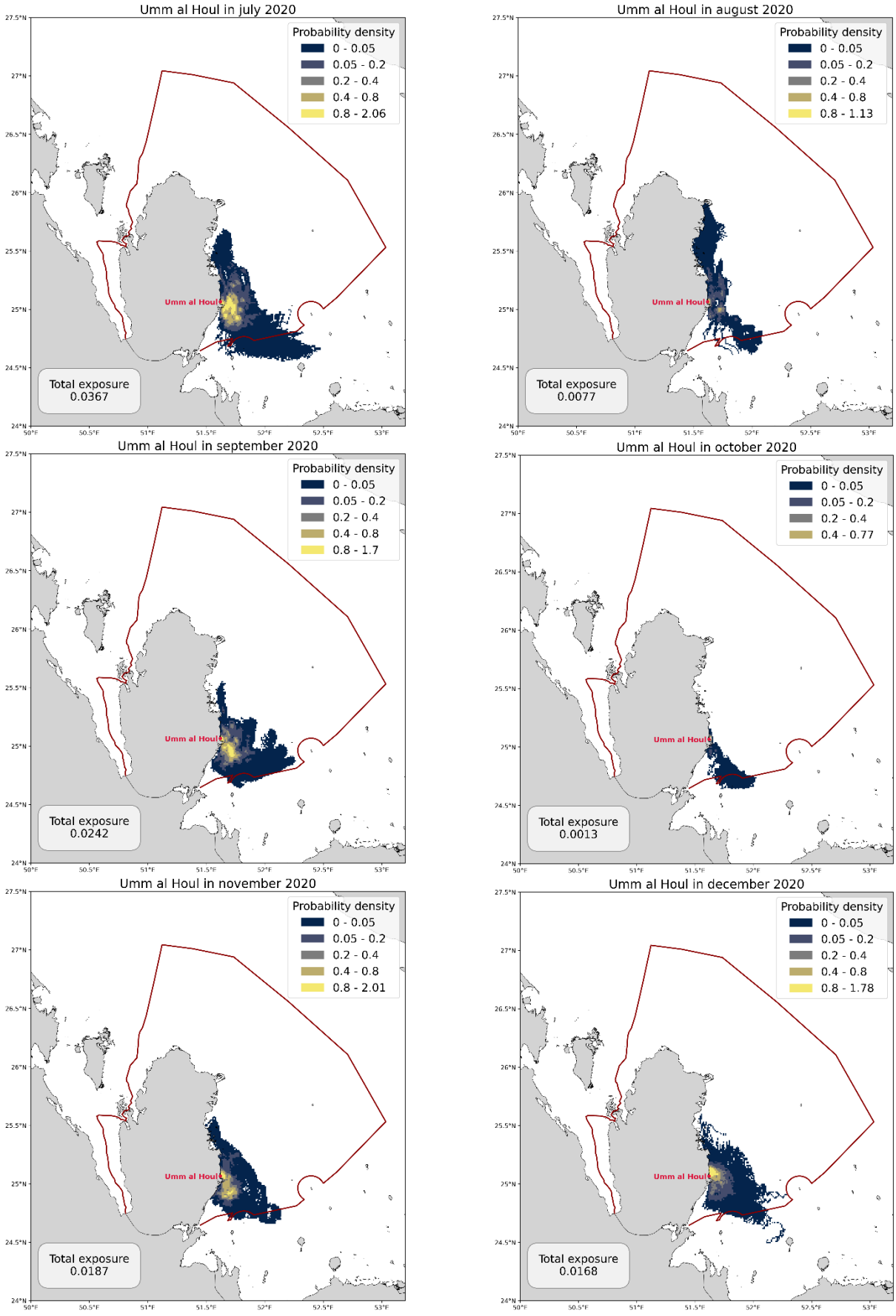
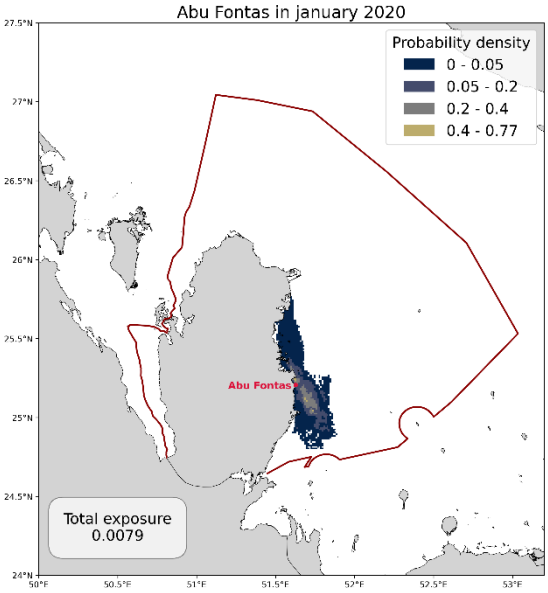
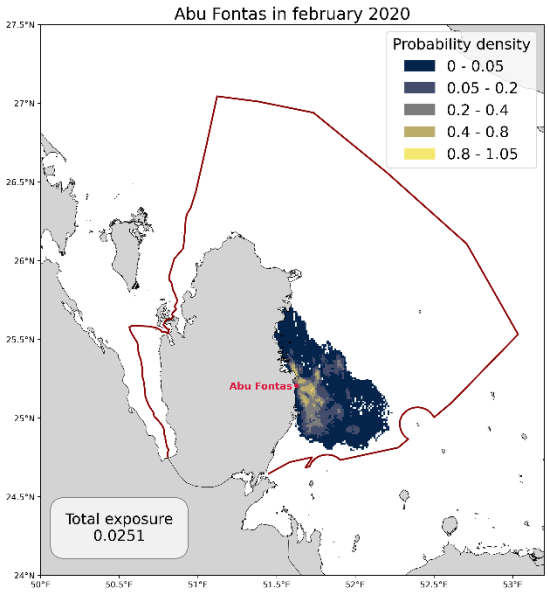
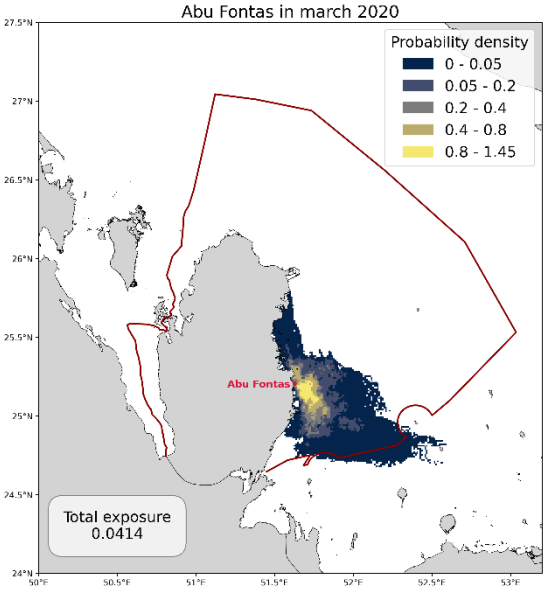
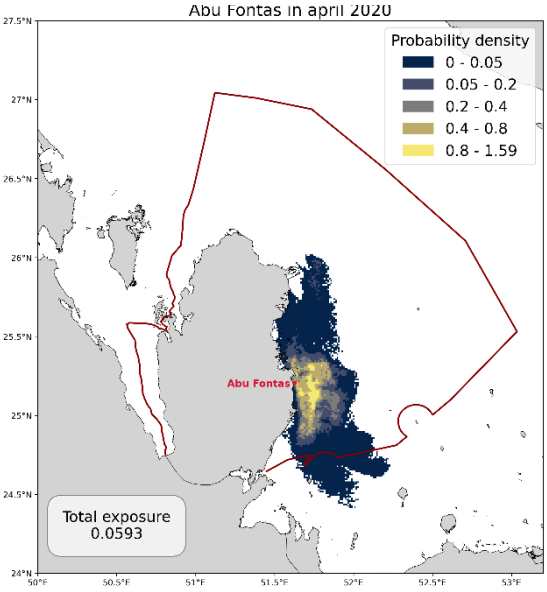


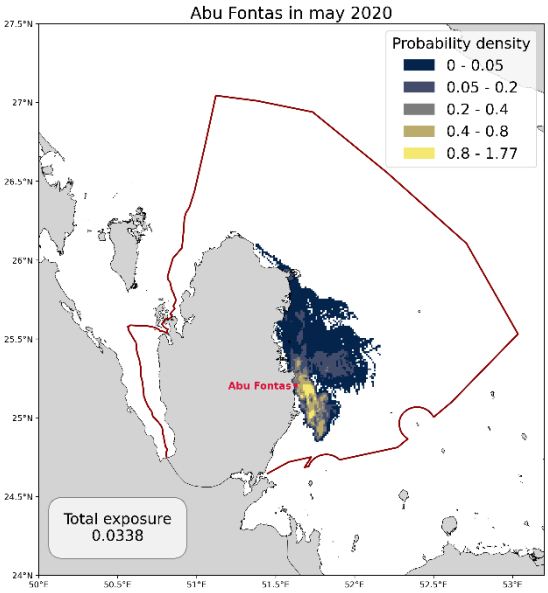
Figure 7.18 : Exposure to ships oil spills for Umm al Houl in 2020

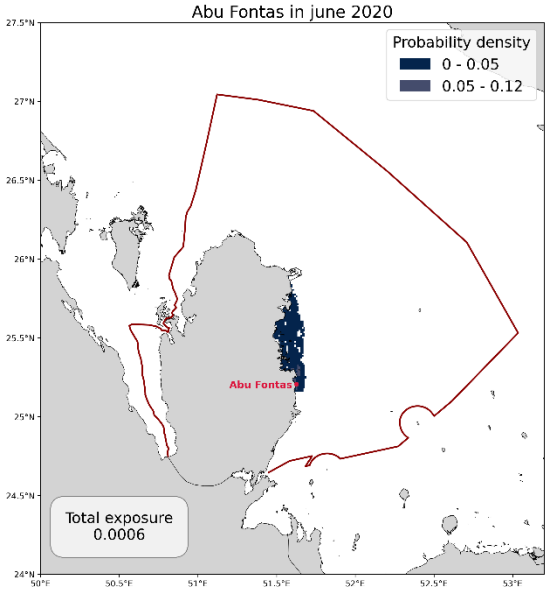

Abu Fontas in january 2020
Probability density
0 - 0.05
0.05 - 0.2
0.2 - 0.4
0.4 - 0.77
Abu Fontas
Total exposure
0.0079


Abu Fontas in february 2020
Probability density
0 - 0.05
0.05 - 0.2
0.2 - 0.4
0.4 - 0.8
0.8 - 1.05
Abu Fontas
Total exposure
0.0251


Abu Fontas in march 2020
Probability density
0 - 0.05
0.05 - 0.2
0.2 - 0.4
0.4 - 0.8
0.8 - 1.45
Abu Fontas
Total exposure
0.0414


Abu Fontas in april 2020
Probability density
0 - 0.05
0.05 - 0.2
0.2 - 0.4
0.4 - 0.8
0.8 - 1.59
Abu Fontas
Total exposure
0.0593


Abu Fontas in may 2020
Probability density
0 - 0.05
0.05 - 0.2
0.2 - 0.4
0.4 - 0.8
0.8 - 1.77
Abu Fontas
Total exposure
0.0338


Abu Fontas in june 2020
Probability density
0 - 0.05
0.05 - 0.12
Abu Fontas
Total exposure
0.0006

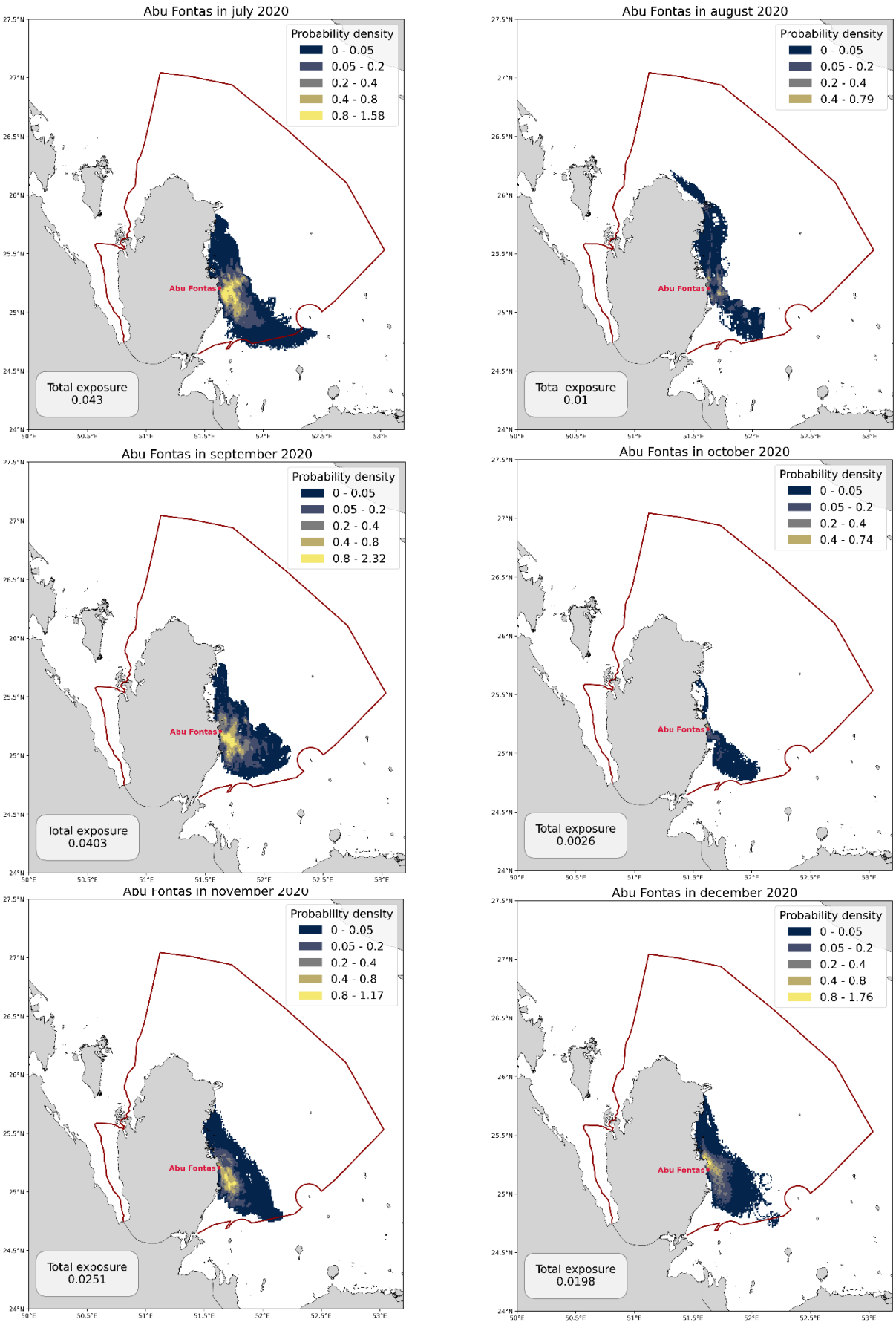
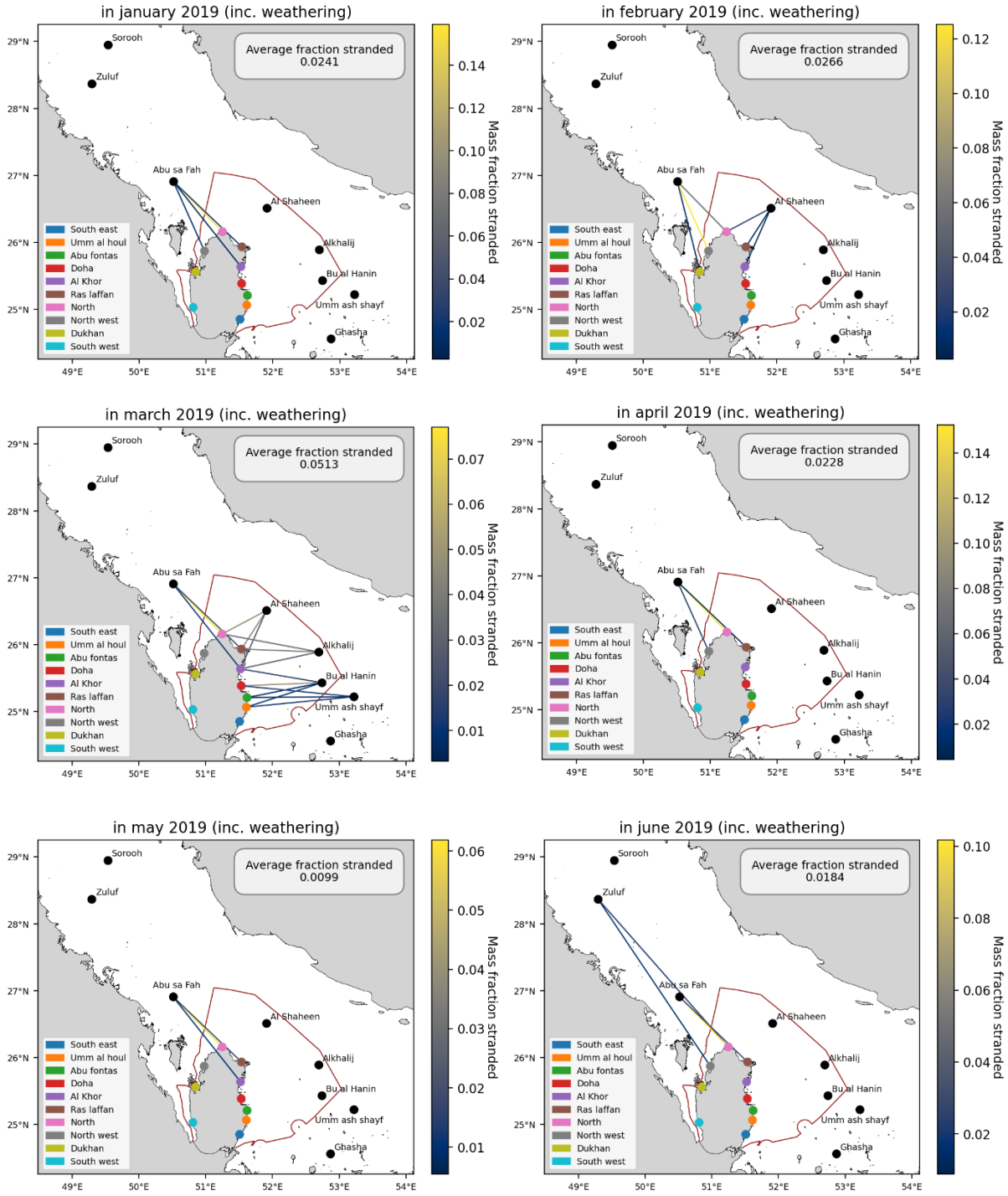


Figure 7.19 : Exposure to ships oil spill for Abu Fontas in 2020

E. Qatari coasts exposure to oil from oil fields



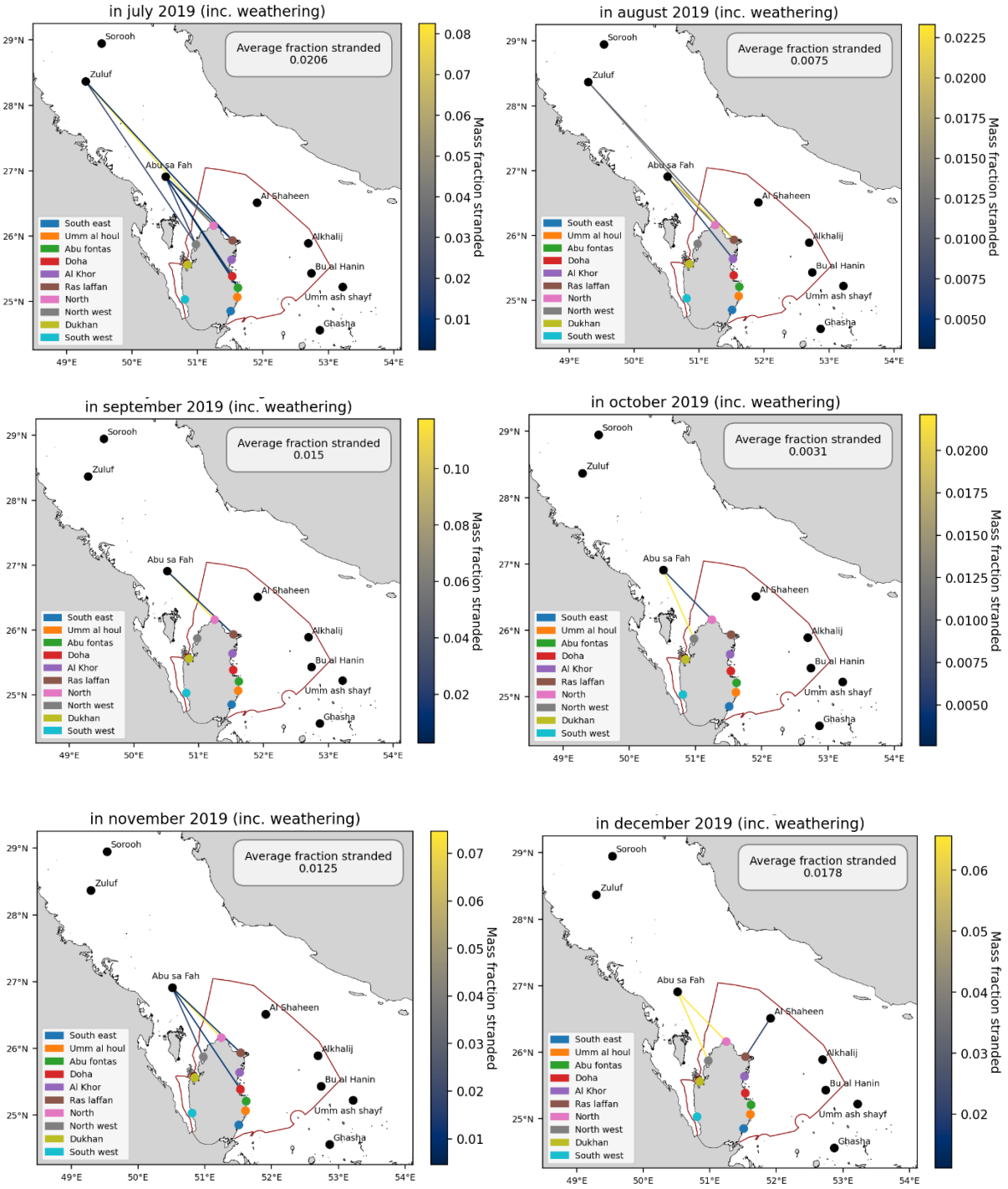
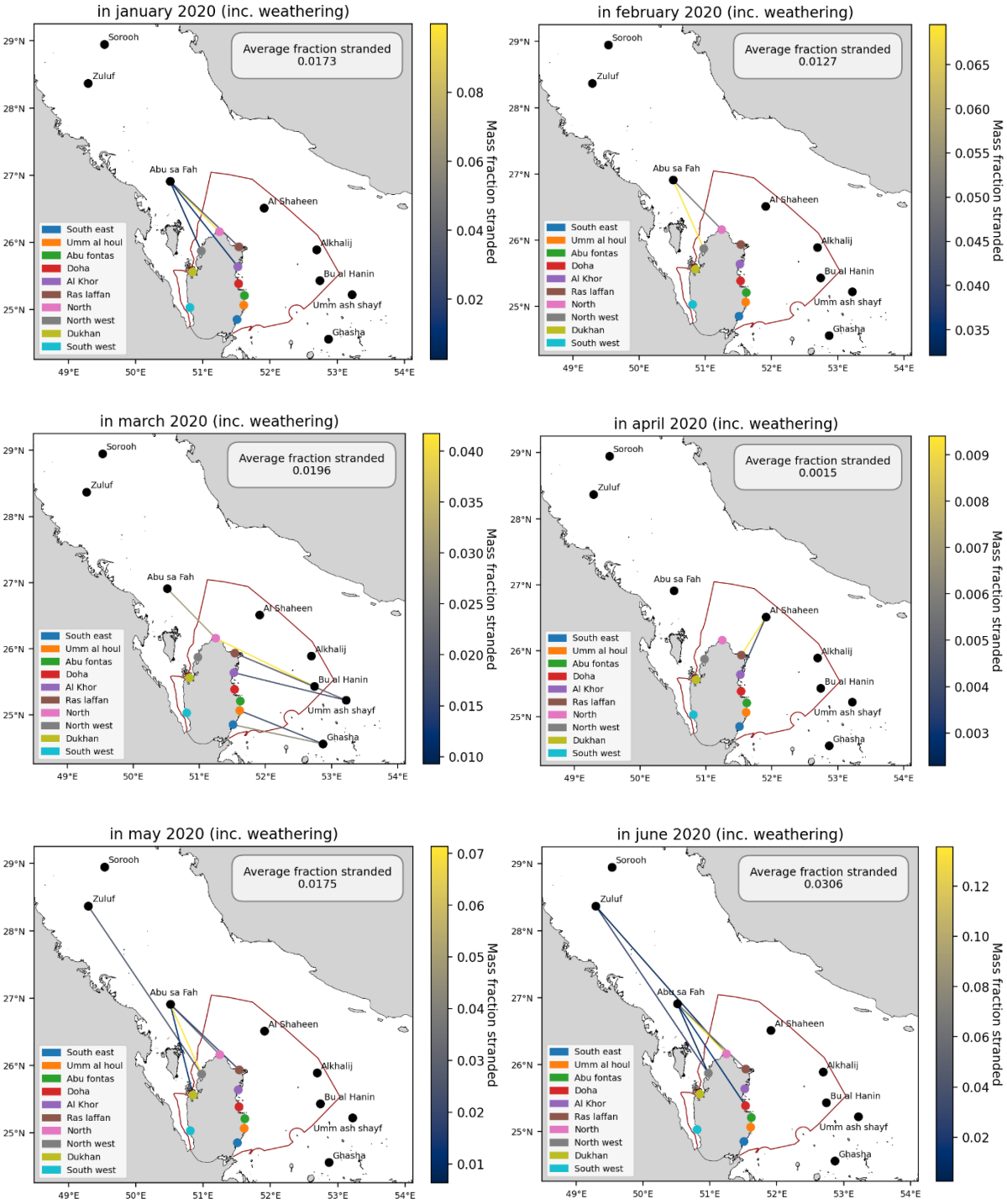


Figure 7.20 : Oil mass fraction stranded on Qatari coasts originating from oil rigs in 2019


in january 2020 (inc. weathering)
Average fraction stranded
0.0173
in february 2020 (inc. weathering)
Average fraction stranded
0.0127
in march 2020 (inc. weathering)
Average fraction stranded
0.0196
in april 2020 (inc. weathering)
Average fraction stranded
0.0015
in may 2020 (inc. weathering)
Average fraction stranded
0.0175
in june 2020 (inc. weathering)
Average fraction stranded
0.0306
Mass fraction stranded
Sorooh
Zuluf
Abu sa Fah
Al Shaheen
Alkhalij
Bu al Hanin
Umm ash shayf
Ghasha
South east
Umm al houl
Abu fontas
Doha
Al Khor
Ras laffan
North
North west
Dukhan
South west
29°N
28°N
27°N
26°N
25°N
49°E
50°E
51°E
52°E
53°E
54°E

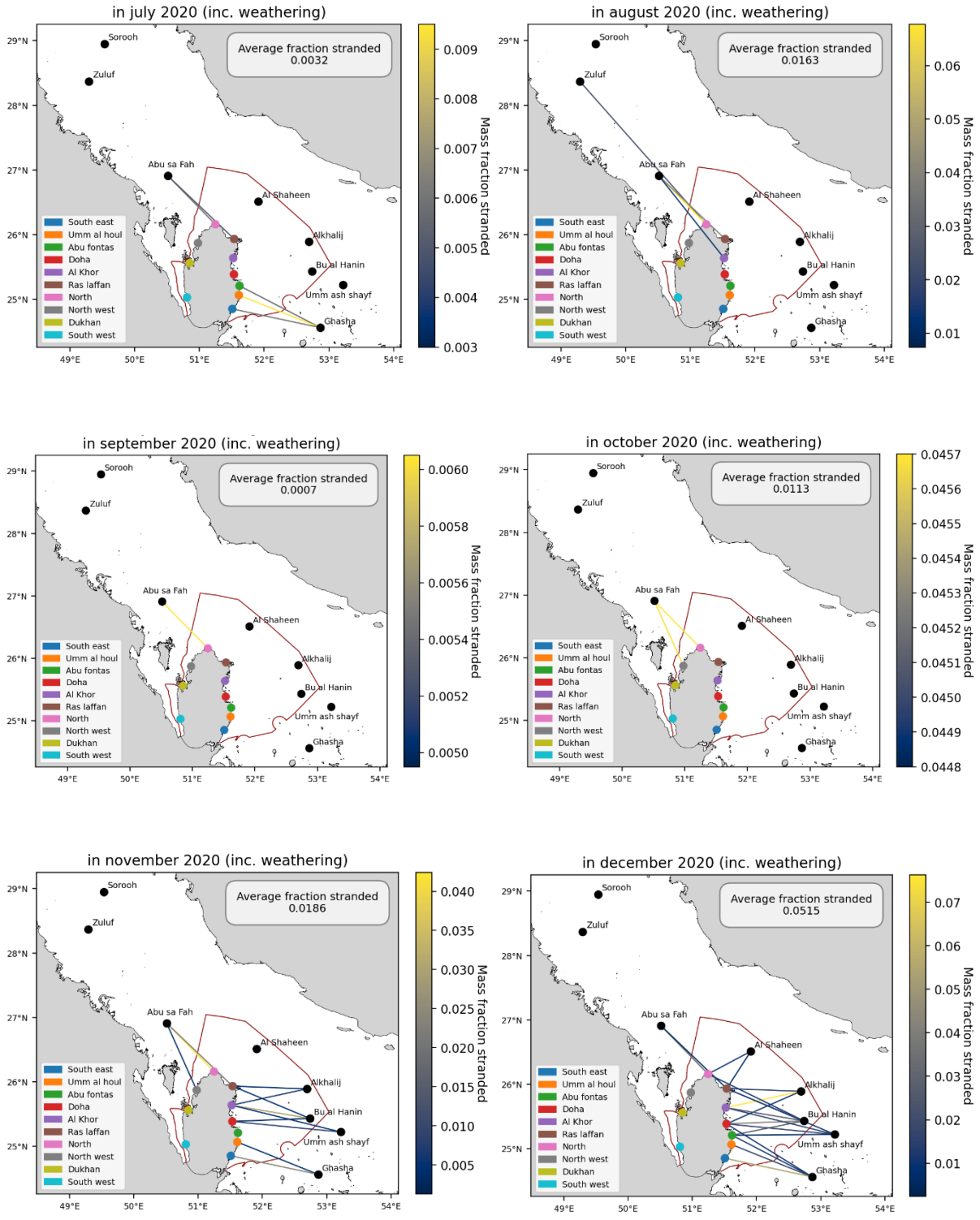


Figure 7.21 : Oil mass fraction stranded on Qatari coasts originating from oil rigs in 2020

Vulnerability assessment of Qatar desalination plants to oil spills

Thomas Anselain

Water scarcity is an issue at least once a year for 70% of the global population. As water scarcity increases, desalination plants are on the rise. Today, desalinated water represents about half of the entire water supply of Qatar. However, the desalination plants and, by extension, Qatar are very sensitive to oil spill pollution. The Arabian Gulf being one of the most oil-polluted environment in the World, Qatar is continuously threatened by oil spills, which could lead to the closure of desalination plants. To efficiently manage its water supply, Qatar needs to monitor its coastal waters in order to detect as early as possible oil spills that could potentially threaten its desalination plants. In this study, we perform a vulnerability assessment of Qatar desalination plants to oil pollution originating from both shipping activities and offshore oil platforms. In order to simulate oil drift dispersal, we used the open-source model OpenOil, which takes into account the different physical processes driving oil dispersal as well as most of the oil weathering processes. To assess the exposure to oil pollution originating from shipping activities, we first identify the oil risk area around a desalination plant and then combine this risk information with the density of ships in the Gulf. In a second step, a connectivity study was performed to highlight which oil fields are the most dangerous for Qatar. Overall, the results show a strong seasonal variability of the oil exposure patterns, which reflects changes in the atmospheric and oceanic in the Gulf. When Shamal winds are blowing in summer and winter, risk is usually located mostly Northwest of Qatar. However, when winds weaken in spring and autumn, the risk area tends to shift East and be more isotropic. It is during summer, that the circulation is the most intense and hence that oil spills could travel the largest distances before reaching a desalination plant. Higher temperatures and more intense wave activity however increase the oil weathering rate and hence reduce the associated risk. Among Qatar's three main desalination plants, Ras Laffan, located on the northeastern coast of Qatar, is the one most at risk of being impacted by oil spills. Despite the model is not validated by previous oil spill observations, our results could inform Qatar authorities on ways to optimize their oil spill management strategy. This study could also inspire new research about desalination plants vulnerability throughout the Arabian Gulf and promote the development of oil spills forecasting and monitoring capacities in order to reduce the impact of oil pollution on water production.

UNIVERSITÉ CATHOLIQUE DE LOUVAIN
Faculté des bioingénieurs
Croix du Sud, 2 bte L7.05.01, 1348 Louvain-la-Neuve, Belgique | **www.uclouvain.be/agro**